In vivo ^{1}H NMR methods to study dynamics of chloroplast water and thylakoid membrane lipids in leaves and in photosynthetic microorganisms

Shanthadevi Pagadala

Thesis committee

Promotor

Prof. Dr H. Van Amerongen
Professor of Biophysics
Wageningen University & Research

Co-promotor

Dr H. Van As
Associate professor, Laboratory of Biophysics
Wageningen University & Research

Other members

Prof. Dr L. F. M. Marcelis, Wageningen University & Research
Prof. Dr J. A. Killian, Utrecht University, The Netherlands
Dr C. P. M. Van Mierlo, Wageningen University & Research
Dr A. Pandit, Leiden University, The Netherlands

In vivo ^{1}H NMR methods to study dynamics of chloroplast water and thylakoid membrane lipids in leaves and in photosynthetic microorganisms

Shanthadevi Pagadala

Thesis

submitted in fulfilment of the requirements

for the degree of doctor

at Wageningen University

by the authority of the Rector Magnificus

Prof. Dr. A. P. J. Mol,

in the presence of the

Thesis Committee appointed by the Academic Board

to be defended in public

on Tuesday 6 June 2017

at 11.00 a.m. in the Aula.

Shanthadevi Pagadala

In vivo ^{1}H NMR methods to study dynamics of chloroplast water and thylakoid membrane lipids in leaves and in photosynthetic microorganisms

130 pages.

Contents

1

Introduction

1.1 Section I

Plants experience varying environmental conditions such as high light, low light and high temperature in daily life. Flexibility of chloroplast thylakoid membrane proteins is essential for plant fitness and survival during such fluctuations[1]. The aim of this thesis is to study dynamics of chloroplast water, thylakoid membrane lipids and proteins in different environmental conditions. To get insight into the significance of the mobility (dynamics) of proteins and lipids, I refer to the chapter "Role of Lipids in the Dynamics of Thylakoid membrane" (title of the book is **Lipids in Photosynthesis**) written by C. W. Mullineaux and H. Kirchhoff[2]. The authors describe how important the mobility of proteins and lipids is in photosynthesis, and some examples are plastoquinol diffusion during electron transport, LHCII mobility during state transitions and membrane biogenesis, and in turnover & repair of thylakoid membrane proteins. An overview of various methods to measure thylakoid membrane dynamics and advantages & limitations of these methods taken from that chapter is listed below.

Fluorescence Recovery After Photobleaching is one of the best techniques so far to probe the mobility

1) of photosynthetic pigment-protein complexes by visualizing the native fluorescence from fluorescent pigments
2) *in vivo* of specific thylakoid membrane proteins genetically tagged with Green Fluorescent Protein (GFP)
3) *in vitro* of proteins tagged with fluorescent antibodies
4) of lipids and membrane fluidity in general by staining membranes with lipophilic fluorophores.

Although FRAP is able to probe the mobility of proteins and lipids (as mentioned above) it is limited by its spatial resolution. It can resolve mobility only at relatively large scales of a micron or more. In addition FRAP can only measure the mean behaviour of a large number of fluorophores and the bleaching during FRAP may perturb the behaviour of the membrane being examined. These limitations can often be overcome by using Fluorescence Correlation Spectroscopy and Single Particle Tracking, but both techniques cannot employ the native fluorescence from photosynthetic pigments since they are too densely packed in the membrane whereas a relatively low density of fluorescent tags is required. However, both techniques can be used *in vitro* by labelling specific membrane proteins with fluorescent antibodies at low density.

Very recently, structural dynamics of thylakoid membranes were visualized using live cell imaging in combination with deconvolution[3]. By observing chlorophyll fluorescence in the antibiotics-induced macrochloroplast in the moss *Physcomitrellapatens* it was concluded that both the structural stability and flexibility of thylakoid membranes are essential for dynamic protein reorganization under fluctuating light environments[3].

In conclusion, the fluorescence techniques are applicable to probe the mobility of proteins and lipids either *in vivo* or *in vitro* by using external labels such as GFP, fluorescent antibodies and lipophilic fluorophores. Any of these methods might lead to non-native conditions. However, the fluorescence techniques clearly give some insight into the mobility of the thylakoid membrane proteins and lipids.

The fluidity of the thylakoid membrane in isolated thylakoid membrane suspensions of cyanobacteria and various mutants has been studied by Klodawska *et al.* using Spin label Electron Paramagnetic Resonance spectroscopy[4]. The relative fluidity of membranes was estimated from EPR spectra by using the outermost splitting parameter in the temperature range from 15°C to 45°C. The data suggested that the overall fluidity of native photosynthetic membranes in cyanobacteria may be influenced by the ratio of polar to nonpolar carotenoid pools under different environmental conditions[4]. However, the technique has its limitations because it requires the use of external labels.

Coming to the chloroplast water dynamics, chloroplast water was discriminated from other cellular water signals in leaf discs by McCain *et al.* using NMR spectroscopy[5,6] on the basis of shifted resonances, but the approach was not correct (as will be detailed in Chapter 2 of this thesis) while McCain *et al.* also calculated water permeability of chloroplast envelope membranes using saturation transfer NMR[7]. Musse *et al.* characterized various cell compartments in *Brassica napus* leaves while monitoring leaf senescence using low field ^{1}H NMR relaxometry, light and electron microscopy[8]. They concluded that chloroplast water can easily be discriminated from other water pools using NMR relaxation time measurements. But, translational dynamics of chloroplast water are not studied so far to the best of our knowledge. This thesis describes Pulsed field gradient ^{1}H NMR methods (DOSY and DRCOSY) to study the dynamics of chloroplast water and the thylakoid membrane lipids and protein complexes at a time scale of milliseconds in leaf disks and in photosynthetic microorganisms under changing environmental conditions in

complete *in vivo* conditions. Study of chloroplast water dynamics at this time scale provides information regarding viscosity of stroma and chloroplast membrane permeability. Also, it is possible to probe the mobility of the thylakoid membrane proteins and lipids at this time scale as their mobility is very slow.

1.2 Section II

Pulsed field gradient Nuclear Magnetic Resonance is a non-invasive technique to measure diffusion of water, lipids and proteins not only in model membrane systems[9] but also in intact biological membranes and biological cells. The main advantage of this Pulsed Field Gradient NMR is that it does not require any external labelling as it makes use of naturally available probe molecules such as water, lipids and proteins. Also, mobility can be resolved at length scales of a few hundreds of nm. However, the technique still has the limitation that it measures diffusion of an ensemble of spins. Moreover, it is hard to distinguish proteins and lipids having the same resonances and diffusing at the same rate. However, one can overcome this problem by selecting particular coherence pathways using more advanced pulse sequences[10]. In order for the reader to understand the following chapters which describe diffusion NMR experiments I will next explain the details of the diffusion NMR experiments.

1.2.1 Basic principles of diffusion NMR:

Diffusion is measured by attenuating NMR signals using a combination of pulsed field gradients. The pulsed field gradients spatially manipulate the external magnetic field B_0 across the sample volume, which results in a distribution of spatial frequencies which can be referred to spatial labelling of the spins. The first gradient spatially encodes the spins with different frequencies (Fig. 1.1) and the second one decodes them. If there is no diffusion in between the gradients there is no signal attenuation; the faster the diffusion the higher the attenuation. The equation of the NMR signal intensity as a function of attenuation, $S(q)$, is as follows:

$$S(q) \cong S_0 \sum_i P_i e^{-q^2 D_i (\Delta - \frac{\delta}{3})}$$

where $q = \gamma \delta g$. S_0 is the NMR signal intensity in the absence of gradients, γ the gyromagnetic ratio, P_i the fraction of molecules i, δ the duration of the gradient pulse, g the gradient strength, D_i the diffusion coefficient of fraction

i and Δ the diffusion observation time, the time between the two gradient pulses.

Diffusion is measured by varying any of the three experimental parameters: Δ, δ and g and fixing the other two. We measure the signal attenuation as a function of gradient strength at fixed Δ and δ. By fitting the attenuation vs. gradient strength with the above equation we get the apparent diffusion coefficient (ADC).
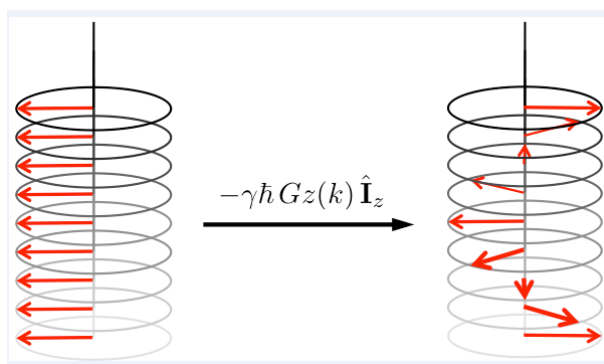

Figure 1.1: Effect of pulsed field gradient on XY-magnetization (Source: https://www.chemie.uni-hamburg.de/nmr/insensitive/tutorial/en.lproj/gradients.html).

In order to measure diffusion of molecules (bearing NMR active nuclei) accurately the NMR signal from the molecules must be attenuated from 2 % to 95 %. One can get the proper attenuation by varying any of the three experimental parameters: Δ, δ and g. However, varying Δ is not very useful as the attenuation is only linearly proportional to the diffusion observation time whereas it is quadratically proportional to g and δ, and varying g is even more advantageous to minimise T_2 weighting during δ. Using stronger gradients to measure diffusion of very slow molecules (for instance membrane lipids or proteins) also has a disadvantage, namely that the stronger gradients produce eddy currents but the eddy[11] currents can be minimised using bipolar[11] gradients.

In general, one of the following two pulse sequences can be used to measure diffusion: the pulsed field gradient spin-echo sequence and the pulsed field gradient stimulated echo sequence.

1.2.2 Pulsed Field Gradient Spin-Echo sequence: A PFG Spin-echo sequence is shown in Fig. 1.2. The first 90° RF pulse shifts the net

magnetization to the XY-plane. The first gradient encodes the spins spatially with different precession frequencies as shown in Fig. 1.1. As the 180° RF pulse inverts the spins the second gradient decodes the spins in the opposite direction resulting in complete refocusing in case of no diffusion and in echo attenuation in case of diffusion. The echo attenuation is measured as a function of g or δ to obtain the apparent diffusion coefficient of the spins.
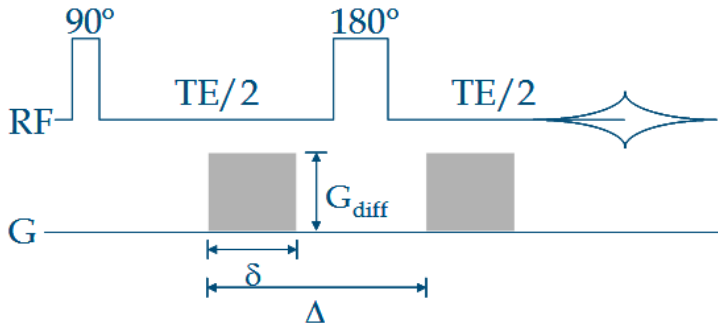

Figure 1.2: Pulsed Field Gradient Spin-Echo sequence.

1.2.3 Pulsed Field Gradient Stimulated Echo sequence: In this PFG stimulated echo sequence (Fig. 1.3) the 180° RF pulse of the spin echo sequence is split into two 90° RF pulses. During the time between these two 90° RF pulses half of the net magnetization is along the Z-axis that makes the sequence more useful than the spin-echo sequence to measure the diffusion of spins with shorter T_2's. Because when the net magnetization is along the Z-axis, the spins have T_1 relaxation which is in general greater than or equal to T_2 relaxation. However, the sequence is limited by a lower S/N ratio as only half of the signal is measured.
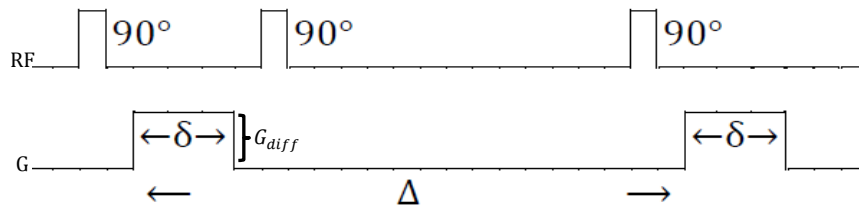

Figure 1.3: Pulsed Field Gradient Stimulated Echo sequence.

Although the above two pulse sequences are the most basic ones to measure diffusion, there are many more advanced sequences derived from

these two for special purposes. For instance, we used a stimulated echo bipolar pulse sequence[12,13,14,15] to minimize the eddy currents and also to measure the diffusion of spins with shorter T_2's (such as lipids and proteins).

1.3 Section III

As the goal of the thesis is to study the dynamics of the chloroplast water, thylakoid membrane lipids and proteins, I provide here a brief introduction to them and their importance. Chloroplasts are plastids found in plant cells and eukaryotic algae that perform photosynthesis. Photosynthesis is probably the most essential process for life on this planet as plants use photosynthesis to make food from carbon dioxide and water with the assistance of sunlight, and animals in turn obtain their food from plants. In addition to the food (carbohydrates), oxygen is another product of photosynthesis that most living creatures need in order to obtain energy via respiration. In addition to energy, carbon dioxide and water are produced again when food is burned to provide energy while using oxygen. Because photosynthesis is very important to fix CO_2, people even are nowadays attempting to build artificial leaves[16,17] to fix additional CO_2, amongst others released by industry and traffic, but also to create and store energy.

Coming back to the chloroplasts, the structure of a chloroplast is shown in Fig. 1.4. A chloroplast has two envelope membranes and a third inner envelope membrane called thylakoid. Stack(s) of thylakoid membranes is (are) called granum (grana) and the space enclosed by a thylakoid membrane is called lumen. The internal fluid surrounded by the inner envelope membrane is called stroma.

The process of photosynthesis occurs in two overall steps, light dependent and light independent. Light-dependent reactions largely take place in the thylakoid membrane and light-independent reactions in the stroma. A schematic structure of a typical thylakoid membrane from plants is shown in Fig. 1.5, and it contains the following major protein complexes: photosystem II (PSII), cytochrome b_6f, photosystem I (PSI), ferredoxin NADP reductase (FNR) and ATP synthase. Both photosystems I&II contain reaction centres with P700 & P680 as their primary electron donors, respectively. These reaction centres consist of proteins and are surrounded by light-harvesting antenna complexes often containing chlorophyll molecules and carotenoids in plants and algae.

1.3.1 Light reactions: Pigments in the light-harvesting antenna complexes absorb light energy and the energy is further converted into chemical energy in the form of NADPH and ATP. Photolysis (water splitting) is also a part of light reactions which produces oxygen which is imperative for life on earth.
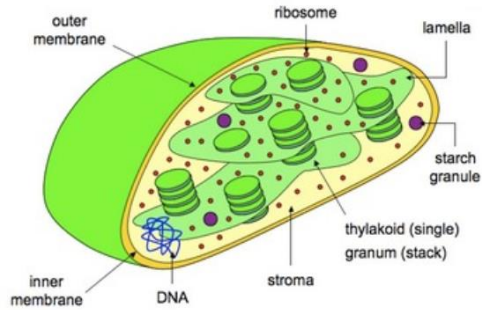

Figure 1.4: Cartoon of the structure of a chloroplast (Source: http://www.vce.bioninja.com.au/aos-1-molecules-of-life/biochemical-processes/photosynthesis.html).
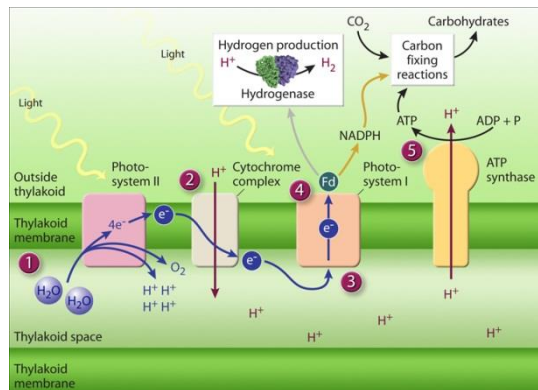

Figure 1.5: Representation of light reactions in a thylakoid membrane (source: http://genomics.energy.gov).

1.3.2 Dark reactions (light-independent reactions): also known as Calvin-Benson-Bassham (CBB) cycle, Calvin–Benson–Bassham (CBB) cycle occurs in the stroma.

During the dark reactions sugar molecules are being produced in the Calvin-Benson-Bassham (CBB) cycle while ATP and NADPH, produced during the light reactions, are being consumed and CO_2 from the atmosphere is being used.

1.4 Section IV

A very brief introduction to the various chapters is given below.

Chapter 2 describes the ^{1}H NMR methods (DOSY and DRCOSY) to discriminate chloroplast water from other cellular water compartments in leaf disks. Orientation-dependent ^{1}H NMR spectra were observed for leaf discs of *Ficus benjamina* and *Acer platanoides*. However, discrimination of chloroplast water from other cellular water compartments based on spectra is not correct anymore, but it can be done using T_2 and ADC determination.

Chapter 3 describes the effect of drought stress on these compartments. Chloroplasts appeared to be less sensitive than other compartments (such as vacuoles for instance) to moderate drought stress in leaf disks of both *F. Benjamina* and *A. platanoides*. With extended drought stress chloroplasts became equally sensitive as vacuoles in *A. platanoides* but they were still less sensitive in *F. Benjamina* because of subepidermal cells.

In chapter 4 we studied the effects of nutrient stress and salt stress on the dynamics of chloroplast water, (thylakoid) membrane lipids and protein complexes in *Chlamydomonas reinhardtii*. Accumulated lipid bodies were observed upon nutrient stress and salt stress in *C. reinhardtii* and their dynamics were also studied.

Chapter 5 deals with the detection of Synechocystis water and comparison of the *Synechocystis* membrane lipids to that of *C. reinhardtii* and spinach thylakoids in order to check the differences in water dynamics and also in thylakoid membrane composition and dynamics.

Chapter 6 provides a general discussion regarding the different systems studied. Chloroplast water pool was discriminated in leaf disks of *F. benjamina* and *A. platanoides* and also in *C. reinhardtii* suspension. Translational dynamics of the chloroplast water in the above mentioned three systems is about comparable in the order of 3×10^{-11} m^2 s^{-1} at $\Delta=25$ ms. Observed changes in the dynamics of the chloroplast water, under various environmental conditions, at short diffusion times indicate the changes in viscosity of the stroma and at long diffusion times indicate the changes in chloroplast membrane permeability. By proper suppression of the abundant water signals more proton pools such as lipids and large protein (membrane) complexes are observed in *C. reinhardtii* and in *Synechocystis*. Chapter 7 summarizes all the chapters.

References:

1) Iwai, M., Pack, C. G., Takenaka, Y., Sako, Y., and Nakano, A. (2013). Photosystem II antenna phosphorylation-dependent protein diffusion determined by fluorescence correlation spectroscopy. Scientific reports **3**.

2) W. Mullineaux and H. Kirchhoff (2010). Role of Lipids in the Thylakoid membrane dynamics. Advances in Photosynthesis and Respiration **30**, pp 283-294.

3) Iwai, M., Yokono, M., and Nakano, A. (2014). Visualizing structural dynamics of thylakoid membranes. Scientific reports **4**.

4) Klodawska, K., Malec, P., Kis, M., Gombos, Z., and Strzalka, K. (2012). EPR study of thylakoid membrane dynamics in mutants of the carotenoid biosynthesis pathway of Synechocystis sp. PCC6803. Acta Biochimica Polonica **59**(1): 87.

5) McCain, D. C., Selig, T. C., and Markley, J. L. (1984). Some plant leaves have orientation-dependent EPR and NMR spectra. Proceedings of the National Academy of Sciences **81**: 748-752.

6) McCain, D. C. (1995). Nuclear magnetic resonance study of spin relaxation and magnetic field gradients in maple leaves. Biophysical Journal **69**: 1111-1116.

7) McCain, D. C. and J. L. Markley (1985). Water permeability of chloroplast envelope membranes: in vivo measurement by saturation-transfer NMR. FEBS Letters **183**: 353-358.

8) Musse, M., De Franceschi, L., Cambert, M., Sorin, C., Le Caherec, F., Burel, A., and Leport, L. (2013). Structural Changes in Senescing Oilseed Rape Leaves at Tissue and Subcellular Levels Monitored by Nuclear Magnetic Resonance Relaxometry through Water Status. Plant Physiology **163**: 392-406.

9) Lindblom, G. and Orädd G. (2009). Lipid lateral diffusion and membrane heterogeneity. Biochimica et Biophysica Acta (BBA)-Biomembranes **1788** (1): 234-244.

10) Melkus, G., Mörchel, P., Behr, V. C., Kotas, M., Flentje, M., and Jakob, P. M. (2009). Sensitive J-coupled metabolite mapping using Sel-MQC with selective multi-spin-echo readout. Magnetic Resonance in Medicine **62** (4): 880-887.

11) Sørland, GH. (2014). Dynamic Pulsed-field-gradient NMR. Berlin: Springer.

12) Cotts, R. M., Hoch, M. J. R., Sun, T., and Markert, J. T. (1989). Pulsed field gradient stimulated echo methods for improved NMR

diffusion measurements in heterogeneous systems. Journal of Magnetic Resonance (1969) **83** (2): 252-266.

13) Vasenkov, S., Böhlmann, W., Galvosas, P., Geier, O., Liu, H., and Kärger, J. (2001). PFG NMR study of diffusion in MFI-type zeolites: Evidence of the existence of intracrystalline transport barriers. The Journal of Physical Chemistry B **105** (25): 5922-5927.

14) Stallmach, F., Gröger, S., Künzel, V., Kärger, J., Yaghi, O. M., Hesse, M., and Müller, U. (2006). NMR Studies on the Diffusion of Hydrocarbons on the Metal-Organic Framework Material MOF-5. Angewandte Chemie International Edition **45** (13): 2123-2126.

15) Paoli, H., Methivier, A., Jobic, H., Krause, C., Pfeifer, H., Stallmach, F., and Kärger, J. (2002). Comparative QENS and PFG NMR diffusion studies of water in zeolite NaCaA. Microporous and mesoporous materials **55** (2), 147-158.

16) Zhou, H., Fan, T., and Zhang, D. (2011). An insight into artificial leaves for sustainable energy inspired by natural photosynthesis. ChemCatChem **3** (3): 513-528.

17) Concepcion, J. J., House, R. L., Papanikolas, J. M., and Meyer, T. J. (2012). Chemical approaches to artificial photosynthesis. Proceedings of the National Academy of Sciences **109** (39): 15560-15564.

18) Karp, G., and Pruitt, N. L. (1996). Cell and molecular biology: concepts and experiments. New York: John Wiley and Sons.

2

Chloroplast water in leaves as viewed by ^{1}H DOSY and DRCOSY NMR

Abstract

Although chloroplasts represent a substantial fraction of the total leaf water, a very limited number of NMR studies of chloroplasts *in vivo* in relation to leaf water content has been published. It is not clear if the published approaches to discriminate chloroplast and non-chloroplast water are fully effective. Here, we present results of high-field ^{1}H DOSY and low-field time domain (TD) DRCOSY experiments to detect and identify chloroplast water and thylakoid membrane lipids.

In suspensions of isolated chloroplasts, exchange between water pools outside and inside the chloroplasts turned out to be fast, limiting the possibility to study size and membrane permeability of chloroplasts and to characterize relaxation times of chloroplast water. In algae suspension, two water pools (cell, chloroplast) could be easily discriminated from the medium water pool on the basis of (restricted) diffusion and relaxation behaviour. In leaf disks of *Ficus benjamina* and *Acer platanoides*, water in chloroplasts could be clearly discriminated from vacuolar water in palisade, spongy, epidermal and sub-epidermal cells. Both water in chloroplasts and water in vacuoles of palisade and spongy cells showed resonances in the high field part of the spectra (with respect to pure water), in contrast to what has been reported in literature.

2.1 Introduction

Plants depend on light and the photosynthetic apparatus to manufacture energy rich complex organic molecules such as ATP and NADPH. The photosynthetic apparatus of plants and algae is located in chloroplasts. Chloroplasts are surrounded by a double envelope membrane and contain a third inner membrane, called the thylakoid membrane, which forms long folds within the organelle. In chloroplasts, light-dependent photosynthetic reactions mainly take place in the thylakoid membranes whereas dark reactions occur in the stroma. The thylakoid membrane consists of 20–30 % lipids and 70–80 % proteins, a large part of which in the photosynthetic supercomplexes photosystem I and II (LHC-I/PSI and LHC-II/PSII)[1].

Photosynthetic activity is directly coupled to changes in chloroplast volume. Chloroplast volume regulation (CVR) is a process by which chloroplasts import or export osmolytes to maintain a constant volume in a changing environment. The process was first studied by Robinson in suspensions of isolated chloroplasts[2]. By measuring stromal volumes using a centrifugation technique he concluded that the chloroplasts maintained constant volumes over a range of water potentials. Robinson also observed correlation between photosynthetic oxygen production and chloroplast volume changes; chloroplast volumes much above or below the optimum evolved very little O_2. Later, Gupta and Berkowitz confirmed that the process also occurs in isolated chloroplast[3]. Below a critical value of the leaf water potential, CVR failed: photosynthetic rates dropped suddenly at the same water potential, as did chloroplast volumes[3]. Santakumari and Berkowitz studied CVR in chloroplasts isolated from plants with and without water stress. CVR extended to lower water potentials in chloroplasts isolated from plants with water stress in comparison to the chloroplasts isolated from plants without water stress[4]. Measured in the dark, this critical water potential value is lower in sun leaves than in shade leaves[5], and it also depends on physiological levels of osmotic solutes[6]. Recently, it was shown that in addition to chloroplasts, organelles that experience osmotic stress from within the cytoplasm during normal growth conditions, also perform volume control by opening mechanosensitive ion channels under hypoosmotic stress[7]. It was concluded that plastids are under hypoosmotic stress during normal plant growth and dynamic response to this stress requires mechanosensitive ion channels.

These studies show that CVR is necessary for an efficient photosynthesis. They were performed only *in vitro*. McCain *et al.* studied CVR for the first

time in intact leaf disks using ^{1}H NMR spectroscopy, based on the assumption that the peak shifted with respect to the resonance frequency of pure water represents chloroplast water[8]. The frequency shift of the chloroplast water with respect to the non-chloroplast water was explained to depend on the high concentration of weakly bound Mn^{2+} ions near the outer surface of the thylakoid membrane, and on the geometry of palisade cells: the mechanical effect of pressing an ellipsoidal chloroplast against the cylindrical inner wall of a palisade cell aligns the shortest chloroplast axis along a radius vector perpendicular to the axis of the cell, and the longest chloroplast axis parallel to the cell's axis[9]. The approach presented by McCain *et al.* is not generally applicable, since it depends on the spectral shift of chloroplast water with respect to that of non-chloroplast water, which is not observed in all leaves.

More recently, Musse *et al.* characterized various cell compartments in *Brassica napus* leaves by monitoring leaf senescence using low field ^{1}H NMR relaxometry, light and electron microscopy[10]. They concluded that chloroplast water can be observed as a water pool with T_2 of about 20 ms, and can easily be distinguished from the T_2 of other water pools. Multi-modal T_2 relaxation can be used to identify different water pools in plant/biological tissue[10,11]. However, interpretation of such multi-exponential decay is not always straightforward because of exchange between water pools. The number of observed decay components depends on the exchange rate between these water pools, which complicates the assignment of the components to compartments. Two-dimensional diffusion-relaxation correlation spectroscopy (DRCOSY[12]) and diffusion-ordered spectroscopy (DOSY[13], correlation of diffusion coefficient with chemical shift) measurements have been demonstrated to be very useful to further unravel water pools in the presence of exchange. However, in the interpretation of DRCOSY results obtained in (leaves of) chive chloroplast water was not considered at all[12].

Here, we present results obtained by high field ^{1}H DOSY and low field ^{1}H DRCOSY measurements to discriminate chloroplast water pool from others and also to characterize the various water pools in isolated chloroplasts, algae and intact leaf disks. In addition to the water pools we were able to detect and characterize membrane lipids using high field ^{1}H DOSY measurements. Leaves have been chosen that show spectral characteristics as reported by McCain *et al*, i.e. splitting of the water peak depending on orientation of the leaves with respect to the main magnetic field.

2.2 Materials and Methods

2.2.1 Isolated chloroplasts

Chloroplasts were isolated from fresh spinach leaves using the method described by Rödiger *et al*[14].

2.2.2 Leaf disks

Leaf disks were obtained from *F. benjamina* and *A. platanoides.* Randomly-picked leaves were used for NMR measurements. Midribs were discarded, remaining tissue was cut into rectangular pieces of 1 cm length for measurements along the main magnetic field and into circular discs for measurements perpendicular to the field. Water resonance was used as a reference for the leaf spectra.

2.2.3 Algae

Wild-type *C. reinhardtii* (137C) cells were grown under continuous white-light illumination in Tris-acetate-phosphate medium[15]. Cells were shaken in a rotary shaker (100 rpm) at 30 °C and illuminated by a white lamp at 10 μmol.m^{-2}.s^{-1}. All cells were grown in 250 mL flasks with a growing volume of 200 mL and maintained in the logarithmic growth phase. The 200 mL suspension was further centrifuged to get about 800 μL of very concentrated cells.

2.2.4 Time-domain ^{1}H Relaxometry

^{1}H T_2 relaxation was measured with the Carr-Purcell-Meiboom-Gill experiment at 0.7 T field strength (30 MHz ^{1}H Larmor frequency) using a Maran Ultra spectrometer. An interecho time of 1 ms was used and 6k echoes were recorded. The experimental repetition time was 3 s and the number of averages was 4. Echo decays were analysed using CONTIN (Provencher, 1979)[16], which fits a continuous distribution of T_2 decays (i.e. Laplace inversion).

DRCOSY

Diffusion-relaxation experiments were performed at 0.7 T using a Maran Ultra spectrometer equipped with a gradient coil capable of delivering a 1.2 T m^{-1} field gradient. A stimulated echo-based diffusion experiment, using unipolar gradients and rectangular pulse shapes, was combined with a time-

domain CPMG experiment. The effective gradient pulse duration δ was set to 2 ms. The effective diffusion time Δ was varied between 20 and 100 ms. Gradient strength was varied between 0.2 and 1.0 T m⁻¹. An echo time of 0.3 ms for isolated chloroplast and algae samples, and 6k echoes were recorded.

DOSY and Diffusion Associated NMR Spectra

All high-field ^{1}H NMR diffusometry experiments were performed at 7 T (300 MHz ^{1}H Larmor frequency) and at 11 T (500 MHz) using a Bruker Avance II and III spectrometers, respectively. The 7 T spectrometer was equipped with a Bruker diff25 diffusion probehead, which delivers maximum field gradient strengths of 10 T m⁻¹. The 11 T spectrometer was equipped with a conventional Bruker z-gradient inverse ^{1}H/^{13}C/BB 5-mm probe which delivers maximum field gradient strengths of 0.5 T m⁻¹.

In NMR diffusometry, the echo attenuation as a function of the experimental parameters can be described by the Stejskal-Tanner equation[17]

$$\frac{I}{I_0} = \sum_i A_i e^{-(\gamma \delta g)^2 \left(\Delta - \delta/3\right) D_i},$$

where $\frac{I}{I_0}$ is the echo attenuation, A_i the amplitude of the NMR signal of component i, γ the gyromagnetic ratio of the relevant nucleus (rad T⁻¹ s⁻¹), δ the effective gradient pulse duration (s), g the gradient strength (T m⁻¹), Δ the effective diffusion time (s), and D_i the diffusion coefficient of component i (m² s⁻¹).

All DOSY experiments were carried out using a stimulated echo experiment in combination with bipolar sine-bell shaped gradients. Stimulated echo was used because it allows the detection of short T_2 components at longer diffusion observation times[18]. Bipolar gradients were used to compensate for internal field gradients, which are present at high field strengths in inhomogeneous samples. The effective gradient pulse duration δ was set to 2 ms. The effective diffusion time Δ was varied between 12 and 300 ms. Gradient intensity was varied between 0.05 and 8.5 T m⁻¹. The attenuation of NMR spectra as a function of gradient intensity was analysed by fitting 1 to 4 exponential decays to the spectra using SplMod (Provencher, 1982)[19], which was set to perform a coupled exponential fit of the spectral data points. This resulted in 1 to 4 diffusion-associated NMR spectra (DANS). The procedure is similar to the DECRA curve resolution method described elsewhere, but SplMod is preferred because it can handle both linear and logarithmic sampling of the gradient axis[17].

In case of *C. reinhardtii*, the effective gradient pulse duration δ was set to 2 ms and the effective diffusion time Δ was set to 30ms. Gradient intensity was varied between 0.7 and 5.2 T m^{-1} for 7 T DOSY. For 11 T DOSY, the effective gradient pulse duration δ was set to 4ms, the effective diffusion time Δ was varied between 20 to 60 ms and gradient intensity was varied between 0.0067 and 0.3 T m^{-1}.

Analysis of restricted diffusion behaviour

The time dependent diffusion coefficient $D(\Delta)$ was analysed using the Mitra equation[20]

$$\frac{D(\Delta)}{D_0} = 1 - \frac{S}{V}\frac{4}{9\sqrt{\pi}}\sqrt{D_0\Delta}$$

where D_0 is the unrestricted diffusion coefficient and $\frac{S}{V}$ the surface-to-volume ratio of the compartment.

Size estimation of the compartments:

Dimensions of the compartments were estimated using the above equation. First, D_0 was calculated by extrapolating a plot of $D(\Delta)$ vs. $\sqrt{\Delta}$ linearly to $\Delta=0$ ms. Only four points were used (for *F. benjamina*) to calculate the slope of the plot $D(\Delta)$ vs. $\sqrt{\Delta}$ for the components 2 and 3 because of the exchange between those and component 1.The intercept equals D_0. The slope of the line equals $-\frac{S}{V}\frac{4}{9\sqrt{\pi}}D_0^{3/2}$. As we know D_0 from the extrapolation, the surface-to-volume ratio follows from $\frac{S}{V} = -\frac{9\sqrt{\pi}}{4}D_0^{-\frac{3}{2}}$x slope. Assuming that the shape of the compartment is spherical, the size (diameter) *d* of the compartment is $d = \frac{6V}{S}$.

T$_2$-associated NMR spectra

^{1}H *T$_2$* relaxation was measured at 7 T (300 MHz ^{1}H Larmor frequency) with a Bruker Avance II spectrometer applying a CPMG sequence with constant TE = 200 μs and a variable number of 180 pulses from 4-9500 in 32 steps before acquisition of the echo to record the spectra of 15K data points with a dwell time of 41 μs.

Echo time dependence of the spectra was analysed with 1 to 4 T$_2$-associated spectra using SplMod (Provencher, 1982)[19], which was set to

perform a coupled exponential fit of the spectral data points using T_2 attenuation equation $I_t = I_0 \sum_i A_i e^{-t/T_{2,i}}$, where $t = NECH \times TE$ with $NECH$- number of echoes and TE- interecho time, A_i and $T_{2,i}$ are the amplitude and T_2 of component i, respectively. This resulted in 1 to 4 T_2-associated NMR spectra.

Saturation transfer experiment

A saturation transfer experiment as described by McCain was used[21]. The leaf disks were oriented perpendicular to the main magnetic field B_0. The upfield peak was saturated using a selective saturation pulse of width 25 ms for a range of saturation recovery times from 5 ms to 3.5 s in 32 steps. The spectrum for each recovery time was subtracted from the spectrum with recovery time of 3.5 s to determine the amount of saturation from the difference spectra.

2.2.5 Confocal Microscopy

Viability of chloroplasts was evaluated by confocal laser scanning microscopy. Images were acquired using a Zeiss LSM 510 (Jena, Germany) confocal microscope. Chlorophyll molecules were excited using an Argon laser by selecting the 514 nm laser line, and their fluorescence was captured using a 650-nm long pass filter. Images with a pixel matrix of 512x512 were obtained using a 40 oil immersion objective (numerical aperture of 1.2) and the pinhole was set at 1 Airy unit. Confocal images were analyzed using Zeiss LSM software, version 3.2.0.70.

2.2.6 Chlorophyll Fluorescence

Fluorescence measurements were performed with a PAM 101 chlorophyll fluorometer (Heinz Walz GmbH, Effeltrich, Germany) using a fibre optic system as described by Schreiber (1986). Saturating pulses (800 ms) of white light (4000 µmol m^{-2} s^{-1}) were provided by a KL 1500 light source (Schott, Wiesbaden, Germany). PSII efficiency (F_v/F_m) was measured using measuring beam intensity of (0.005 µmol m^{-2} s^{-1}) and saturation pulse.

2.3 Results

2.3.1 Isolated chloroplasts

In concentration-dependent DRCOSY experiments of isolated chloroplast suspensions of spinach, only a single component was observed. For a

concentration of 3.4 g L^{-1}, a single T_2 of ~100 ms was found with an associated apparent diffusion coefficient (ADC) of 1.5×10^{-9} m^{2}s^{-1}. Both T_2 and ADC were concentration dependent (Fig. 2.1), which indicates fast exchange across the chloroplast envelope membrane of water inside the chloroplasts with water in the medium. The maximum quantum yield of PSII of the isolated chloroplasts, measured by PAM fluorometry, was about 70 % and also CLSM images revealed that chloroplasts were intact. Apparently, on the level of protons/water the envelope membrane of isolated chloroplasts was leaky, resulting in an average NMR signal of the water protons inside and outside the chloroplasts, as was also observed by Goldfeld *et al*[22].
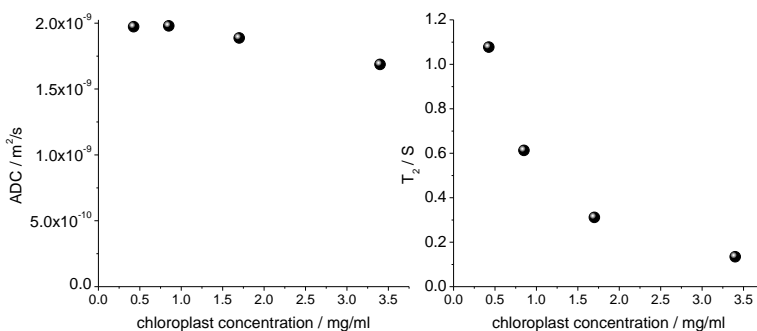
Figure 2.1: ADC and T_2 values (0.7 T[1]H DRCOSY experiments) as a function of chloroplast concentration of isolated chloroplasts suspensions of spinach leaves. A single, concentration dependent component was observed, pointing to fast exchange of water across the chloroplast envelope membrane.

2.3.2 Algae

In order to check if chloroplast water could be observed in an *in vivo* system, DRCOSY experiments were performed on an algae suspension of *Chlamydomonas reinhardtii*. *C. reinhardtii* is a unicellular microorganism containing a single chloroplast that occupies about 60 % of the total cellular volume. The cup-shaped chloroplast is ~6 μm in diameter. Since algae have a strong cell wall and are naturally growing microorganisms we expected to observe at least two water pools.^{1}H DRCOSY experiments were performed at 0.7 T for a set of diffusion-observation times ranging from 10 ms to 60 ms. A resulting D–T_2 correlation map for a diffusion observation time Δ=20 ms is shown in Fig. 2.2. Three T_2's with maxima around 90 ms, 80 ms and

15 ms and only two correlated ADCs of 2×10^{-9} m^2 s^{-1} (for T_2=90 ms) and 1.8×10^{-10} m^2 s^{-1} (for T_2=80 ms and T_2=15 ms), respectively, were observed. The signal with the longest T_2 and fastest diffusion coefficient did not show any restrictive diffusion behaviour, and was therefore assigned to medium water. The signals with shorter T_2's and slower ADCs could be either from water inside algae and/or from non-water protons.
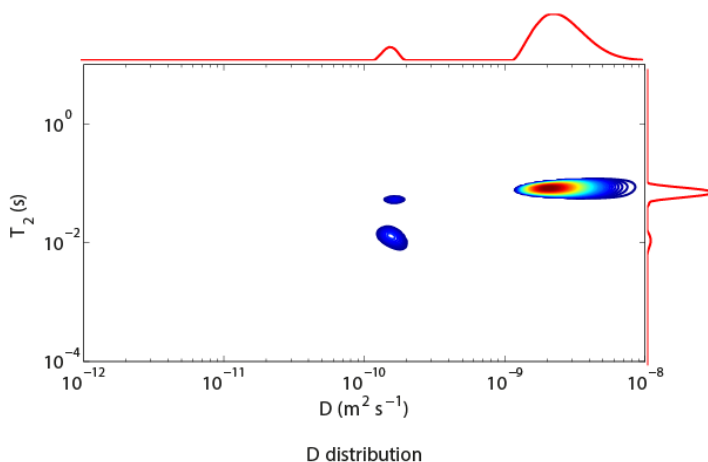

D distribution

Figure 2.2: A 0.7 T ^{1}H NMR D–T_2 correlation map of a *C. reinhardtii* suspension, Δ = 20 ms. Besides the water signal of the medium, two other signals are present.

To clarify this we performed DOSY NMR experiments at 11 T with diffusion observation times ranging from 10 ms to 60 ms. Due to the limited gradient values available at the 11 T machine (max 0.5 T/m) we were able to decompose the spectra only into two components with different associated diffusion coefficients (Diffusion Associated NMR Spectra, DANS) by coupled fitting of the attenuation of the individual spectral points for each Δ. The DANS for Δ = 20 ms (Fig. 2.3a) showed two ADCs around 2×10^{-9} m^2 s^{-1} and 1.8×10^{-10} m^2 s^{-1} at the water resonance (~4.7 ppm). This showed that both proton pools are water-bound. The signal with highest diffusion coefficient did not show any restrictive diffusion behaviour (Fig. 2.3b), and can therefore be assigned to medium water. The slower diffusing fraction showed restricted diffusion (Fig. 2.3b). From the $D(\Delta)$ curve, a compartment size of 9 μm from low-field DRCOSY and 11μm from high-field DOSY measurements was calculated, assuming a spherical compartment. These values correspond quite well to the dimension of the algae (around 10 μm), indicating that this signal is from water inside algae. The fraction of the

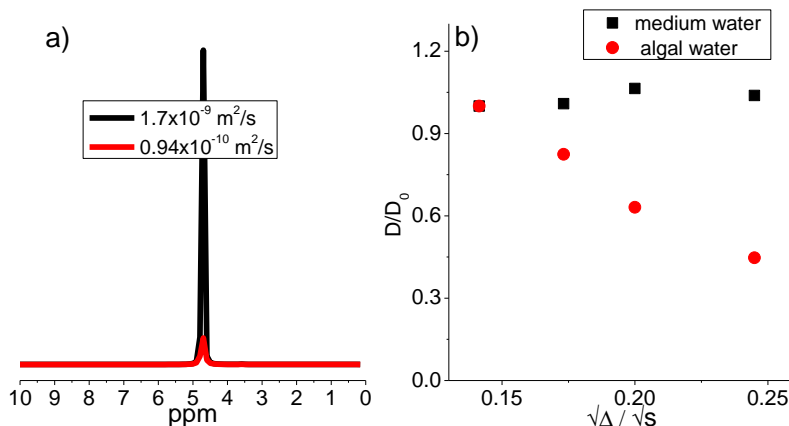water inside the algae was about 10 % of the total signal, representing the concentration of algae in the medium.

Figure 2.3: a) Diffusion associated NMR spectra (DANS) (11 T ^{1}H DOSY experiment), of a *C. reinhardtii* suspension at $\Delta = 20$ ms. Both components have a resonance at 4.7 ppm. b) Normalized diffusion behaviour of the two water signals of *C. reinhardtii* suspension as a function of the diffusion time Δ. Rectangles correspond to the largest fraction with the longest T_2 of Fig. 2.2. This fraction showed unrestricted diffusion (water in the medium). Circles correspond to the smaller fraction (about 10 %) with the shorter T_2 and clearly show restricted diffusion (water inside the algae).

In an attempt to measure the chloroplast water signal at 7 T with a high gradient diffusion probe (gradient max 10 T/m), we suppressed the signal of the medium water using a diffusion filter. For that, the first gradient step for diffusion weighting in a DOSY experiment was chosen to be 0.7 T/m and the spectra were recorded as a function of gradient to a maximum of 5.2 T/m. Again multiple proton pools, rather than one, were observed: one with a diffusion coefficient of order 3×10^{-10} m^2 s^{-1} and the other of order 4×10^{-11} m^2 s^{-1} for $\Delta=30$ ms (Fig. 2.4a). The first proton pool (component 1) had two resonances, at 4.7 ppm and 3.6 ppm. The signal at 4.7 ppm was assigned to algal water as its ADC coincides very well to the above mentioned algal water and 4.7 ppm is typical for water protons. The signal at 3.6 ppm was assigned (based on the ADC) to non-water protons (three CH$_2$ groups of Tris(hydroxymethyl)-aminomethan) in the medium which are visible also in Fig. 2.2 with T_2 80 ms and D of 1.8×10^{-10} m^2 s^{-1}. The second proton pool

(component 2) had only one resonance at 4.7 ppm and the estimated compartment size from its restricted diffusion (Fig. 2.4b) was about 6μm, indicating that this component represents chloroplast water.
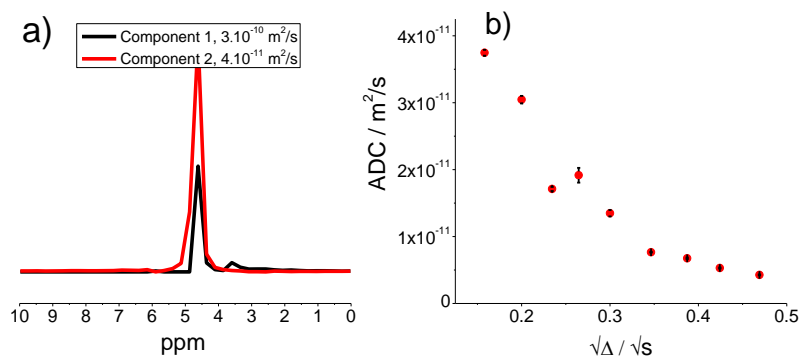

Figure 2.4: a) Diffusion-associated ^{1}H NMR spectra of *C. reinhardtii* (7 T) after suppression of the largest fractions of mobile water (water in the medium and part of the water inside the algae) by diffusion editing (first gradient step 0.7 T/m) : δ=2 ms, Δ=30 ms and *g*: 0.7-5.2 T/m. Now two components were observed. b) ADC as a function of Δ for the slower diffusing component. Clear restricted diffusion was observed. Based on this dependence a radius of 4.6 μm was calculated, which is about the dimension of the chloroplasts inside *C. reinhardtii*.

2.3.3 Leaves

Leaves of specific plants show orientation-dependent NMR and EPR spectra[8]. Fig. 2.5a shows ^{1}H NMR spectra (7 T) of *F. benjamina* leaves and 5b of *A. platanoides* leaves. Both leaves showed orientation dependency of the ^{1}H NMR spectra. In order to check susceptibility effects on the spectra resulting from air spaces in the leaves, they were treated by perfluorodecalin – a substance used to fill air spaces in the leaf[23]. The leaf disks were treated by perfluorodecalin in two ways. First, leaf disks were dipped in perfluorodecalin for 10 mins and then the leaf disks were shifted to NMR tube to measure the spectrum. Second, leaf disks were dipped in perfluorodecalin that is in NMR tube and then the spectrum was measured. The spectra of perfluorodecalin-treated leaves were identical to those of untreated leaves (data not shown), indicating that susceptibility effects due to air pockets on the shape of the spectra were negligible.
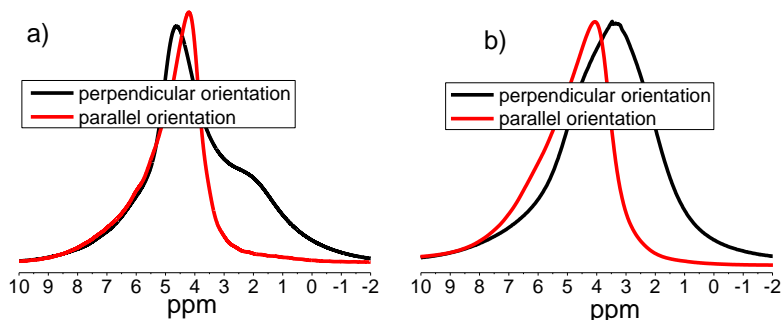
Figure 2.5: 7 T ^{1}H NMR spectra of oriented a) *F. benjamina* and b) *A. Platanoides* leaf disks (leaf surface is perpendicular to B_0 (black) and parallel to B_0 (red)).

To further unravel the NMR spectra of leaves and to test if the peaks shifted with respect to the water resonance (4.7 ppm) originate from chloroplast water, we performed ^{1}H DOSY experiments at 7 T. For both leaf species, we studied both parallel and perpendicular orientations for diffusion observation times ranging from 12 to 290 ms and *g* values between 0.05 and 8.5 T/m. Fig. 2.6 shows diffusion-attenuated spectra of *A. platanoides* leaves for Δ = 25 ms oriented parallel (a) and perpendicular (b) to B_0.

The diffusion attenuated ^{1}H NMR spectra were analysed by fitting the diffusion attenuation curve with a discrete sum of (attenuation) exponentials with different (apparent) diffusion coefficients, resulting in DANS. A four-component fit was found to be the best for Δ = 25 ms for both leaf species, because the sum of residuals did not significantly decrease by adding a fifth component. The results for *A. platanoides* leaves oriented both parallel and perpendicular to B_0 at Δ = 25ms are shown in Fig. 2.6c and d, respectively. The results clearly reveal that the different diffusion components have different spectral characteristics. The spectra of almost all components contained resonances shifted from the water resonance (4.7 ppm). The shifts were dependent on the orientation, except for component 4. The fastest-diffusing protons (representing the largest fraction) showed resonances close to the water position (4.7 ppm), slower diffusing protons from 10 ppm to 1 ppm with maxima at 4.9 ppm for the parallel orientation and at 2.6 ppm for the perpendicular orientation and the slowest components from 10 ppm to -2 ppm, with maxima at 4.7 ppm for the parallel orientation and 2.3 ppm and 3.3 ppm for components 3 and 4, respectively,
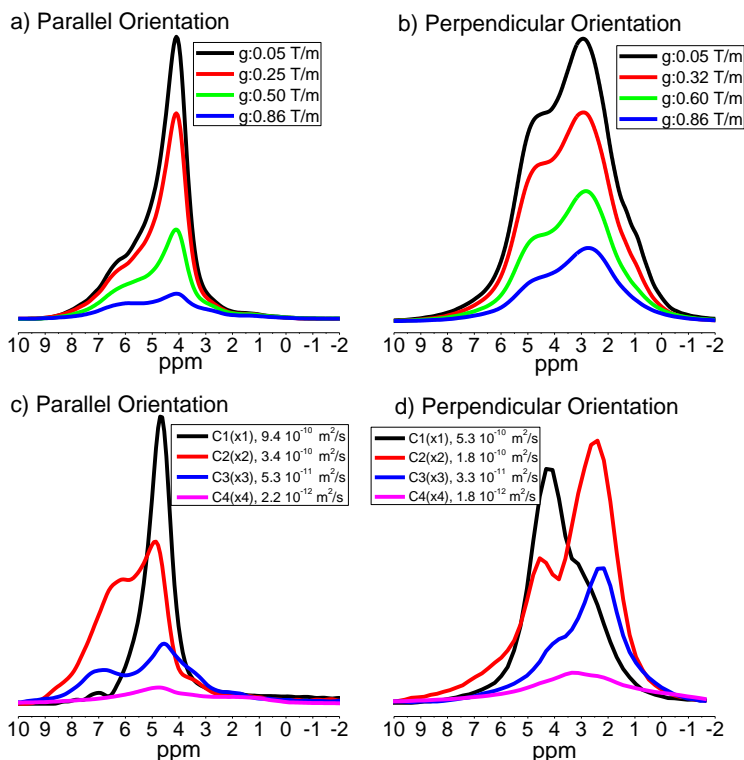
Figure 2.6: Diffusion-attenuated ^{1}H NMR spectra of *A. platanoides* leaf disks at $\Delta=25$ ms a) oriented parallel to B$_0$ and b) perpendicular to B$_0$ (g = 0.05 up to 8.5 T m^{-1}) and their corresponding Diffusion-associated ^{1}H NMR spectra c) *parallel* orientation and d) *perpendicular* orientation. Note the different scaling factors for the different components in c and d.

for the perpendicular orientation. For components 2 and 3, most of the signal appeared at lower ppm values for the perpendicular orientation whereas they appeared at higher ppm for the parallel orientation. In Fig. 2.7a, the Δ dependencies of the spectra of the four components for *A. platanoides* leaf disks in perpendicular orientation are presented. A four-component fit was found to be the best because the sum of residuals did not significantly decrease by adding a fifth component for all the diffusion-observation times. The spectral shapes of each of the four components at the different Δ values were very stable; only the amplitudes decreased with increasing Δ. The rate of the decrease increased going from component 1 to 4, and is most probably only related to relaxation behaviour of the different

25

components. The behaviour of the ADCs of these components as a function of Δ (Fig. 2.7b) revealed that all components showed restricted diffusion behaviour and the estimated dimensions were as follows: 15 µm for component 1, 9 µm for component 2 and 3.6 µm for component 3.
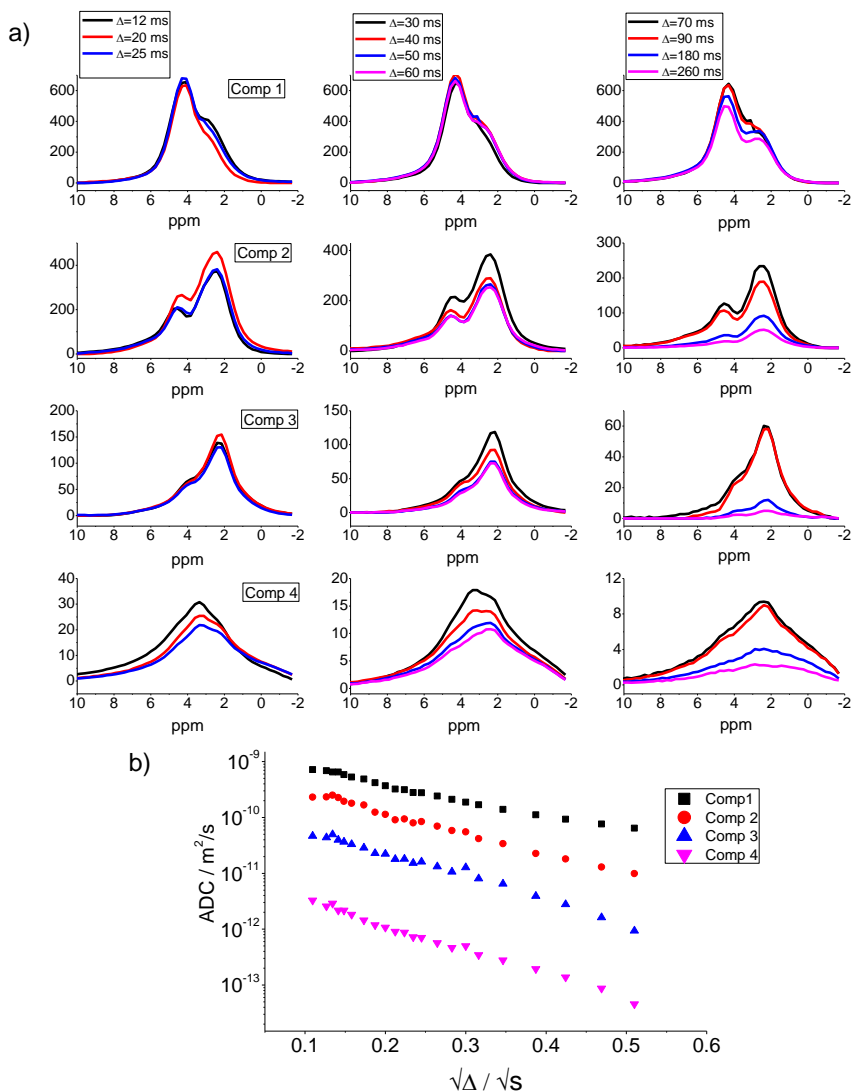

Figure 2.7: Diffusion time dependency (see columns) of diffusion-associated ^{1}H NMR spectra of components 1-4 (rows) (a) and of ADC's (b) from *A. platanoides* leaf disks oriented perpendicular to B$_0$.

In Fig. 2.8 the Δ dependency of the spectra of the components (a) and of the related ADCs (b) for *F. benjamina* leaf disks in perpendicular orientation are presented. A four component fit was found to be optimal (based on residuals) from 12 ms – 25 ms (first column Fig. 2.8a), three component fit from 30 ms – 60 ms(second column Fig. 2.8a) and two component fit from 65 ms – 290 ms (third column Fig. 2.8a).
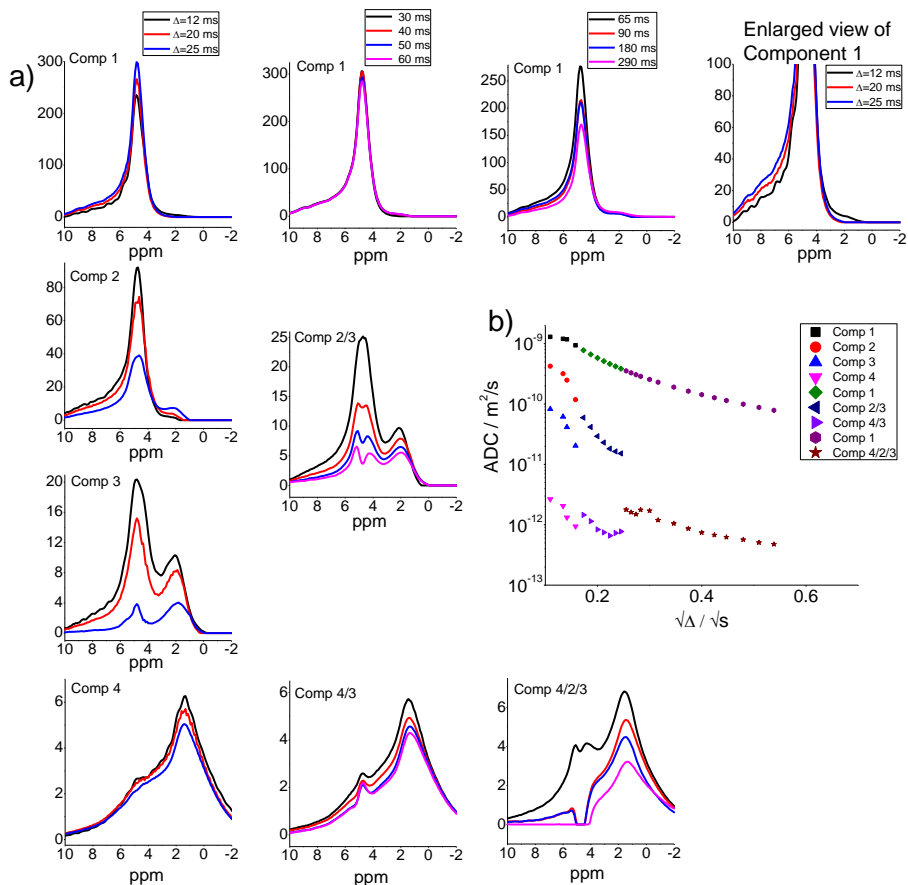

Figure 2.8: Diffusion time dependency (columns) of diffusion-associated ^{1}H NMR spectra for the different components (rows) (a) and the related ADCs (b) of *F. benjamina* leaf disks oriented perpendicular to B_0.

Striking changes in amplitudes were observed with increasing Δ's up to around 40 ms. We summarize the changes in the amplitudes for three resonances: 7, 4.7 and 2 ppm, respectively, component 1: +10, +63, -4;

component 2: -10, -53, +6; component 3: -4, -16, -6. These changes in the amplitudes cannot be explained by relaxation effects alone, and suggest exchange between the components 1, 2 and 3. Moreover, the decrease in the amplitude of the two peaks of component 3 showed different Δ dependency although they have the same ADC, which might indicate that the spectrum of component 3 does present different proton pools with different T_1 and/or different exchange behaviour. The behaviour of the ADCs as a function of Δ is presented in Fig. 2.8b. Based on this figure we conclude that component 2 and 3 merge to a single one and later that component merges with component 4. Although component 1 takes part of the intensity of components 2 and 3 the ADC behaviour is hardly affected, most probably because the increase in amplitude is relatively small compared to its original amplitude.

To test if there was exchange between the components, a saturation transfer experiment on *F. benjamina* leaves was performed[21]. From the plot of saturation intensity vs. recovery time, a rise of the downfield peak was observed because of saturation transfer from the upfield peak (data not shown), which clearly indicated exchange between upfield and downfield signal. The downfield peak rose until a recovery time of 100 ms, about 1.5 times larger than observed in *Liriodendron tulipifera* (tulip tree) leaves[21]. The maximum was observed around 30-50 ms.

Low field (0.7 T) T_2 experiments were performed on *F. benjamina* leaves to investigate whether the chloroplast water signal can be observed separately. Multi-exponential signal decay was observed. Analysis by SplMod resulted in four components and also CONTIN analysis showed a T_2 distribution with four peaks (Fig. 2.9a). The observed T_2 distributions for *F. benjamina* are comparable to those observed in *Brassica napus* leaves[10]. To measure T_2 values of the diffusion associated spectra (DANS), T_2-weighted spectra were measured for *F. benjamina* leaf disks at 7 T. The two-dimensional data set (spectra as a function of echo time) was fitted by a discrete number of components to obtain T_2-associated NMR spectra (Fig. 2.9b). A four-component fit was found to be optimal (based on the residuals). The two shorter T_2 values (5 and 31 ms) are similar to the low-field results and the two longer T_2 values (88 and 260 ms) are shorter than the ones from low field (190 and 750 ms). Different leaves have been used.
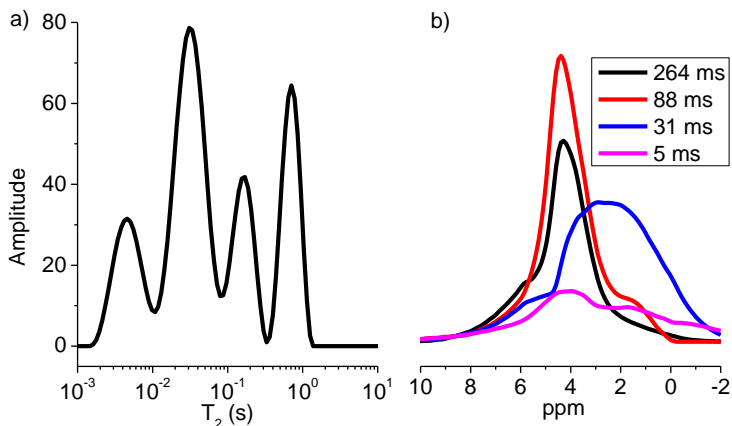
Figure 2.9: T_2 distribution of *F. benjamina* leaf disks, measured at field strength of 0.7 T (a) and T_2 associated ^{1}H NMR spectra of perpendicularly oriented *F. benjamina* leaf disks, measured at field strength of 7 T. The corresponding T_2 values of the spectra are presented in the legend (b).

2.4 Discussion

Diffusion NMR helps to focus on specific signals of interest by spectral editing. This was achieved by choosing proper diffusion attenuation windows. In the *Chlamydomonas reinhardtii* algae suspensions, we used a diffusion filter to suppress the water signal of the medium (component 1). This way, the less abundant slow(er) diffusing components for instance algal water (component 2) can be resolved. A third signal was observed in both 0.7 T DRCOSY (ADC$\cong$2×10^{-10} m^2 s^{-1} and T_2=80 ms for Δ=20 ms, Fig. 2.2) and 7 T DOSY experiments (ADC$\cong$3×10^{-10} m^2 s^{-1} for Δ=30 ms and had a resonance at 3.6 ppm, Fig. 2.4a) but not in 11 T DOSY experiments (Fig. 2.3a) because of different levels of attenuation. The parameters were optimized for detecting chloroplast water signal. In general the choice of the attenuation parameter settings (gradient range, Δ and the number of gradient steps) in combination with the differences in ADCs, volume fractions of the components and size of the compartments, will influence the results and will determine which and how much components can be discriminated. So, they have to be selected with care. One should also be aware that non-water components with large molecular weight will have a smaller ADC, even if present in the medium and without any restricted diffusion behaviour. That explains why the signal of the medium water was

already suppressed and still we could observe the 3.6 ppm signal from the TRIS buffer (third component in Fig. 2.2).

Intact leaves

For *A. platanoides* leaf disks oriented perpendicular to B_0, four components were observed at all diffusion times (Fig. 2.7). This leaf consists of upper and lower epidermis cells, palisade mesophyll cells and spongy mesophyll cells all containing chloroplasts. Table 1 shows summary of the water fractions, calculated D_0's and estimated sizes of all the compartments for both leaf disks in both orientations. Actual water fractions depend on history of the plant such as well watered or water stressed and position of the leaf on the plant. The size of the compartment to which this component 1 belongs, as estimated from restricted diffusion behaviour, was ~15 μm. Therefore, we assigned component 1 to vacuolar water of palisade cells, since in this orientation the palisade cells were oriented with their longest axis (which is about 20-25 μm)[24] in the gradient direction. Possibly, a small part of the spongy cells contribute to this component as well, because spongy cells are curved-cylindrical and oriented in different directions.

The size of the compartment associated with component 2 as estimated from its restricted diffusion behaviour was ~9μm. This is the dimension we expect for spongy cells and epidermal cells (in the direction perpendicular to the leaf surface)[24]. Therefore, component 2 was assigned to vacuole water of spongy cells plus epidermal cell water. Size estimated from hindered diffusion behaviour of component 3 was 3.6μm. Its fraction was 12 % (actual fraction can be larger if T_2 weighting was reduced) at Δ=12ms. This dimension is of the order of the chloroplast compartment size. Also, the D_0 of the component is in the order of the D_0 of chloroplast water detected in *C. reinhardtii*. Therefore, component 3 was assigned to chloroplast water.

The D_0 of component 4 was 5.3×10^{-12} m^2/s and diffusion time dependency of this component showed hindered behaviour. This diffusion coefficient is in the order of that of lipids in membranes[25]. The spectrum of this component was independent of the orientation of the leaf disks with respect to the main magnetic field. Galactolipids are the main structural components of chloroplast envelope membranes and thylakoid membranes, and the predominant lipids in this class are monogalactosyl-diacylglycerol (MGDG) and digalactosyl-diacylglycerol (DGDG), which have resonances at 4.0 ppm, 4.2 ppm, 4.4 ppm, 4.6 ppm and 4.8 ppm[26,27]. Lipid terminal methyl groups

Table 1: Summary of the water fractions, calculated D_0's and estimated sizes of all the compartments for both leaf disks in both orientations.

Type of leaf disks	Component	Perpendicular orientation	Parallel orientation
F. benjamina	1	Vacuoles of palisade and subepidermal cells (21 µm, 59 %) $D_0=2.1\times10^{-9}$ m^2/s	Subepidermal cells (19.3 µm, 20 %) $D_0=2.3\times10^{-9}$ m^2/s
	2	Vacuoles of spongy cells and epidermal cells (8.7 µm, 30 %) $D_0=1.1\times10^{-9}$ m^2/s	Vacuoles of palisade, spongy and epidermal cells (9 µm, 66 %) $D_0=1.4\times10^{-9}$ m^2/s
	3	Chloroplast (3.8 µm, 11 %) $D_0=2.2\times10^{-10}$ m^2/s	Chloroplast (4 µm, 14 %) $D_0=2.2\times10^{-10}$ m^2/s
A. platanoides	1	Vacuoles of palisade and (part of the) spongy cells (15 µm, 54 %) $D_0=1.1\times10^{-9}$ m^2/s	Epidermal and (part of the) vacuoles of spongy cells (18.6 µm, 60.5 %) $D_0=1.8\times10^{-9}$ m^2/s
	2	Vacuoles of (part of the) spongy and epidermal cells (9 µm, 34 %) $D_0=5.1\times10^{-10}$ m^2/s	Vacuoles of palisade and (part of the) spongy cells (11 µm, 25 %) $D_0=8.8\times10^{-10}$ m^2/s
	3	Chloroplast (3.6 µm, 12 %) $D_0=0.8\times10^{-10}$ m^2/s	Chloroplast (5 µm, 14.5 %) $D_0=1.7\times10^{-10}$ m^2/s

and choline groups have resonances at 0.8 ppm and 1.3 ppm. So, component 4 most probably originates from membrane lipids. Better resolved resonances of membrane lipids have been observed in *C. reinhardtii* suspensions under conditions of heavy diffusion filtering (chapter 4).

For *F. benjamina* leaf disks oriented perpendicular to B_0, the number of components decreased with increasing diffusion times (Fig. 2.8) because of exchange between the components 1, 2 and 3. Component 1 was present for diffusion times from 12 ms to 290 ms. The size estimated from restricted diffusion behaviour was around 21μm with 60 % of the intensity at shortest diffusion time. The spectrum of this component was similar to the spectrum of T_2-component 1 in Fig. 2.9b (T_2 = 260 ms). *F. benjamina* leaves have bigger epidermal cells as compared to *A. platanoides* leaves and in addition to the epidermal cells *F. benjamina* leaves also have quite large subepidermal cells[24,28,29], located in between the upper epidermis and the palisade cells. In *F. benjamina* leaf epidermal cells are approximately 10-20μm and subepidermal cells 20-50μm large, the length of the palisade cells in the direction perpendicular to the leaf surface (which was the gradient direction for diffusion measurements) is in the same order. Therefore, component 1 was assigned to vacuole water of palisade cells and also to subepidermal cell water.

The size estimated from hindered diffusion behaviour of component 2 was around 8.7μm. The spectrum of this component was similar to the T_2 spectrum of component 2 in Fig. 2.9b (T_2 = 88 ms). The total fraction of components 1 and 2 together was about 63 % for the T_2 measurements. Therefore, component 2 was assigned to vacuole water of spongy cells and also to epidermal cell water. These two longest T_2 values (88 ms and 260 ms) obtained from high-field measurements were shorter than those (190 ms and 750 ms) obtained from low-field measurements. These differences between high and low field T_2 values can originate from the contribution of chemical exchange between protons with different resonant frequencies and from susceptibility effects due to the presence of chloroplasts, resulting in shifted resonances which create local magnetic field gradient (which are stronger at higher field strengths) and diffusion through these local field gradients contribute to shorten T_2. In addition, T_2 of vacuolar water depends on leaf development (age) and senescence[10].

The size estimated from hindered diffusion behaviour of component 3 was around 3.8μm. This size is in the order of the chloroplast compartment size.

T_2 of the component was around 31 ms (component 3 from T_2 measurements). This T_2 value is in agreement with the T_2 value reported for chloroplast water in *Brassica napus* L. leaves (Musse *et al.*, 2013)[10]. These T_2 and D_0 values are also in good agreement to those observed for chloroplast water in *C. reinhardtii*. Therefore, the component was assigned to chloroplast water.

In Fig. 2.8a, total amplitude decreased by an amount 3 % from Δ 12 ms to 25 ms most probably due to (T_1) relaxation. At the same time striking changes in amplitudes were observed for the individual components. Component 1: +10, +63, -4; component 2: -10, -53, +6; component 3: -4, -16, -6 (at 7, 4.7 and 2 ppm, respectively). This indicates exchange among various compartments. The saturation transfer experiment confirmed this view, but form the diffusion associated spectra we observed by far more details. The effect of exchange is always an increase in amplitude of the component with the longest relaxation time (and highest diffusion coefficient)[30]. Chloroplasts in palisade and spongy cells (component 3) can exchange water with vacuoles in palisade (part of component 1) and spongy cells (component 2), respectively, explaining the fast decrease in amplitude of component 3 and the increase in component 1. Although part of component 3 (chloroplast water) will go to component 2 (spongy cells), exchange between subepidermal cells (part of component 1) and epidermal cells (part of component 2) results in a net decrease of component 2.

This assignment is further supported by comparing the results of the measurements in different orientations of the leaves. These results are summarized in Table 1. Subepidermal cells (part of component 1) are about spherical and therefore the dimension based on restricted diffusion measurements will be independent of the orientation. Palisade cells have cylindrical shapes and are oriented perpendicular to the leaf surface, making diffusion to be dependent on orientation with respect to the gradient direction. When the diffusion was measured parallel to *F. benjamina* leaf surface component 1 had only about 20 % of the intensity whereas component 2 had about 66 % and component 3 had about 14 % at Δ 12 ms. Estimated sizes of the compartments in this orientation were 19.3μm for component 1, 9μm for component 2 and 4μm for component 3. In this orientation only the sub-epidermal cells have a large dimension, and the palisade cells have a comparable size as the spongy cells. Thus component 1 now originates only from subepidermal cells, component 2 had

contributions from vacuoles of both palisade and spongy cells and also from epidermal cells and component 3 represents chloroplast water.

When the diffusion was measured parallel to *A. platanoides* leaf surface intensities amounted as follows: 60.5 % for component 1, 25 % for component 2 and 14.5 % for component 3. The intensities of individual components did not change substantially for *A. platanoides* leaf disks in contrast to *F. Benjamina* leaf disks because of different anatomy. *A. platanoides* leaves do not have subepidermal cells. Moreover epidermal cells of *A. platanoides* leaves are not spherical and they are quite long in the parallel direction. Thus, epidermal cells contribute to component 1 in parallel orientation ($\approx$18.6μm) and to component 2 in perpendicular orientation (9μm). Also, spongy cells can contribute with the long dimension to components 1 and 2 in both orientations as they are not spherical, but curved cylindrical in different directions. The palisade cells will contribute to component 1 in perpendicular orientation and to component 2 in the parallel orientation. In all orientations component 3 is about constant and the observed dimension are in agreement with the expected chloroplast dimension.

The D_0 of component 4 was 6.7×10^{-12} m^2/s and the component showed restricted diffusion. T_2 of the component was around 5 ms. T_2 of membrane lipids is indeed in the order of 5 ms[31,32].

2.5 Conclusions

Suspensions of isolated chloroplasts showed fast exchange, most probably introduced by the isolation procedure, between chloroplast water and the medium water. In contrast, in suspensions with intact *C. reinhardtii* three water pools could be resolved: water in the medium, water inside the algae and water inside the chloroplasts. The size of the algae and their chloroplasts could be estimated from restricted diffusion of the algal water and the chloroplast water.

In leaves of *F. benjamina* and *A. platanoides* that show orientation dependent NMR spectra, detection of chloroplast water on the basis of shifted resonances as suggested by McCain *et al*[8] is problematic. In addition to chloroplast water, water in other compartments like vacuoles of palisade and spongy cells contain resonances shifted from the standard 4.7 ppm water resonance. In addition, chloroplast water contains a contribution at 4.7 ppm in both *F. benjamina* and *A. platanoides* leaves.

However, on the basis of diffusion behaviour, in combination with spectroscopic or relaxation time information, different cell water compartments can be discriminated and identified. Chloroplast water was observed to have a T_2 of about 30 ms (high field measurements) and around 20-40 ms from TD NMR measurements at low field and a D_0 in the order of 2.2×10^{-10} m^2/s. The observed T_2 value is in agreement with the one reported by Musse *et al*[10]. Based on these T_2 and ADC values we can discriminate chloroplast water even if the spectrum does not contain a shifted peak with respect to the normal water resonance. So, discrimination of chloroplast water based on T_2 is possible, although exchange can affect the apparent T_2 values. Exchange effects can be minimised by applying diffusion measurements with short diffusion times. We conclude that combined (two-dimensional) D-T_2 (DRCOSY) measurement is the best approach to discriminate chloroplast water pool from others. In this way we can potentially study chloroplast water in intact leaves using (low field) (unilateral) TD NMR. It is also possible to study effects of environmental factors such as water or light on chloroplasts using T_2 and restricted diffusion of chloroplast water.

In leaves, membrane lipids were observed in addition to chloroplast water. To the best of our knowledge, no other lipid diffusion measurements in intact leaf systems have been reported. T_2 of the membrane lipids is on the order of 5 ms, their apparent diffusion coefficient is 2.7×10^{-12} m^2/s at Δ=12 ms and 5×10^{-13} m^2/s at Δ=290 ms. Hindered diffusion of the lipids was also observed. It would be possible to probe changes in membrane dynamics under changing environmental conditions using the hindered diffusion of membrane lipids.

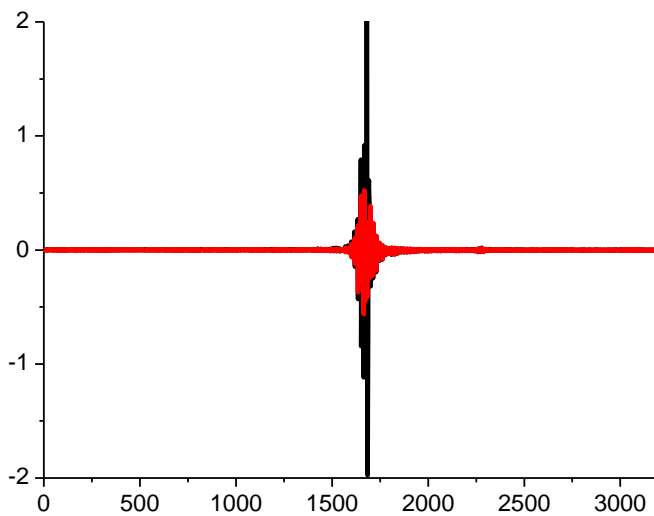**Supporting information**

Supporting information is included below: **S2.1.** Residual plot (1-component fit (black) and 2-component fit (red)), of DANS (11 T ^{1}H DOSY experiment), of a *C. reinhardtii* suspension at Δ = 20 ms. **S2.2.** Residual plot (2 (black), 3 (red), 4 (blue) and 5 (magenta) component fits), of *C. reinhardtii* (7 T) after suppression of the largest fractions of mobile water (water in the medium and part of the water inside the algae) by diffusion editing (first gradient step 0.7 T/m): δ=2 ms, Δ=30 ms and *g*: 0.7-5.2 T/m. **S2.3.** Residual plots (3 (black), 4 (red) and 5 (blue) component fits) of DANS (for various diffusion observation times) of *A. platanoides* leaf disks oriented perpendicular to B$_0$. **S2.4.** Residual plots (labels of each subplot show the number of components) of DANS (for various diffusion observation times) of *F.*

benjamina leaf disks oriented perpendicular to B_0. It is clear from the plots that number of components decrease with increasing diffusion observation time. **S2.5.** Residual plot (3 (black), 4 (red) and 5 (blue) component fits) of T_2 associated ^{1}H NMR spectra of perpendicularly oriented *F. benjamina* leaf disks, measured at field strength of 7 T.

Acknowledgements

Figure S2.1: Residual plot (1-component fit (black) and 2-component fit (red)), of DANS (11 T ^{1}H DOSY experiment), of a *C. reinhardtii* suspension at Δ = 20 ms, clearly indicates that 2-component fit is better.
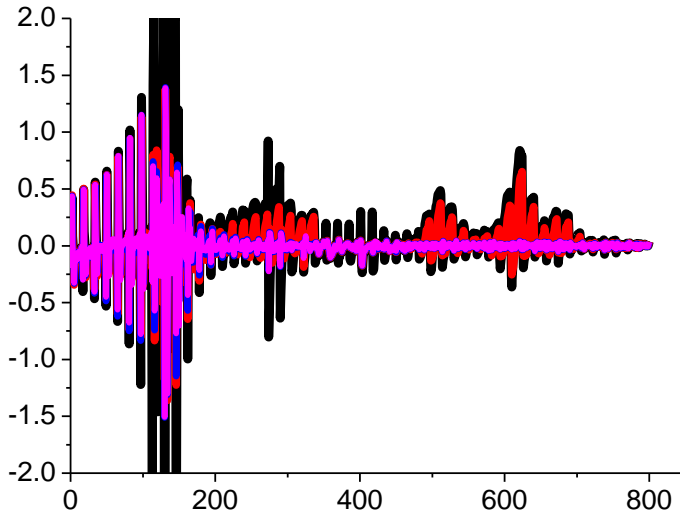
Figure S2.2: Residual plot (2 (black), 3 (red), 4 (blue) and 5 (magenta) component fits), of *C. reinhardtii* (7 T) after suppression of the largest fractions of mobile water (water in the medium and part of the water inside the algae) by diffusion editing (first gradient step 0.7 T/m): δ=2 ms, Δ=30 ms and *g*: 0.7-5.2 T/m. In addition to the water signals (algal and chloroplast) lipid bodies and membrane lipids were also observed here.
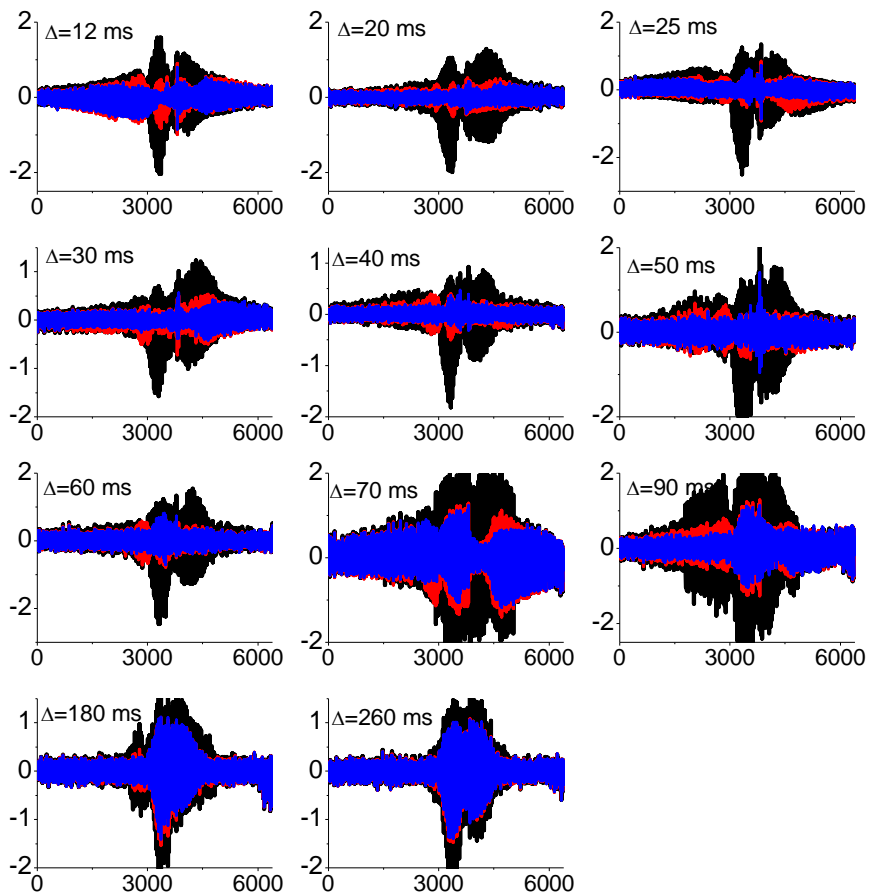
Figure S2.3: Residual plots (3 (black), 4 (red) and 5 (blue) component fits) of DANS (for various diffusion observation times) of *A. platanoides* leaf disks oriented perpendicular to B_0. It is clear from the plots that 4-component fit is better for all the observed diffusion times.
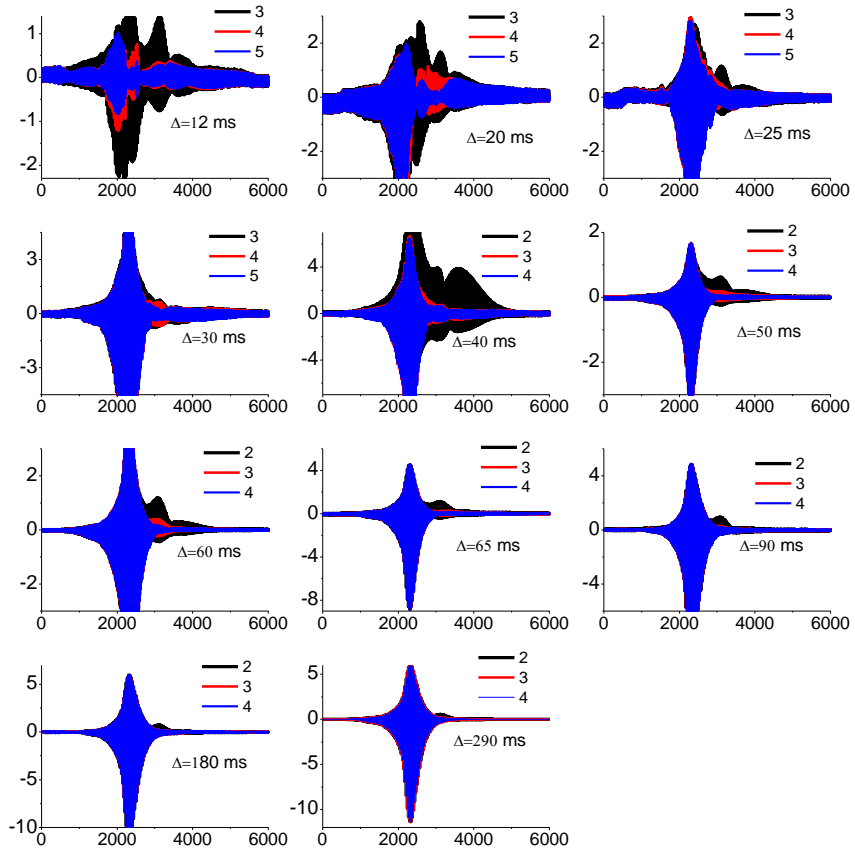
Figure S2.4: Residual plots (labels of each subplot show the number of components) of DANS (for various diffusion observation times) of *F. benjamina* leaf disks oriented perpendicular to B_0. It is clear from the plots that number of components decrease with increasing diffusion observation time.
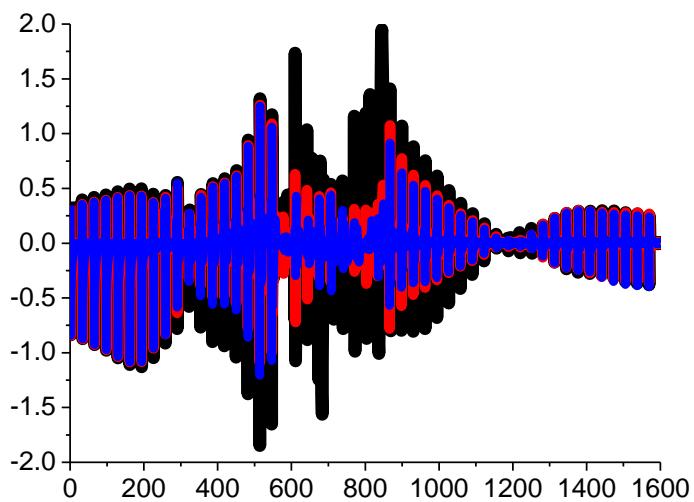
Figure S2.5: Residual plot (3 (black), 4 (red) and 5 (blue) component fits) of T_2 associated ^{1}H NMR spectra of perpendicularly oriented *F. benjamina* leaf disks, measured at field strength of 7 T. It is clear from the plot that 4-component fit is better.

References

1) Croce, R. and H. van Amerongen. (2014). Natural strategies for photosynthetic light harvesting. *Nature Chemical Biology* **10**(7): 492-501.

2) Robinson, S. P. (1985). Osmotic adjustment by intact isolated chloroplasts in response to osmotic stress and its effect on photosynthesis and chloroplast volume. *Plant Physiology* **79**(4): 996-1002.

3) Gupta, A. S. and Berkowitz, G. A. (1988). Chloroplast osmotic adjustment and water stress effects on photosynthesis. *Plant Physiology* **88**(1): 200-206.

4) Santakumari, M. and Berkowitz, G. A. (1991). Chloroplast volume: cell water potential relationships and acclimation of photosynthesis to leaf water deficits. *Photosynthesis Research* **28**(1): 9-20.

5) McCain, D. C. (1995). Combined effects of light and water stress on chloroplast volume regulation. *Biophysical Journal* **69**(3): 1105.

6) McCain, D. C. and Markley, J. (1992). In vivo study of chloroplast volume regulation. *Biophysical Journal* **61**: 1207-1212.

7) Veley, K. M., Marshburn, S., Clure, C. E., and Haswell, E. S. (2012). Mechanosensitive channels protect plastids from hypoosmotic stress during normal plant growth. *Current Biology* **22**(5): 408-413.

8) McCain, D. C., Selig, T. C., and Markley, J. L. (1984). Some plant leaves have orientation-dependent EPR and NMR spectra. *Proceedings of the National Academy of Sciences* **81**: 748-752.

9) McCain, D. C. and Markley, J. L. (1985). A theory and a model for interpreting the proton nuclear magnetic resonance spectra of water in plant leaves. *Biophysical Journal* **48**(5): 687.

10) Musse, M., De Franceschi, L., Cambert, M., Sorin, C., Le Caherec, F., Burel, A., and Leport, L. (2013). Structural changes in senescing oilseed rape leaves at tissue and subcellular levels monitored by Nuclear Magnetic Resonance Relaxometry through water status. *Plant Physiology* **163**: 392-406.

11) Van As, H. (2007). Intact plant MRI for the study of cell water relations, membrane permeability, cell-to-cell and long distance water transport. *Journal of Experimental Botany* **58**(4): 743-756.

12) Qiao, Y., Galvosas, P., and Callaghan, P. T. (2005). Diffusion correlation NMR spectroscopic study of anisotropic diffusion of water in plant tissues. *Biophysical Journal* **89**: 2899-2905.

13) Johnson Jr, C. S. (1999). Diffusion ordered nuclear magnetic resonance spectroscopy: principles and applications. *Progress in Nuclear Magnetic Resonance Spectroscopy* **34**: 203-256.

14) Rödiger, A., Baudisch, B., and Klösgen, R. B. (2010). Simultaneous isolation of intact mitochondria and chloroplasts from a single pulping of plant tissue. *Journal of Plant Physiology* **167**(8): 620-624.

15) Gorman, D. S. and Levine, R. P. (1965). Cytochrome f and plastocyanin: Their sequence in the photosynthetic electron transport chain of *Chlamydomonas reinhardtii*. *Proceedings of National Academy of Sciences* USA **54**: 1665-1669.

16) Provencher, S. W. (1979). Inverse problems in polymer characterization: direct analysis of polydispersity with photon correlation spectroscopy. *Die Makromolekulare Chemie* **180**(1): 201-209.

17) Stejskal, E. O. and Tanner, J. E. (1965). Spin diffusion measurements: spin echoes in the presence of a time-dependent field gradient. *Journal of Chemical Physics* **42**:288–292.

18) Antalek, B. (2002). Using Pulsed Gradient Spin Echo NMR for chemical mixture analysis: How to obtain optimum results. *Concepts in Magnetic Resonance***14**: 225-258.

19) Provencher, S. W. (1982). A constrained regularization method for inverting data represented by linear algebraic or integral equations. *Computer Physics Communications* **27**(3): 213-227.

20) Mitra, P. P., Sen, P. N., Schwartz, L. M., and Le Doussal, P. (1992). Diffusion propagator as a probe of the structure of porous media. *Physical Review Letters* **68**(24): 3555.

21) McCain, D. C. and Markley, J. L. (1985). Water permeability of chloroplast envelope membranes: in vivo measurement by saturation-transfer NMR. *FEBS Letters* **183**: 353-358.

22) Gol'dfel'd MG, Vozvyshaeva, LV. and Iushmanov, VE. (1979). Magnetic relaxation of water protons and the state of the water photodissociation system in chloroplasts. *Biofizika* **24**: 264.

23) Littlejohn, G. R., Gouveia, J. D., Edner, C., Smirnoff, N., and Love, J. (2010). Perfluorodecalin enhances in vivo confocal microscopy resolution of Arabidopsis thaliana mesophyll. *New Phytologist* **186**(4): 1018-1025.

24) Dineva, S. B. (2006). Development of the leaf blades of *Acer platanoides* in industrially contaminated environment. *Dendrobiology* **55**: 25-32.

25) Kana, R. (2013). Mobility of photosynthetic proteins. *Photosynthesis Research* **116**(2-3): 465-479.

26) Jouhet, J., Maréchal, E., Baldan, B., Bligny, R., Joyard, J., and Block, M. A. (2004). Phosphate deprivation induces transfer of DGDG galactolipid from chloroplast to mitochondria. *The Journal of Cell Biology* **167**: 863-874.

27) Nuzzo, G., Gallo, C., d'Ippolito, G., Cutignano, A., Sardo, A., and Fontana, A. (2013). Composition and quantitation of microalgal lipids by ERETIC 1H NMR method. *Marine Drugs* **11**: 3742-3753.

28) Labunskaya, E. A., Zhigalova, T. V., and Choob, V. V. (2007). Leaf anatomy of the mosaic *Ficus benjamina* cv. Starlight and interaction of source and sink chimera components. *Russian Journal of Developmental Biology* **38**(6): 397-405.

29) McCain, D. C., Croxdale, J., and Markley, J. L. (1993). The spatial distribution of chloroplast water in *Acer platanoides* sun and shade leaves. *Plant, Cell & Environment* **16**(6): 727-733.

30) Van der Weerd, L., Melnikov, S. M., Vergeldt, F. J., Novikov, E. G., and Van As, H. (2002). Modelling of self-diffusion and relaxation time NMR in multicompartment systems with cylindrical geometry. *Journal of Magnetic Resonance* **156**(2): 213-221.

31) Wang, T., Cady, S. D., and Hong, M. (2012). NMR determination of protein partitioning into membrane domains with different curvatures and application to the influenza M2 peptide. *Biophysical Journal* **102**(4): 787-794.

32) Deese, A. J., Dratz, E. A., Hymel, L., and Fleischer, S. I. D. N. E. Y. (1982). Proton NMR T1, T2, and T1 rho relaxation studies of native and reconstituted sarcoplasmic reticulum and phospholipid vesicles. *Biophysical Journal* **37**(1): 207-216.

3

The effect of dehydration on leaf cellular compartments in relation to the water buffering role of subepidermal cells studied by ^{1}H DOSY

Abstract

We studied the effects of dehydration (from moderate to severe) on the distribution of water in different cellular compartments in leaf disks of *F. benjamina* and *A. platanoides* using ^{1}H DOSY NMR. These leaves differ with respect to subepidermal cells which are present only in *F. benjamina*. Such cells may act as a water storage, buffer pool during drought. We clearly showed the effect of this storage pool on the dehydration behaviour of the other tissues in the leaves and cell compartments therein. This pool prevented the fast loss of water from the chloroplasts.

PSII efficiency was measured by PAM and correlated to the changes in chloroplast water volume observed in both leaves. In case of moderate dehydration the PSII efficiency of the *A. platanoides* leaf disks was very comparable to that of *F. benjamina* leaf disks, although the amount of water in the chloroplasts relative to the amount of chloroplast water in the fresh leaf disks of *F. benjamina* and *A. platanoides* was quite different. In case of severe dehydration, although both leaf disks lost same amount of their initial water, their PS II efficiencies were quite different because of the difference in the amount of water in chloroplasts relative to fresh leaf disks. This indicates a (non-linear) correlation between PSII efficiency and chloroplast water content.

3.1 Introduction

Drought impacts on plants include growth, yield, membrane permeability and integrity, pigment content, osmotic adjustment, water potential and water pools and photosynthetic activity[1,2,3]. Schapendonk *et al.* studied water stress on photosynthesis in five potato cultivars using chlorophyll fluorescence and gas exchange measurements[4]. They concluded that water stress reduced photosynthesis, initially as a consequence of stomatal closure, but after 3 days increasingly by inhibiting directly the photosynthetic capacity (mesophyll limitation). Stomatal closure correlated with the reduction in photosynthesis, but it was not the sole cause of this reduction because the internal CO_2 concentration in the leaves was not affected by the water stress[4]. Under conditions of drought, reduction in chloroplast volume might also lead to desiccation within the chloroplast, which in turn leads to conformational changes in rubisco[5]. Drought stress conditions are also known to acidify the chloroplast stroma, resulting in inhibited rubisco activity[5,6]. It has also been shown that at higher water deficits chlorophyll content decreased by a significant level in *Helianthus annuus*[1,7] and in *Vaccinium myrtillus*[1,8]. The foliar photosynthetic rate of higher plants is known to decrease as the relative water content and leaf water potential decreases[1,9]. Although photosynthetic rates were observed to decrease with leaf water content, changes in photosynthetic rates with chloroplast water content were not studied in intact leaf systems. The reason is that non-invasive methods that allow us to discriminate water in the different leaf tissues are hardly available. Recently we have demonstrated that ^{1}H NMR Diffusion Ordered SpectroscopY (DOSY) and Diffusion Relaxation Correlation Spectroscopy (DRCOSY) methods allow us to discriminate between different water and proton pools in *Ficus benjamina* and *Acer platanoides* leaves on the basis of their (restricted) diffusion behaviour (Chapter 2). These leaves clearly differ with respect to large subepidermal cells, which are present only in *F. benjamina*. In fresh leaf disks of *A. platanoides,* with their surface oriented perpendicular to the main magnetic field, we were able to discriminate the following water and lipid pools: vacuolar water of palisade cells plus large spongy cells (component 1), vacuolar water of small spongy cells plus epidermal cells(component 2), chloroplast water (component 3) and membrane lipids (component 4) and for fresh leaf disks of *F. benjamina,* in addition to the abovementioned ^{1}H pools subepidermal cellular water was also observed (cf. Tables 1 and 2).

Here we use the previously developed ^{1}H NMR DOSY-DANS approach to study the two different types of leaves *F. benjamina* and *A. platanoides*

during dehydration. The main focus is to study the effect of dehydration on the (re)distribution of water in the different water pools in those two types of leaf disks and also to answer the question if the subepidermal cells in *F. benjamina* act as a water storage/buffer pool during dehydration, to protect other compartments like the chloroplasts. Fresh leaves of well-watered plants (100% amount of water relative to fresh (AWRF)), leaves with a 20–50% AWRF (moderate dehydration) and leaves with 5–15% AWRF (severe dehydration) are compared. In this way we reveal the effect of subepidermal cells in *F. benjamina* on the water volume of chloroplasts, and the correlation with PSII efficiency upon dehydration.

3.2 Materials and Methods

3.2.1 Leaf disks

Leaf disks were obtained from *F. benjamina* and *A. platanoides.* Randomly-picked leaves were used for NMR measurements. Midribs were discarded, remaining tissue was cut into circular disks. The surface of leaf disks was kept perpendicular to the magnetic field B_0 in a standard NMR (shigemi) tube. The resonance of pure water in an identical tube was used as a reference (4.7 ppm). In order to study dehydration the same leaf disks were kept aside in the lab after the NMR measurements of the fresh leaf disks. Depending on the initial water content of the fresh leaves (which can differ due to different water gift history and position on the plant) the dehydration time to reach moderate hydration and severe hydration differed. For leaves of very well-watered plants it took 80 hours to reach moderate dehydration and an additional 20 hours to reach severe dehydration (cf. Fig. 3.1b).These periods can be much shorter for leaves of drought stressed plants.

3.2.2 Chlorophyll Fluorescence

Fluorescence measurements were performed with a PAM 101 chlorophyll fluorometer (Heinz Walz GmbH, Effeltrich, Germany) using a fibre optic system as described by Schreiber (1986). Saturating pulses (800 ms) of white light (4000 µmol m^{-2} s^{-1}) were provided by a KL 1500 light source (Schott, Wiesbaden, Germany). PSII efficiency (F_v/F_m) was measured using measuring beam intensity of (0.005 µmol m^{-2} s^{-1}) and saturation pulse.

3.2.3 DOSY and Diffusion Associated NMR Spectra

Special NMR (Shigemi) tube was used for all experiments in order to minimise susceptibility differences coming from interface between liquid

sample and air. All ^{1}H NMR diffusometry experiments were performed at 7 T (300 MHz ^{1}H Larmor frequency) using a Bruker Avance II spectrometer equipped with a Bruker diff25 diffusion probehead (Bruker, Germany), which delivers maximum field gradient strengths of 10 T m^{-1}.

All DOSY experiments were carried out using a 13-interval PFG stimulated echo NMR experiment in combination with bipolar sine-bell shaped gradients. The stimulated echo amplitude attenuation as a function of the experimental parameters can be described by the Stejskal-Tanner equation[10] $\frac{I}{I_0} = \sum_i A_i e^{-(\gamma \delta g)^2 \left(\Delta - \delta/3 \right) D_i}$, where $\frac{I}{I_0}$ is the echo attenuation, i the number of the components in the system, A_i the amplitude of the NMR signal of component i, γ the gyromagnetic ratio for ^{1}H (rad T^{-1} s^{-1}), δ the effective gradient pulse duration (s), g the gradient strength (T m^{-1}), and Δ the effective diffusion time (s), and D the diffusion coefficient (m^2 s^{-1}).

Stimulated echo was used because it allows the detection of shorter T_2 components at longer diffusion observation times[11]. Bipolar gradients were used to compensate for internal field gradients, which are present at high field strengths in inhomogeneous samples. The effective gradient pulse duration δ was set to 2 ms. The effective diffusion time Δ was varied between 12 and 300 ms. Gradient intensity was varied between 0.05 and 8.5 T m^{-1}. The attenuation of NMR spectra as a function of gradient intensity was analysed by fitting 1 to 4 exponential decays to the spectra using SplMod (Provencher, 1982)[12], which was set to perform a coupled exponential fit of the spectral data points. This resulted in 1 to 4 diffusion-associated NMR spectra (DANS). The procedure is similar to the DECRA curve resolution method described elsewhere, but SplMod is preferred because it can handle both linear and logarithmic sampling of the gradient axis[10].

Analysis of restricted diffusion behaviour

The time dependent diffusion coefficient $D(\Delta)$ was analysed using the equation[13]

$$\frac{D(\Delta)}{D_0} = 1 - \frac{S}{V} \frac{4}{9\sqrt{\pi}} \sqrt{D_0 \Delta}$$

where D_0 is the unrestricted diffusion coefficient, $\frac{S}{V}$ the surface-to-volume ratio of the compartment and Δ the diffusion observation time.

Size estimation of the compartments:

Dimensions of the compartments were estimated using the above equation. First, $D_0$was calculated by extrapolating a plot of $D(\Delta)$ vs. $\sqrt{\Delta}$ linearly to Δ=0 ms. The intercept equals D_0. The slope of the line equals $-\frac{S}{V}\frac{4}{9\sqrt{\pi}}D_0^{3/2}$. As we know $D_0$from the extrapolation, the surface-to-volume ratio follows from

$\frac{S}{V} = -\frac{9\sqrt{\pi}}{4}D_0^{-\frac{3}{2}}\text{x slope}$. Assuming that the shape of the compartment is spherical, the size (diameter) d of the compartment is $d = \frac{6V}{S}$.

3.3 Results

DOSY experiments *F. benjamina*

^{1}H NMR spectra of *F. benjamina* leaf disks of different levels of dehydration are shown in Fig. 3.1a and the corresponding total amplitudes of the spectra as a function of dehydration time in Fig. 3.1b . Clearly, the signal at higher ppm was more sensitive to the dehydration than at lower ppm.
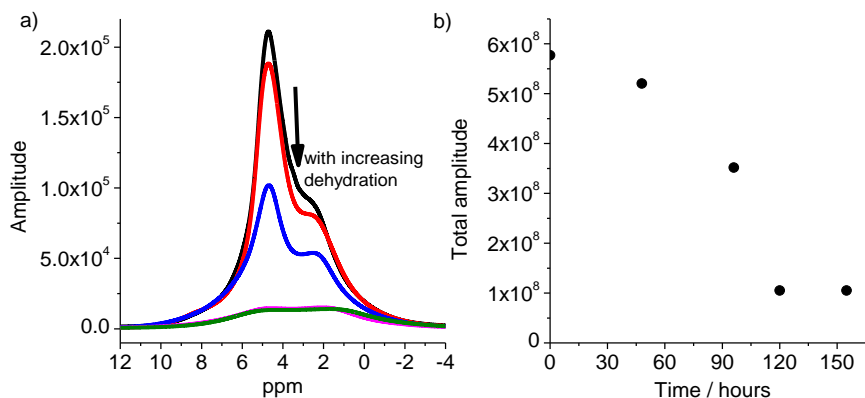
Figure 3.1: Effect of dehydration on ^{1}H NMR spectra of *F. benjamina* leaf disks oriented perpendicular to B_0 (a) and corresponding integrals of the spectra as a function of time (b).

In order to determine the effect of the dehydration on individual components/compartments a DOSY-DANS approach was applied (cf. Chapter 2) and the Apparent Diffusion Coefficient (*ADC*) was measured for

diffusion observation times Δ from 12 – 300 ms. Results of the fresh leaves (100% AWRF) were similar to the ones mentioned in Chapter 2. In Fig. 3.2 the Δ dependency of the spectra and in Fig. 3.3 of the related *ADC*s of the four components for *F. benjamina* leaf disks with moderate dehydration are presented.
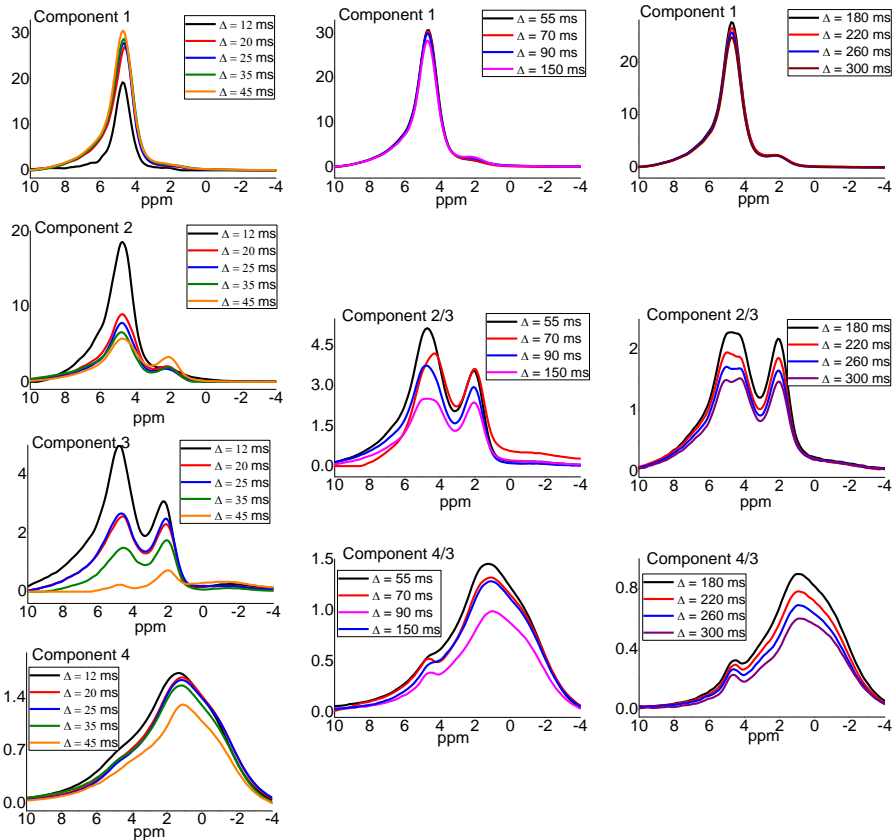

Figure 3.2: Diffusion time dependency of the spectra of the four components for *F. benjamina* leaf disks (oriented perpendicular to B$_0$) with moderate dehydration.

A four component fit was found to be optimal (based on residuals) from 12 ms – 45 ms and a three component fit from 50 ms – 300 ms (Fig. 3.3). In fresh leaf disks, a four component fit was found to be the best from 12 ms – 25 ms, a three component fit from 30 ms – 60 ms and a two component fit from 65 ms – 290 ms (Chapter 2, Fig. 2.8). The differences in the observed

number of components, as a function of Δ, were due to the changes in relative amplitude fractions of the components. At Δ=12 ms, total amplitude fractions of the components for fresh leaf disks were 60% for component 1, 30% for component 2 and 11% for component 3 and the fractions changed as 30% for component 1, 48% for component 2 and 21% for component 3 as a result of moderate dehydration.
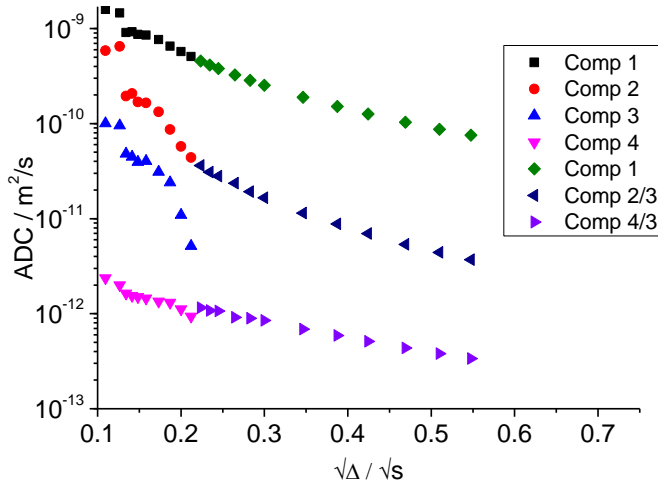

Figure 3.3: Diffusion time dependency of the apparent diffusion coefficients (*ADC*) of the four components for *F. benjamina* leaf disks (oriented perpendicular to B$_0$) with moderate dehydration.

The amplitude of component 1 of *F. benjamina* (Fig. 3.2) increased with increasing Δ up to around 45 ms for all resonances. The maximum at 4.7 ppm increased with about 109 arbitrary units and at 7 ppm with about 22.7. A small increase of about 6.4 could be observed around 2 ppm. The amplitude of component 2 in the 3 to 10 ppm range decreased, the maximum at 4.7 ppm with about 127 and at 7 ppm with about 11. In contrast, the resonance centred around 2 ppm increased with about 16. The amplitude of component 3 clearly decreased for all resonances, at 7 ppm 13, at 4.7 ppm 47.6 and at 2 ppm 24. These changes in the amplitudes cannot be explained by relaxation effects only, and suggested exchange as observed for fresh leaf disks.

The sizes estimated from hindered diffusion behaviours of components 1, 2 and 3 were very comparable to those of components 1, 2 and 3 in fresh leaf disks (cf. Table 1). The compartments subepidermal cells and vacuoles of

palisade cells lost 78% of water, epidermal cells and vacuoles of spongy cells about 28% and chloroplasts about 15%as a result of drying (cf. Table 1).Component 4 had a D_0 of $3.6×10^{-12}$ m^2/s. The component remained with same amplitude upon moderate dehydration indicating stability of (thylakoid) membranes.
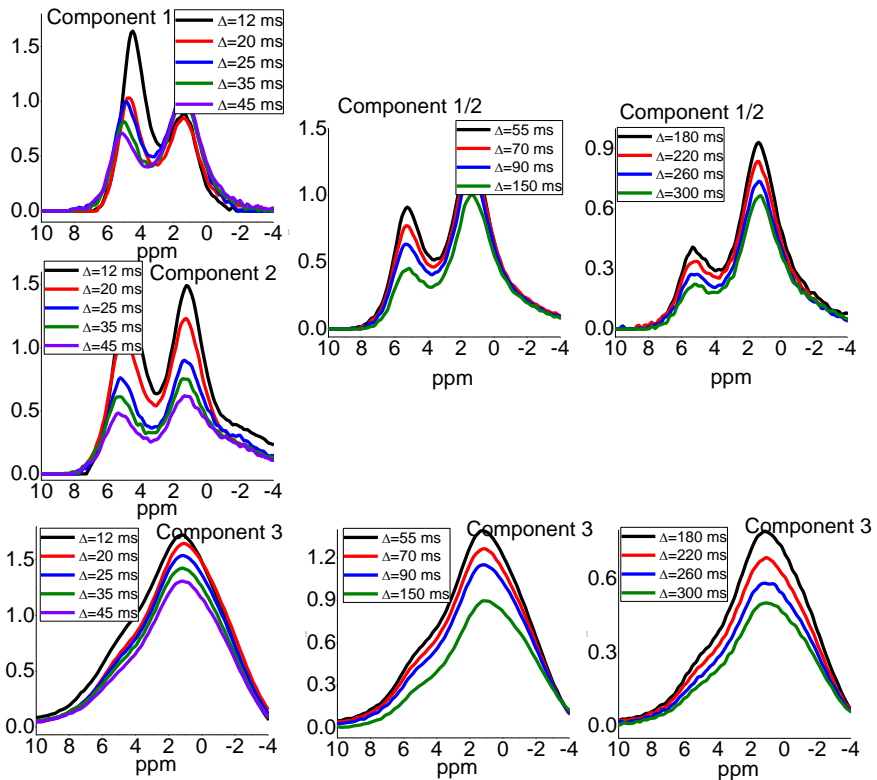

Figure 3.4: Diffusion time dependency of the spectra of the three components for *F. benjamina* leaf disks (oriented perpendicular to B$_0$) with severe dehydration.

In Fig. 3.4 the Δ dependency of the spectra and in Fig. 3.5 of the related *ADC*s of the components for *F. benjamina* leaf disks with severe dehydration are presented. Now a three component fit was found to be optimal (based on the residuals) from 12 ms – 50 ms and a two component fit from 55 ms – 300 ms. The decrease in the amplitude of the two peaks of component 1 showed different Δ dependency although they have the same *ADC*, which might indicate that the spectrum of component 1 does present

different proton pools with different T_1 and/or different exchange behaviour. The amplitude of the total spectrum of component 1 (and 3!) increased going from Δ=45 to 55 ms and a small part of component 2 goes to the component 3 which amplitude increased with Δ from 45 ms to 55 ms as a result of going from 3 to 2 component fit. Most of the signal of component 2 goes to component 1.
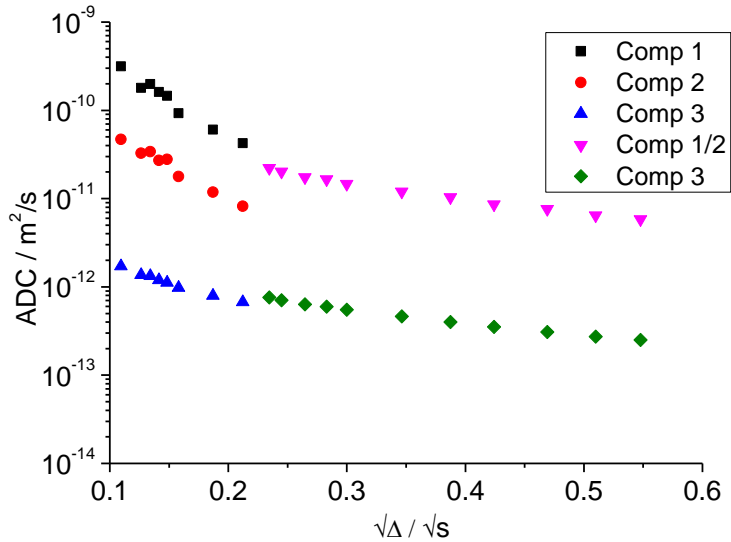

Figure 3.5: Diffusion time dependency of the apparent diffusion coefficients (*ADC*) of the three components for *F. benjamina* leaf disks (oriented perpendicular to B_0) with severe dehydration.

Component 1 had a D_0 of 7.3×10^{-10} m^2/s which is substantially lower than that of component 1 from leaves with moderate dehydration (2.3×10^{-9} m^2/s) and the estimated size from its hindered diffusion behaviour was about 8±2 μm. Component 2 had a D_0 of 1.1×10^{-10} m^2/sand estimated size from its hindered diffusion behaviour was about 3±1 μm. Thus, component 1 from leaves with severe dehydration contains components 1 and 2 of fresh leaf disks and of leaf disks with moderate dehydration. The compartments epidermal cells, subepidermal cells and vacuoles of both palisade cells and spongy cells remained only with 2.5% of their initial water due to severe dehydration (cf. Table 1). Component 2 from severely drought stressed leaves was the same as component 3 of fresh and moderate dehydrated leaf disks. Chloroplasts still had 33% of its initial water.

In Table 1 the absolute total amplitudes, D_0's and dimensions of the three components are summarized.

Table 1: Total amplitudes of the components at Δ=12 ms, D_0's and estimated sizes of the components with different levels of dehydration for *F. benjamina* leaf disks oriented perpendicular to B_0

Component	Fresh (100% AWRF)	Moderate dehydration (44% AWRF)	Severe dehydration (6% AWRF)
1	Vacuoles of palisade cells + subepidermal cells d: 21 ± 10 µm, Total amplitude: 1240 AWRF:100% D_0=2.1×10^{-9} m^2/s	Vacuoles of palisade cells d: 20 ± 6 µm, Total amplitude: 276 AWRF: 22% D_0=2.3 ×10^{-9} m^2/s	Vacuoles of palisade cells and spongy cells + epidermal and subepidermal cells d: 8 ± 2 µm, Total amplitude: 47 AWRF: 2.5% D_0=7.3×10^{-10} m^2/s
2	Vacuoles of spongy cells + epidermal cells d: 9 ± 2 µm, Total amplitude: 610 AWRF: 100% D_0=1.1×10^{-9} m^2/s	Vacuoles of palisade cells and spongy cells + epidermal and subepidermal cells d: 12 ± 5 µm, Total amplitude: 440 AWRF: 72% D_0=1.1×10^{-9} m^2/s	
3	Chloroplast d: 4 ± 1 µm, Total amplitude: 230 AWRF: 100% D_0=2.2×10^{-10} m^2/s	Chloroplast d: 5 ± 1 µm, Total amplitude: 195 AWRF: 85% D_0=1.9×10^{-10} m^2/s	Chloroplast d: 3 ± 1 µm, Total amplitude: 76 AWRF: 33% D_0=1.1×10^{-10} m^2/s

In Fig. 3.6 the effect of the dehydration on the diffusion behaviour of the components is presented. Due to moderate dehydration *ADC*s of water molecules in both vacuoles of palisade cells and subepidermal cells slowed down by about a factor of 1.3 at short diffusion times and remained same at longer diffusion times. The slow dynamics could be due to cell's shrinkage resulting from dehydration. The comparable calculated D_0's and *ADC*s at longer diffusion times indicate that the membrane permeability of the compartments remained comparable with moderate dehydration (Sibgatullin *et al.*, 2010)[14]. Due to moderate and severe dehydration water molecules in both vacuoles of spongy cells and epidermal cells and also in chloroplasts

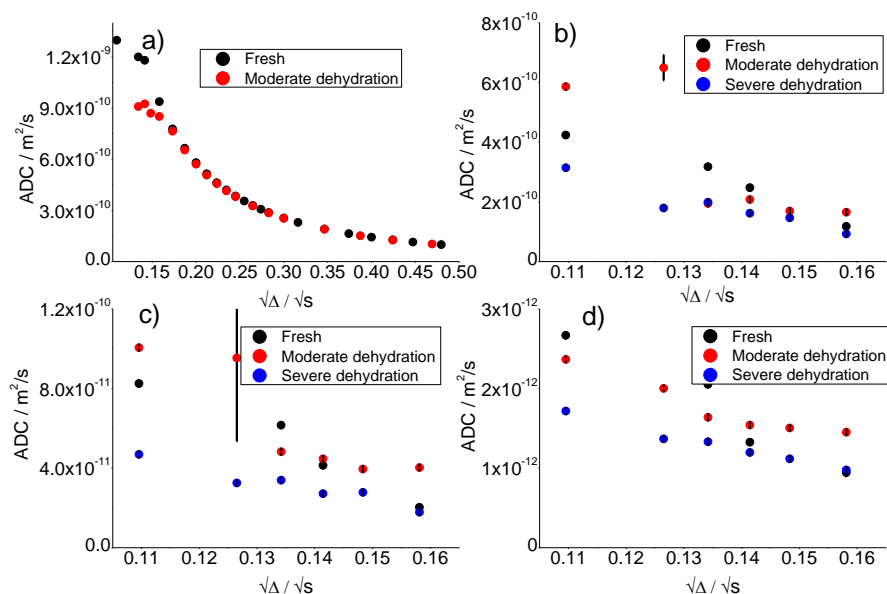experienced more severe restricted diffusion indicating the shrinkage of the compartments.

Figure 3.6: Effect of dehydration on diffusion behaviour of the components for *F. benjamina* leaf disks oriented perpendicular to B_0. Component 1 (a), 2 (b), 3 (c) and 4 (d) are shown.

DOSY experiments *A. platanoides*

In order to study dehydration effects also in leaf disks of *A. platanoides* DOSY experiments were performed for diffusion observation times from 12–300 ms on the leaf disks with no dehydration, moderate dehydration and severe dehydration. The results of the fresh leaves were similar to the ones mentioned in chapter 2. In contrast to *F. benjamina* leaf disks, the four components were observed at all levels of dehydration and for all diffusion observation times from 12–300 ms. In Fig. 3.7 the effect of the dehydration on the DANS of the four components for Δ=12 ms is presented. The amplitude of component 4 was not constant with dehydration, perhaps because of deterioration of thylakoid membranes (will be discussed in the following section). In Table 2 the changes in total amplitudes and dimensions of the three components 1, 2 and 3 as a result of drying out are summarized.
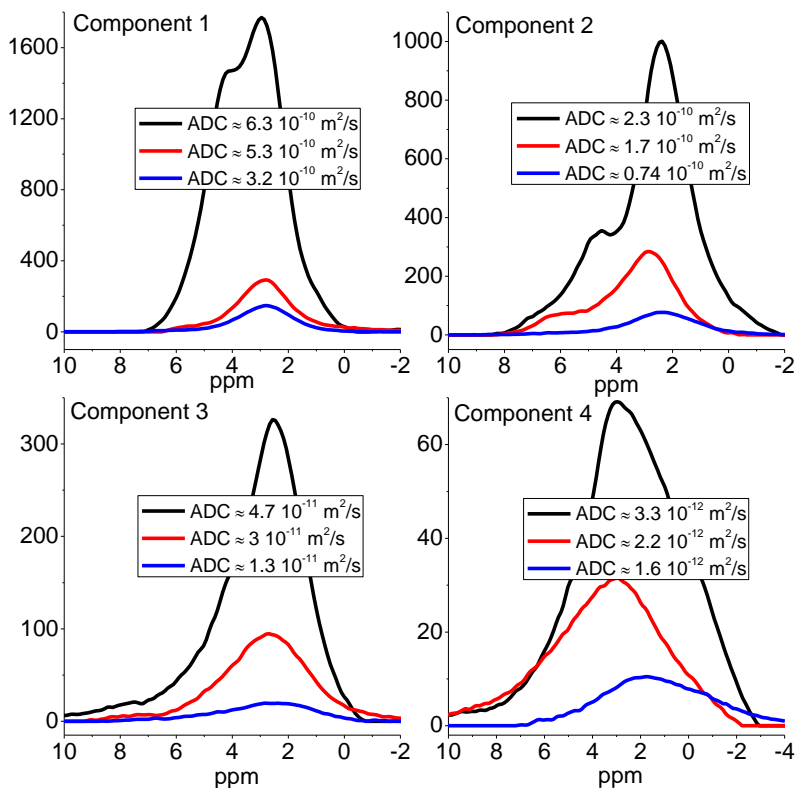
Figure 3.7: Effect of dehydration on the DANS of the four components from *A. platanoides* leaf disks oriented perpendicular to B_0 for $\Delta=12$ ms: black spectra correspond to fresh, red to moderate dehydration and blue to extremely severe dehydration.

The spectral shapes of each of the four components at the different Δ values were very stable (data not shown), not only for fresh leaf disks but also for moderately and severely dehydrated disks; only amplitudes decreased with increasing Δ.

In Fig. 3.8 the effect of the dehydration on the diffusion behaviour of the components is presented. In the case of moderate and severe dehydration ADC of water molecules in vacuoles of palisade cells slowed down by about a factor of 2, in vacuoles of spongy cells by about a factor of 3 and in chloroplasts by about a factor of 2.5 at short diffusion times. Component 4

Table 2: Total amplitudes of the components at Δ=12 ms with different levels of dehydration for *A. platanoides* leaf disks oriented perpendicular to B_0

Component	Fresh (100% AWRF)	Moderate dehydration (22% AWRF)	Severe dehydration (7.5% AWRF)
1	Vacuoles of palisade cells and spongy cells d: 15 ± 1 μm, Total amplitude: 550 AWRF: 100%	Vacuoles of palisade cells and spongy cells d: 13 ± 1.9 μm, Total amplitude: 78 AWRF: 14%	Vacuoles of palisade cells and spongy cells d: 12 ± 2 μm, Total amplitude: 37 AWRF: 7%
2	Vacuoles of spongy cells + epidermal cells d: 9 ± 1.2 μm, Total amplitude: 310 AWRF: 100%	Vacuoles of spongy cells + epidermal cells d: 6.7 ± 3.2 μm, Total amplitude: 89 AWRF: 29%	Vacuoles of spongy cells + epidermal cells d: 9.3 ± 2.2 μm, Total amplitude: 25 AWRF: 8%
3	Chloroplast d: 3.6 ± 0.2 μm, Total amplitude: 110 AWRF: 100%	Chloroplast d: 3.7 ± 2.5 μm, Total amplitude: 37 AWRF: 34%	Chloroplast d: 2.8 ± 1.3 μm, Total amplitude: 8.1 AWRF: 7%

slowed down as a function of dehydration perhaps due to deterioration of thylakoid membranes. The data presented in Figs. 3.7 and 3.8 are from two measurements on different leaves with different dehydration levels. Severe dehydration in Fig. 3.8 was extremely severe thus under extremely severe dehydrated conditions the comp 4 had very low *ADC*s and we could also see scattering of *ADC*s with big delta.

PAM fluorometry

PSII efficiency was measured for leaf disks of both *F. benjamina* and *A. platanoides* with different levels of dehydration using PAM fluorometry. The results are presented in Table 3. PSII efficiency was also measured for fresh

leaf at one particular position and then for the same leaf area after cutting. The measured PSII efficiencies were very similar (about 83%) indicating that the cutting had no effect.
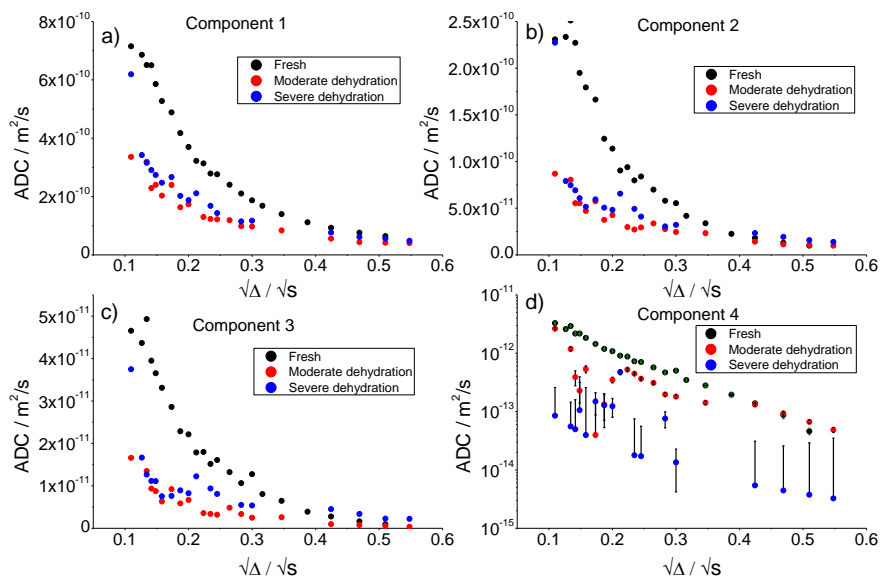

Figure 3.8: Effect of dehydration on the *ADC*s as a function of diffusion labelling time of the four components 1 (a), 2 (b), 3 (c), and 4 (d) from *A. platanoides* leaf disks oriented perpendicular to B_0.

Table 3: PSII efficiencies of leaf disks of both *F. benjamina* and *A. platanoides* with different levels of dehydration

	Without dehydration	Moderate dehydration	Extremely severe dehydration
F. benjamina	0.78	0.50	0.23
A. platanoides	0.79	0.51	0.07

3.4 Discussion

F. benjamina and *A. platanoides* leaves have different structures especially with respect to subepidermal cells. *F. benjamina* leaf has quite big subepidermal cells which are about spherical with a diameter of 20-30 μm[15]. Here we confirm from our NMR measurements that these subepidermal cells serve as water storage pools and help the plant to survive under drought conditions. Component 1 from *F. benjamina* leaf originated from both palisade cells and subepidermal cells. Upon moderate dehydration the component lost about 78% water mainly from subepidermal cells. As a result subepidermal cells got shrunken and, due to the smaller dimension, will become part of component 2. Although the dehydration levels are different at moderate dehydration state for *F. benjamina* leaf disks (AWRF$_{leaf}$ is 44% and AWRF$_{chloroplast}$ about 85%) and *A. platanoides* leaf disks (AWRF$_{leaf}$ is 21% and AWRF$_{chloroplast}$ is only about 34%) the PSII efficiency of the *A. platanoides* leaf disks was very comparable to that of *F. benjamina* leaf disks. In case of severe dehydration, both leaves had lost about 93% of initial water, but the differences in their PSII efficiencies were quite obvious: 23% in *F. benjamina* and only 7% in *A. platanoides.* That may relate to the differences in AWRF$_{chloroplast}$: 33% for *F. benjamina* and only 7% for *A. platanoides.* Thus, we observed a correlation between PSII efficiency and chloroplast water content though it is not linear and different for both leaves. To a critical value of 20% of chloroplast water content, PSII efficiency was high enough and below that level PSII efficiency declined gradually. Saccardy *et al.* observed for *Zea mays* leaves that the efficiency of PSII remained unchanged within the range of 100 to 60% Relative Water Content (RWC) and then declined as RWC declined[16]. Because of subepidermal cells, chloroplasts in *F. benjamina* did not lose much water even in case of severe dehydration that resulted in higher PSII efficiency. However, high PSII efficiency does not mean high photosynthetic rates. Thus in order to study the relation between chloroplast volume and photosynthetic activity under complete *in vivo* conditions our NMR measurements should be combined with other methods such as gas exchange measurements.

In addition to the changes observed in the water signals we also observed substantial changes in amplitude behaviour of component 4 (assumed to represent membrane lipids) as a function of dehydration for the two different leaf disks. For *F. benjamina* the amplitude of component 4 was not very sensitive to dehydration (Figs. 3.2 and 3.4), but for *A. platanoides* the amplitude decreased substantially (Fig. 3.7) probably due to deterioration of

thylakoid membranes. As mentioned above, chloroplasts in leaf disks of *F. benjamina* did not lose much water even in case of severe dehydration that might have protected thylakoid membranes from deterioration. As the *A. platanoides* leaves do not have subepidermal cells, chloroplasts were sensitive to the dehydration and thus loss of chloroplast water might have resulted in deterioration of thylakoid membranes. Because of deterioration of thylakoid membranes membrane lipids could be more mobile and appeared in component 3 particularly in case of severe dehydration. Other components of deteriorated thylakoid membrane, such as proteins, for instance, with more mobility could have appeared in component 4. For *A. platanoides* leaf disks, *ADC*s of the membrane lipids slowed about a factor of 3 at short diffusion times and remained same at long diffusion times in case of the moderate dehydration and in the case of extremely severe dehydration *ADC*s of component 4 slowed about a factor of 10 at short diffusion times and about a factor of 17 at long diffusion times. The slower diffusion of component 4 supports the speculation 'deterioration of thylakoid membrane' caused by extremely severe dehydration. For *F. Benjamina* leaf disks, *ADC*s of the membrane lipids slowed about a factor of 1.5 at all diffusion observation times, which might indicate changes in membrane lipid/protein interactions and/or membrane reorganization as a result of dehydration.

3.5 Conclusion

The ^{1}H NMR DOSY-DANS method allows us to study the behaviour of the different cellular water pools within leaves as a function of water content (induced by drying down). The combination of NMR and PAM measurements indicated a nonlinear correlation between chloroplast water volume and PSII efficiency. In case of moderate dehydration, although the dehydration levels are different for *F. benjamina* leaf disks and *A. platanoides* leaf disks the PSII efficiency of the *A. platanoides* leaf disks was very comparable to that of *F. benjamina* leaf disks.

In case of severe dehydration, both leaf disks had lost about 93% of initial water, but the differences in their PSII efficiencies were quite obvious: 23% for *F. benjamina* leaf disks and only 7% for *A. platanoides* leaf disks. At the same time differences in their $AWRF_{chloroplast}$ were observed: 33% for *F. benjamina* leaf disks and only 7% for *A. platanoides* leaf disks. To a critical value of chloroplast water content, PSII efficiency was high enough and below 20% of $AWRF_{chloroplast}$ PSII efficiency declined gradually. Therefore, we conclude that the subepidermal cells in leaves of *F. benjamina* clearly

serve as water storage pools and help plants to survive under dehydrating conditions by preventing chloroplast water loss. That high chloroplast water content even in extremely severe dehydrated conditions gave high PSII efficiency in *F. benjamina* leaf disks.

The observed changes in *ADC*s of the (thylakoid) membrane lipids in both the leaf disks indicate changes in the membrane lipid/protein interactions and/or membrane reorganization as a result of dehydration.

Supporting information

Supporting information is included below: **S3.1.** Residual plots (labels of each subplot show the number of components) of DANS (for various diffusion observation times) of *F. benjamina* leaf disks subjected to moderate dehydration and oriented perpendicular to B_0. **S3.2.** Residual plots (labels of each subplot show the number of components) of DANS (for various diffusion observation times) of *F. benjamina* leaf disks subjected to severe dehydration and oriented perpendicular to B_0. **S3.3.** Residual plots (labels of each subplot show the number of components) of DANS (for diffusion observation time of 12 ms) of *A. platanoides* leaf disks oriented perpendicular to B_0, subjected to moderate (a) and severe dehydration (b).
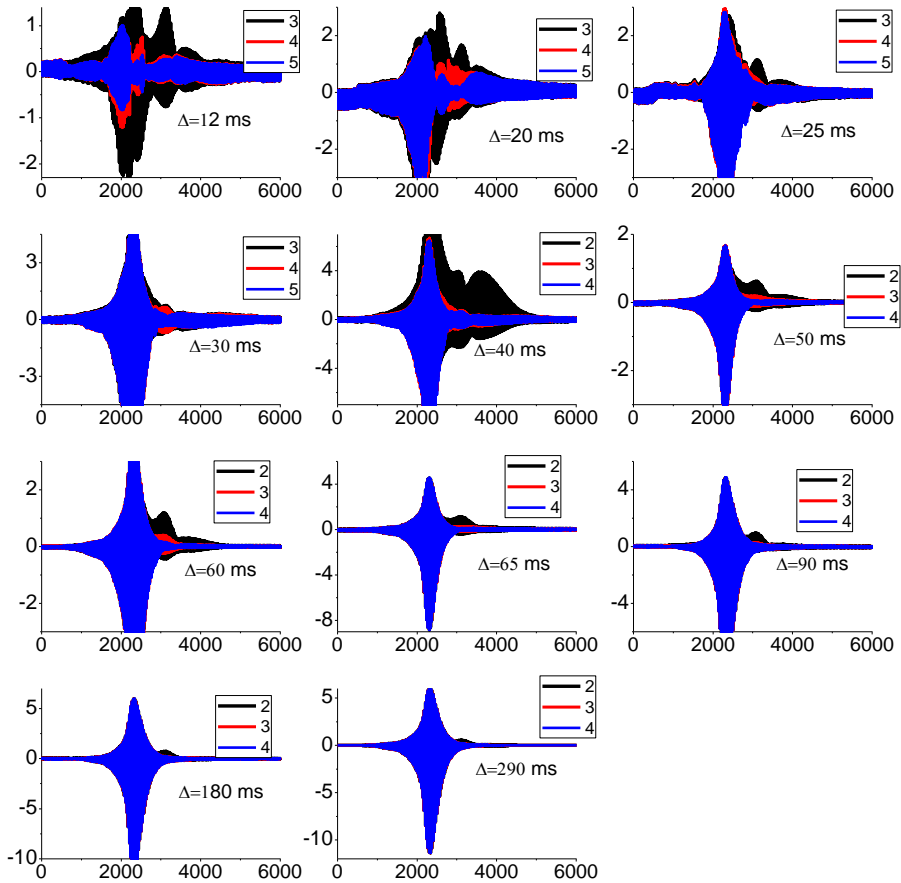
Acknowledgements

Figure S3.1: Residual plots (labels of each subplot show the number of components) of DANS (for various diffusion observation times) of *F. benjamina* leaf disks subjected to moderate dehydration and oriented perpendicular to B_0. It is clear from the plots that number of components decrease with increasing diffusion observation time.
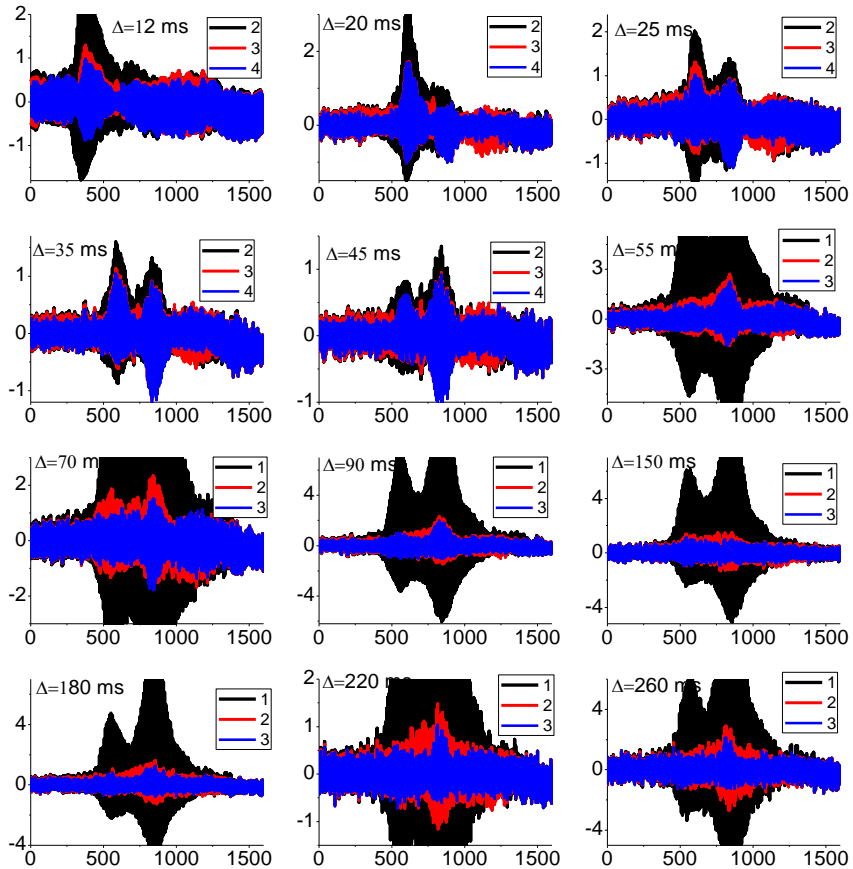
Figure S3.2: Residual plots (labels of each subplot show the number of components) of DANS (for various diffusion observation times) of *F. benjamina* leaf disks subjected to severe dehydration and oriented perpendicular to B_0. It is clear from the plots that number of components decrease with increasing diffusion observation time.
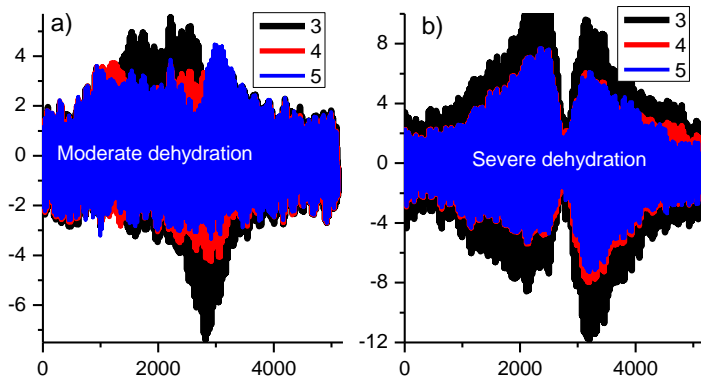
Figure S3.3: Residual plots (labels of each subplot show the number of components) of DANS (for diffusion observation time of 12 ms) of *A. platanoides* leaf disks oriented perpendicular to B_0, subjected to moderate (a) and severe dehydration (b). It is clear from the plots that four component fit is better.

References

1) Fanaei, H. R., Sadegh, H. N., Yousefi, T., and Farmanbar, M. (2015). Influence of drought stress on some characteristics of plants. Biological Forum- An International Journal **7**(1): 1732-1738.
2) Benjamin, J. G., and Nielsen, D. C. (2006).Water deficit effects on root distribution of soybean, field pea and chickpea. Field Crops Research **97**(2): 248-253.
3) Praba, M. L., Cairns, J. E., Babu, R. C., and Lafitte, H. R. (2009). Identification of physiological traits underlying cultivar differences in drought tolerance in rice and wheat. Journal of Agronomy and Crop Science **195**(1): 30-46.
4) Schapendonk, A. H. C. M., Spitters, C. J. T., and Groot, P. J. (1989). Effects of water stress on photosynthesis and chlorophyll fluorescence of five potato cultivars. Potato Research **32**(1): 17-32.
5) Reddy, A. R., Viswanatha Chaitanya, K. and Munusamy, V. (2004). Drought-induced responses of photosynthesis and antioxidant metabolism in higher plants. Journal of Plant Physiology **161**(11): 1189-1202.
6) Meyer, S., and Bernard, G. (1999). Heterogeneous inhibition of photosynthesis over the leaf surface of Rosa rubiginosa L. during water stress and abscisic acid treatment: induction of a metabolic component by limitation of CO2 diffusion. Planta **210**(1): 126-131.
7) Kiani, S. P., Maury, P., Sarrafi, A., and Grieu, P. (2008). QTL analysis of chlorophyll fluorescence parameters in sunflower (Helianthus annuus L.) under well-watered and water-stressed conditions. Plant Science **175**(4): 565-573.
8) Tahkokorpi, M., Taulavuori, K., Laine, K., and Taulavuori, E. (2007). After-effects of drought-related winter stress in previous and current year stems of *Vacciniummyrtillus L*. Environmental and Experimental Botany **61**(1): 85-93.
9) Lawlor, D. W., and Cornic, G. (2002). Photosynthetic carbon assimilation and associated metabolism in relation to water deficits in higher plants. Plant, Cell & Environment **25**(2): 275-294.
10) Stejskal, E. O., and Tanner, J. E. (1965). Spin diffusion measurements: spin echoes in the presence of a time-dependent field gradient. Journal of Chemical Physics **42**:288–292.
11) Antalek, B. (2002). Using Pulsed Gradient Spin Echo NMR for Chemical Mixture Analysis: How to Obtain Optimum Results. Concepts in Magnetic Resonance**14**: 225-258

12) Provencher, S. W. (1982).A constrained regularization method for inverting data represented by linear algebraic or integral equations. Computer Physics Communications **27**(3): 213-227.

13) Olayinka, S. and Ioannidis, M. (2004). Time-dependent diffusion and surface-enhanced relaxation in stochastic replicas of porous rock. Transport in Porous Media **54**(3): 273-295.

14) Sibgatullin, T.A., Vergeldt, F.J., Gerkema, E. and Van As, H. (2010). Quantitative permeability imaging of plant tissues. European Biophysics Journal **39**(4): 699-710.

15) Labunskaya, E. A., Zhigalova, T. V., and Choob, V. V. (2007). Leaf anatomy of the mosaic *Ficus benjamina* cv. Starlight and interaction of source and sink chimera components. Russian Journal of Developmental Biology **38**(6): 397-405.

16) Saccardy, K., Pineau, B., Roche, O. and Cornic, G. (1998). Photochemical efficiency of Photosystem II and xanthophyll cycle components in *Zea mays* leaves exposed to water stress and high light. Photosynthesis Research **56**:57-66.

4

Dynamics of chloroplast water, lipids and thylakoid membrane signals in *Chlamydomonas reinhardtii* studied by non-invasive DRCOSY and DOSY-DANS ^{1}H NMR

Abstract

Mobility of thylakoid membranes and pigment-protein complexes therein is essential for survival of photosynthetic organisms under changing environmental conditions. The published approaches to probe mobility of the thylakoid membrane lipids and protein complexes are either dependent on the use of external labels or used only for *in vitro* studies. Here, we present non-invasive ^{1}H NMR methods (DOSY and DRCOSY) to study dynamics of water in chloroplasts, lipids in oil bodies and in thylakoid membranes and pigment-protein complexes under complete *in vivo* conditions in suspensions of the green alga *Chlamydomonas reinhardtii*. Nutrient stress and excess salt stress resulted in substantial changes in apparent diffusion coefficients of membrane lipids and pigment-protein complexes. Nutrient stress and excess salt stress resulted in accumulated lipid bodies and in striking differences in the dynamics and spectra/composition of the different components.

4.1 Introduction:

Photosynthesis is one of the most important processes for life on earth. In higher plants and algae, photosynthetic light reactions occur in specialized internal membranes of chloroplasts called thylakoids. Photosynthetic organisms are exposed to strong fluctuating environmental conditions (e.g. light and temperature). The organisms switch their behaviour to protect themselves from the unfavourable environmental conditions by a reorganization of the thylakoid membrane in relation to functional switching of specific light-harvesting pigment protein complexes[1,2]. In general, the mobility of photosynthetic proteins and lipids in the thylakoid membranes represents an important factor that affects light-energy conversion in photosynthesis. As such, understanding the dynamics of these molecules in relation to photosynthesis and stressors is fundamental to improve e.g. biomass and crop production[3]. Stress responses are in addition directly reflected in changes in (amount of) chloroplast water, thylakoid membrane and photosynthetic pigment-photosystem complexes and the production of e.g. lipids accumulated in oil bodies[4].

A number of methods has been used to study dynamics of molecules in isolated thylakoid membranes or model systems of it[5]. Blackwell *et al.*[6] estimated lateral diffusion coefficients for PQ-9, decyl PQ and PQ-2 in soybean phosphatidylcholine liposomes and in isolated spinach thylakoid and sub-thylakoid membranes using a pyrene fluorescence quenching technique. The results provided the evidence that PQ lateral mobility within the thylakoid membrane determines the rate of quinol oxidation by the cytochrome b$_6$f complex. They also concluded that plastocyanin rather than PQ must be responsible for rapid electron transport between PS II and PS I and that was in agreement with a similar proposal by Lavergne, Joliot and their co-workers[7,8]. Using Fluorescence Recovery After Photobleaching (FRAP) and Confocal Laser Scanning Microscopy (CLSM), lateral diffusion of light-harvesting complexes and reaction centres in the thylakoid membranes of the cyanobacterium *Dactylococcopsissalina* was measured[9]. It was proposed that the lateral diffusion of the light-harvesting phycobilisomes is involved in the regulation of photosynthetic light harvesting (state 1-state 2 transitions)[9].

Kirchhoff *et al.*[10] also examined the mobility of photosynthetic pigment-protein complexes in unstacked thylakoid regions in the C3 plant *Arabidopsis thaliana* and agranal bundle sheath chloroplasts of the C4 plants *Sorghum bicolor* and *Zea maize* by the FRAP technique. They

concluded that more than 50 % of the protein complexes are mobile in unstacked thylakoid membranes and the number dropped to only about 20 % in stacked grana regions because of the high protein to lipid ratio. Sarcina *et al.*[11] measured diffusion of lipid soluble fluorescent markers in the cyanobacterium *Synechococcus sp.* PCC 7942 in the wild type strain and also in a strain with an increased level of fatty acid unsaturation using the FRAP technique. They observed a six-fold increase in the diffusion coefficient for the fluorescent marker in the strain with increased fatty acid unsaturation at growth temperature. This result provides evidence that the increased lipid desaturation results in an increased lateral diffusion of lipids.

Although the above mentioned techniques (pyrene fluorescence quenching and FRAP) were used to probe the mobility of lipids, electron carriers and protein complexes in thylakoid membranes, their application is limited to isolated thylakoid systems and there is a need for *in vivo* approaches. These methods are also sensitive to artefacts, because e.g. FRAP bleaching may perturb the behaviour of the membrane being examined[12]. Also, the use of external fluorescent labels might result in non-native conditions. Here, we apply the ^{1}H Pulsed Field Gradient (PFG) NMR technique to study dynamics of (chloroplast) water and lipids and molecules in the photosynthetic membrane *in vivo* in *Chlamydomonas reinhardtii* suspensions. PFG NMR is a very useful non-invasive technique to measure diffusion in biological systems. Naturally available ^{1}H bearing NMR probe molecules such as water, lipids, proteins and so on can directly be measured. Thus PFG NMR does not require any external labelling and one can even measure very low diffusion coefficients in the order of 10^{-15} m^2/s as well if a high power gradient diffusion probe is used. Such slow diffusion is for instance expected for supercomplexes (light harvesting complexes) in the photosynthetic membrane[9]. Diffusion coefficients of particular proteins and lipids from different membranes and cell compartments including thylakoid membrane measured by different techniques have been reported by Kana[5].The diffusion coefficient of proteins in eukaryotic plasma membranes is about 2.5×10^{-13}-7.5×10^{-13} m^2/s and that of lipids in eukaryotic membranes is about 1×10^{-12}-4×10^{-12} m^2/s. The diffusion coefficient of lipids in thylakoid membranes is 6×10^{-14}-1×10^{-12} m^2/s, whereas the diffusion coefficient of LHCII in stroma lamellae is about 3×10^{-15} m^2/s and in grana it is 5×10^{-15} m^2/s, whereas the diffusion coefficient of PSII reaction centers (red light adapted) is 2.3×10^{-14} m^2/s[5].

In chapter 2 we reported two water pools that could be discriminated in *C. reinhardtii*. One represents the cell water and the other water in the

chloroplast. Sizes of the alga and its chloroplast were also estimated using the restricted diffusion behaviour of the algal water and chloroplast water (chapter 2). *C. reinhardtii* is a unicellular alga with a relatively large chloroplast compartment and a high concentration of thylakoid membrane. *C. reinhardtii* can be manipulated in a controlled way, allowing us to study the (dynamic) changes in response to environmental manipulations. In this chapter, we demonstrate that in algae more proton pools can be observed *in vivo* by proper suppression of the abundant water signals. Doing so, in addition to the chloroplast water, (membrane) lipids and large (membrane) protein complexes were observed. The (changes in) diffusion behaviour and in amount/composition of these chloroplast and thylakoid membrane related proton pools in wild type *C. reinhardtii* grown in three different media (normal medium, nitrogen free medium and salty medium) was studied.

4.2 Materials and Methods

4.2.1 Wild-type *C. reinhardtii*

Wild-type *C. reinhardtii* (137C) algae were grown under continuous white-light illumination in Tris-acetate-phosphate medium[13]. Algae were shaken in a rotary shaker (100 rpm) at 30 °C and illuminated by a white lamp at 10 μmol.m^2.s^{-1}. All algae were grown in 250 mL flasks with a growing volume of 120 mL and maintained in the logarithmic growth phase. The 120 mL suspension was further centrifuged to get about 800 μL of very concentrated algae.

For the NF (nitrogen free) experiment nitrogen was removed from the normal medium to induce nutrient stress, and the algae were grown in that NF medium for 4 days. To induce the salinity stress, 100 mM NaCl was added to the normal medium and the algae were grown in that for 2 days.

4.2.2 NMR

A special NMR (Shigemi) tube was used for all experiments in order to minimise susceptibility differences coming from interface between liquid sample and air. All NMR diffusometry experiments were performed with a 7 T (300 MHz ^{1}H Larmor frequency) Wide Bore Bruker Avance II spectrometer equipped with a Bruker diff25 diffusion probehead, which delivers a maximum field gradient strength 10 T m^{-1}.

In NMR diffusometry, the echo attenuation as a function of the experimental parameters can be described by the Stejskal-Tanner equation[14]

$$\frac{I}{I_0} = \sum_i A_i e^{-(\gamma \delta g)^2\left(\Delta - \delta/3\right)D_i},$$ where $\frac{I}{I_0}$ is the echo attenuation, A_i the amplitude of the NMR signal, γ the gyromagnetic ratio (26.75 10^7 rad T^{-1} s^{-1} for ^{1}H), δ the effective gradient pulse duration (s), g the gradient strength (T m^{-1}), Δ the effective diffusion time (s), and D the diffusion coefficient (m^2 s^{-1}). A 13–interval pulsed gradient sequence was used[15].

Acquisition parameters were as follows: number of averages–128 for DOSY and 64 for DRCOSY; number of g-steps–16 (linearly distributed) for both DOSY and DRCOSY; TR–0.75 s for DOSY and 1.7 s for DRCOSY and the total time per experiment is 20–25 mins for DOSY and about 30 mins for DRCOSY.

DOSY

All DOSY experiments were carried out using a stimulated echo experiment in combination with bipolar sine-shaped gradients. Stimulated echo was used because it allows the detection of shorter T_2 components at longer diffusion times[16]. Bipolar gradients were used to compensate for internal field gradients, which are present at high field strengths in inhomogeneous samples. The effective gradient pulse duration δ was set to 3ms. The effective diffusion time Δ was varied between 25 and 260 ms. Gradient intensity was varied between 2 and 8 T m^{-1}.

DOSY data analysis

The attenuation of NMR spectra as a function of gradient intensity was analysed by fitting 1 to 4 exponential decays to the spectra using SplMod (Provencher, 1982)[17], which was set to perform a coupled exponential fit of the spectral data points. This resulted in 1 to 4 diffusion-associated NMR spectra (DANS). The procedure is similar to the DECRA curve resolution method described elsewhere[14].

DRCOSY

A stimulated echo-based diffusion experiment, using bipolar gradients and sine-shaped pulses, was combined with a time-domain CPMG experiment. The effective gradient pulse duration δ was set to 3ms. The effective diffusion time Δ was 40 ms. Gradient strength was varied between 2 and 8

T m^{-1}. An echo time TE of 0.2 ms was used and 2k echoes were recorded. The data was analysed using 2D Fast Laplace Inversion[18] (2-dimensional version of CONTN) and also SplMod[19] (discrete fitting with a sum of (limited number of) exponentials).

Analysis D(Δ): In the limit of short Δ, D depends linearly on the square root of the diffusion time. The slope of this dependence is determined by the surface-to-volume ratio (S/V) of the water containing compartment, (Sen, 2004)[20], according to the equation[21]

$$\frac{D(\Delta)}{D_0} = 1 - \frac{S}{V}\frac{4}{9\sqrt{\pi}}\sqrt{D_0\Delta}$$

4.3 Results

4.3.1 DOSY on wild-type C. reinhardtii grown in normal medium (NM)

^{1}H diffusion was measured in C. reinhardtii by PFG DOSY (Diffusion Ordered SpectroscopY) NMR for a set of diffusion times (Δ) from 25 ms to 260 ms. Diffusion attenuated ^{1}H NMR spectra for Δ = 40 ms are shown in Fig. 4.1.
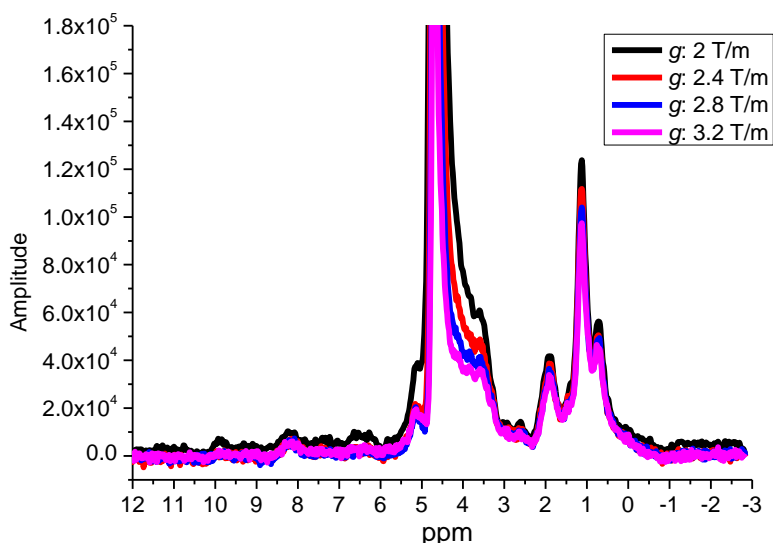
Figure 4.1: Diffusion attenuated ^{1}H NMR spectra of *C. reinhardtii* for Δ= 40 ms, δ=3 ms, g: 2-8 T/m (medium and part of cell water already suppressed).

Medium water, a large part of the cell water and mobile metabolites were already suppressed using a diffusion filter: the first gradient value was 2 T/m. The diffusion attenuated ^{1}H NMR spectra were analysed by fitting the diffusion attenuation curve by a discrete number of components. Four diffusion associated ^{1}H NMR spectra (DANS) related to four different diffusion coefficients were obtained for all the diffusion times from 25 ms up to 260 ms. The result for $\Delta=40$ ms is shown in Fig. 4.2.
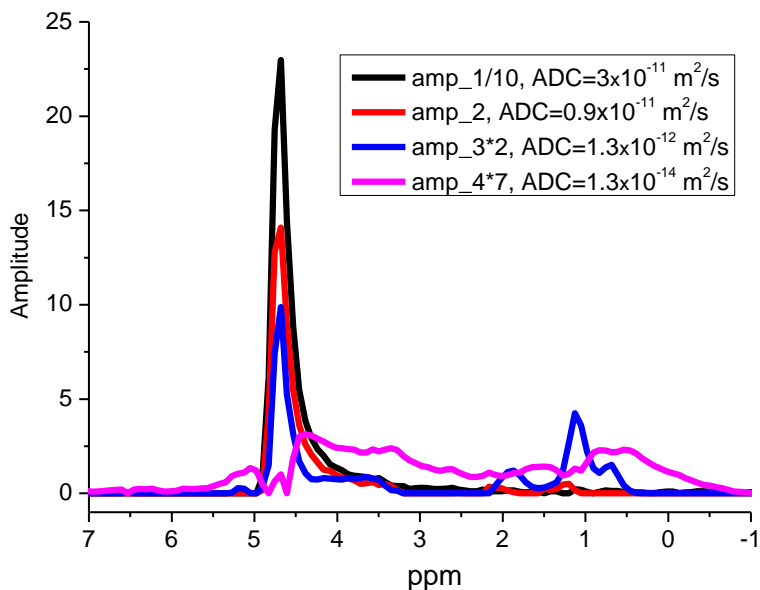

Figure 4.2: Diffusion Associated ^{1}H NMR spectra (DANS) at $\Delta=40$ ms. Note the differences in the scaling factors to make the spectral intensities comparable! The amplitude of component 1 was divided by 10 and of components 3 and 4 were multiplied by 2 and 7, respectively.

DANS and apparent diffusion coefficient (ADC) as a function of Δ for component 1 are shown in Fig. 4.3. The spectrum contained only one peak at the resonance of water and the compartment size estimated from the restricted diffusion was about 4.6±1.2 μm. We assigned this component to chloroplast water because of the estimated dimension which was in the order of chloroplast size in *C. reinhardtii* and also because of its ADC which was in the order of the ADC of chloroplast water in leaves (see chapter 2). This component was the largest fraction after suppressing the medium

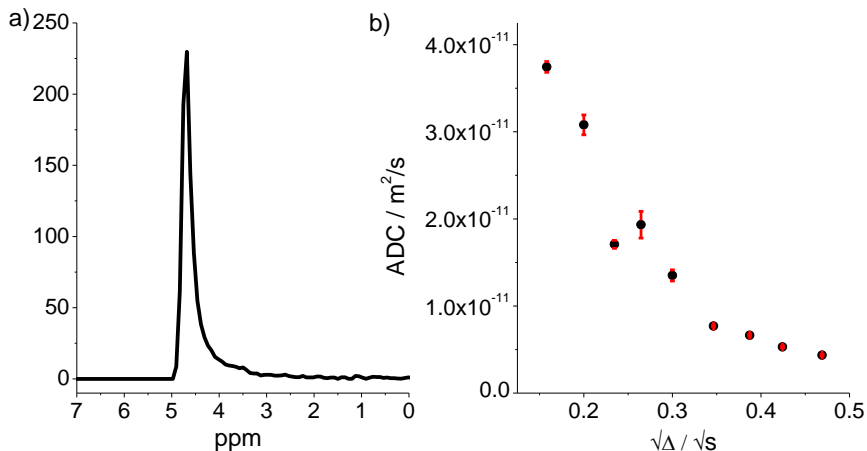water and part of the algal water, representing about 90% of the total remaining signal.

Figure 4.3: DANS (a) and ADC as a function of diffusion labelling time Δ (b) of component 1. Estimated size from its Δ-dependence of D(Δ) is 4.6±1.2 μm: chloroplast water.

Component 2 (Fig. 4.4) has a huge peak at 4.7 ppm, and less intense peaks in the region 1 – 2.5 ppm. Its diffusion coefficient is almost 1000 times lower than that of bulk water. The integral of this component was about 3% of the remaining signal after the initial suppression. Probably it was from both water protons (4.7 ppm) and lipid protons diffusing at about the same rate, but with a different Δ dependence that might have resulted in such a strange diffusion behaviour of the component (Fig. 4.4b). The roughly estimated size from its D(Δ) was about 1.3±1 μm so it might represent lipid bodies. The ADC of the component was 2×10^{-12} m²/s at Δ=220 ms which is close to the ADC (0.79×10^{-12} m²/s at Δ=400 ms) of TAGs in oil bodies in seeds[22].

DANS and diffusion behaviour of component 3 (about 4% (integrated intensity) of the signal) are shown in Fig. 4.5. The spectrum has resonances at chemical shifts of lipid protons such as CH3 at 0.8–0.9 ppm, CH2 at 1.1 ppm, C**H**2CH2COO at 1.62 ppm, C**H**2–CH=CH at 2.02–2.09 ppm, C**H**–OH at 3.4–4 ppm , α,β-glycosidic bonds at 4–5 ppm and CH=CH at 5.2 ppm[22,23]. Its diffusion coefficient is about 2×10^{-12} m²/s at Δ=25 ms, which is similar to what is observed for lateral diffusion of lipids in model membranes[24,25].
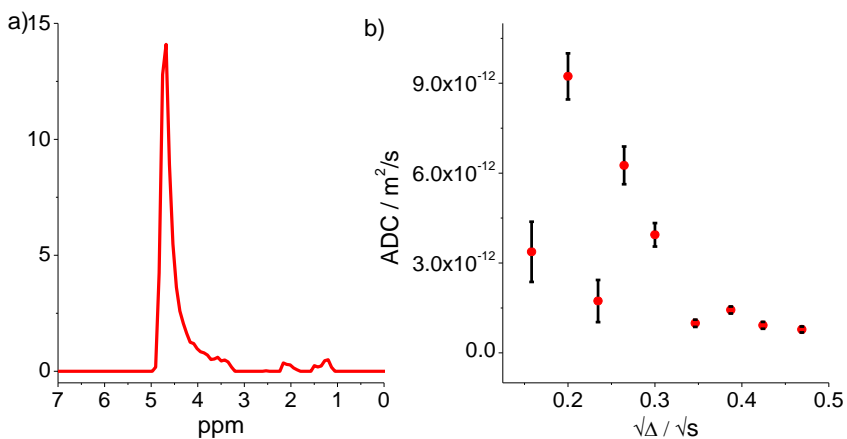
Figure 4.4: DANS (a) and diffusion behaviour (b) of component 2.
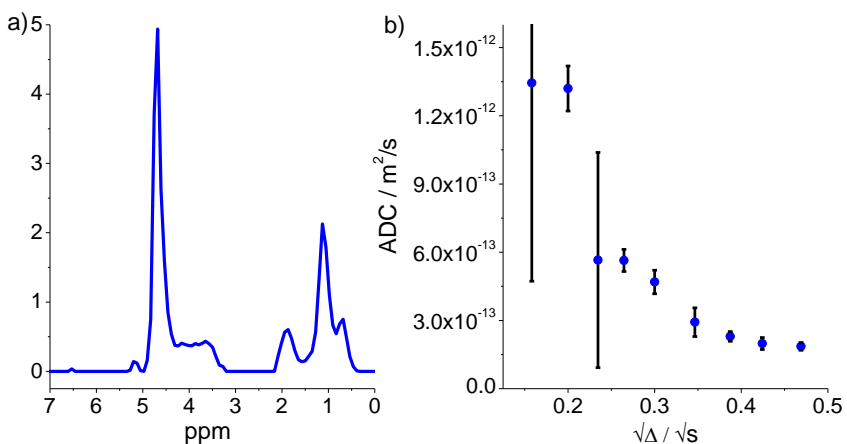

Figure 4.5: DANS (a) and diffusion behaviour (b) of component 3.

Fig. 4.6 shows DANS and diffusion behaviour of component 4. DANS showed resonances in a broad chemical shift range. The integral fraction of the component was about 3% of the signal. The ADC of the component was 2×10^{-14} m^2/s at Δ=25 ms which is in the order of that of membrane protein complexes[5]. The root mean square displacement of component 4 calculated from the restricted diffusion behaviour was ~32 nm for all Δ from 25 ms to

220 ms which indicates that the mobility of this component was severely restricted.
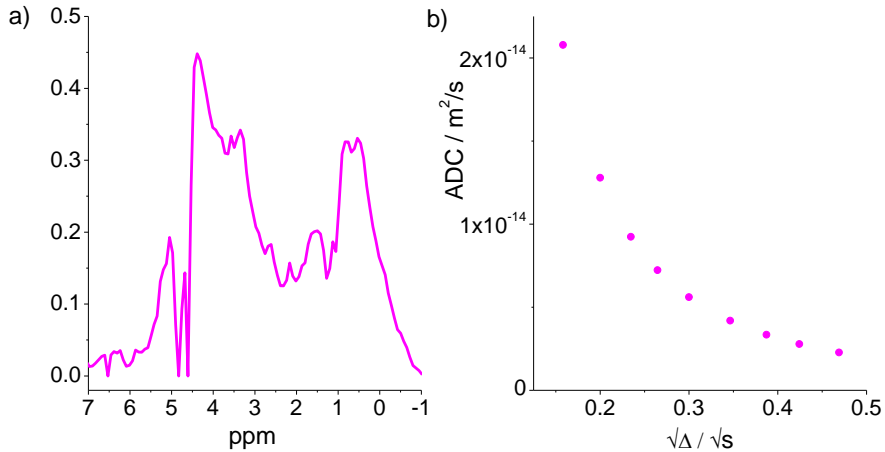

Figure 4.6: DANS (a) and diffusion behaviour (b) of component 4.

Fig. 4.7 shows the diffusion time dependency of the spectra of all components. The integral of component 1 reduced slightly between $\Delta=25$ ms and 40 ms but substantially by about 65% between $\Delta=40$ ms and 55 ms and then gradually from 55 ms till 220 ms. Integral of component 2 increased substantially about 63% from $\Delta=25$ ms to 40 ms and reduced to 31% from $\Delta=40$ ms to 55 ms and then to 53% from $\Delta=55$ ms to 70 ms and then decreased gradually with increasing Δ. The complex behaviour of component 2 with increasing Δ could be coming from the combination of water (either vacuole or lumenal) and lipid bodies diffusing at the same rate. Although the total integral of component 3 decreased gradually with increasing Δ, resonances of component 3 show quite complex behaviour, some resonances decayed faster and some resonances even increased. The integral of component 4 decreased gradually with increasing Δ because of T_1 relaxation.
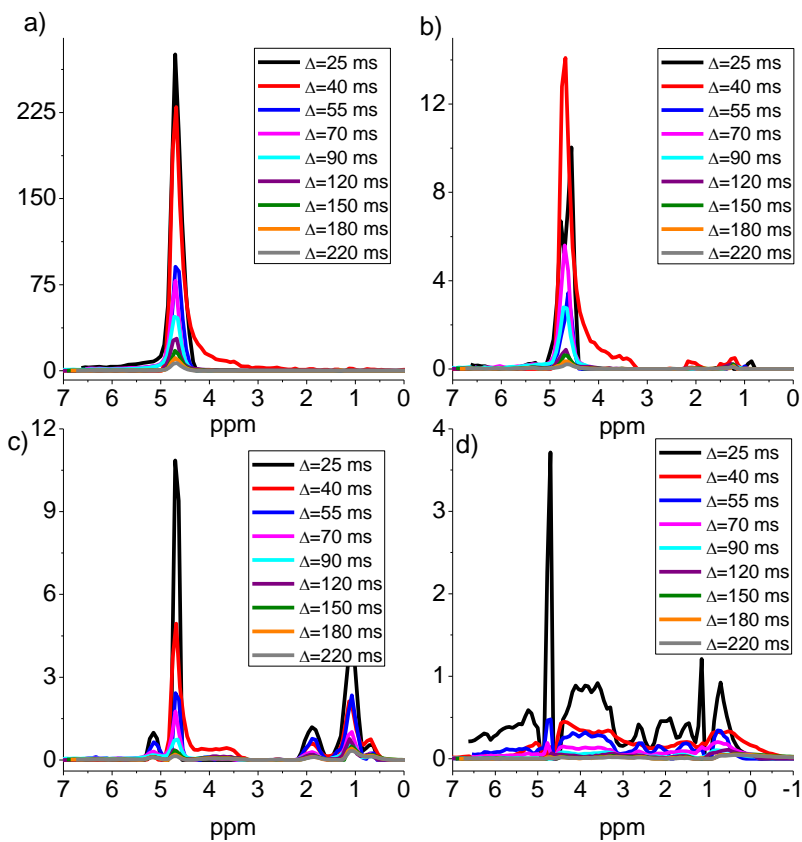
Figure 4.7: DANS as a function of diffusion observation time for component 1 (a), component 2 (b), component 3 (c) and component 4 (d) for NM algae.

4.3.2 DOSY on WT C. reinhardtii grown in nitrogen free (NF) and salty medium (SM)

C. reinhardtii was grown in nitrogen free medium (NF) and also in salty medium (SM, 100 mM NaCl was added to the normal medium and the algae were grown in the salty medium for 2 days). The growth rate of algae was reduced because of the stress and that resulted in a lower concentration of algae in NF and SM. In order to have equal concentration (numerically) of algae in the three different samples, we normalised each sample on its own first diffusion filtered step at Δ=25 ms. Diffusion measurements were performed on both algae separately. A four component fit was found to be

optimal (based on residuals) for the used gradient values (2-8 T/m) and all the diffusion times for the *C. reinhardtii* grown in both media.

The DANS of component 1 (a single peak at water resonance) from both NF and SM algae was quite similar to the one obtained for the NM algae (Fig. 4.8a, Δ= 40 ms) and its ADC at Δ=25 ms was 4.4×10^{-11} m^2/s for NF algae and 2.1×10^{-11} m^2/s for SM algae. The compartment size estimated from the dependence of D(Δ) as a function of Δ (Fig. 4.9a) was 4.9 ± 1.2 μm for NF algae and 3.8 ± 0.5 μm for SM algae. The dimensions were very much comparable for NM algae and NF algae. The size decreased significantly in SM algae indicating that the chloroplasts lost water (smaller volume) because of excess salt stress.
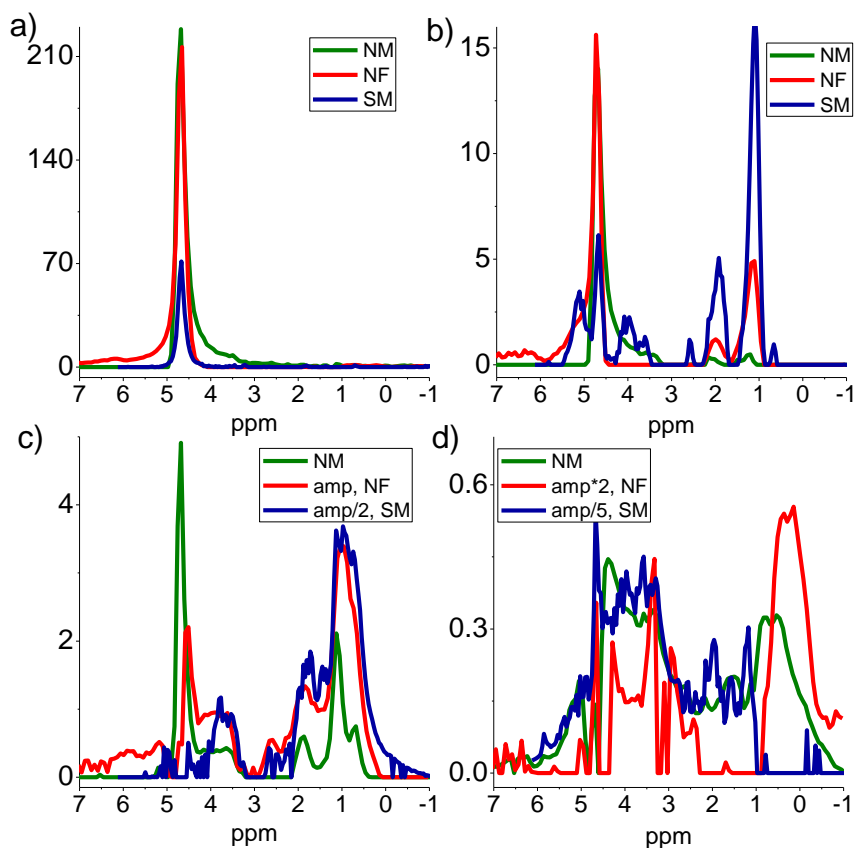

Figure 4.8: DANS of components1 (a), 2 (b), 3 (c) and 4 (d) from NM algae, NF algae and SM algae at Δ= 40 ms.
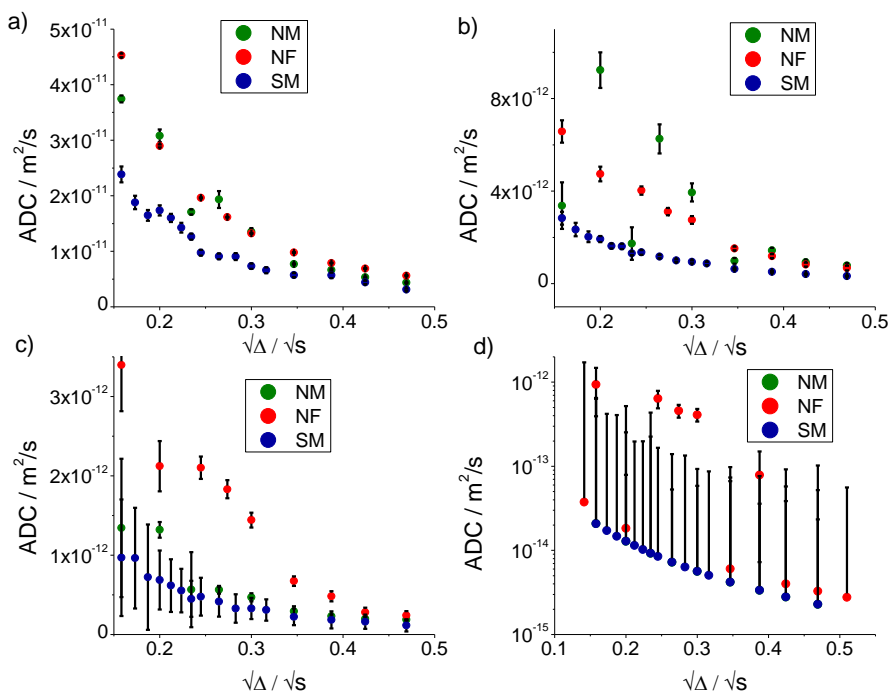
Figure 4.9: *ADC*s of components1 (a), 2 (b), 3 (c) and 4 (d) as a function of diffusion observation time for NM algae (Olive), NF algae (red) and SM algae (royal).

The DANS of component 2 from both NF algae and SM algae show same resonance peaks but with different relative amplitudes (Fig. 4.8b, at Δ=40 ms). Differences in relative amplitudes of the resonances of the spectrum were quite clear. NM algae had a higher intense peak at 4.7 ppm and SM and NF algae had one at 1.14 ppm. The diffusion behaviour of this component was significantly different for NM, NF and SM algae (Fig. 4.9b), maybe because of not well resolved separation of components 1and 2 and/or 2 and 3 (mixing of water protons and lipid protons).

The DANS of component 3 from both NF algae and SM algae had broader resonances than the DANS of component 3 from NM algae (Fig. 4.8c, at Δ=40 ms). Differences in relative amplitudes of the resonances were quite clear, as well in the diffusion behaviour of this component of NF with respect to that of NM and SM (Fig. 4.9c).

The DANS of component 4 from NF algae and SM algae showed substantial changes with respect to DANS of component 4 of NM algae (Fig.

4.8d, at Δ=40 ms). Also, the diffusion behaviour of the components was significantly different (Fig. 4.9d). The ADC was about 35 times faster in NF algae in comparison to NM algae at Δ=120 ms and 22 times at Δ=220 ms and the apparent diffusion was about equal in both NM algae and SM algae. The error bars in the observed ADC's from NM algae (also from SM algae) were quite high because of very slow diffusion. To be able to measure diffusion accurately sufficient signal attenuation by the gradient pulses is a prerequisite. The error bars in the observed ADC's from NF algae were negligible (Fig. 4.9d) because of the faster diffusion, which could be measured accurately with the available maximal gradient strength.
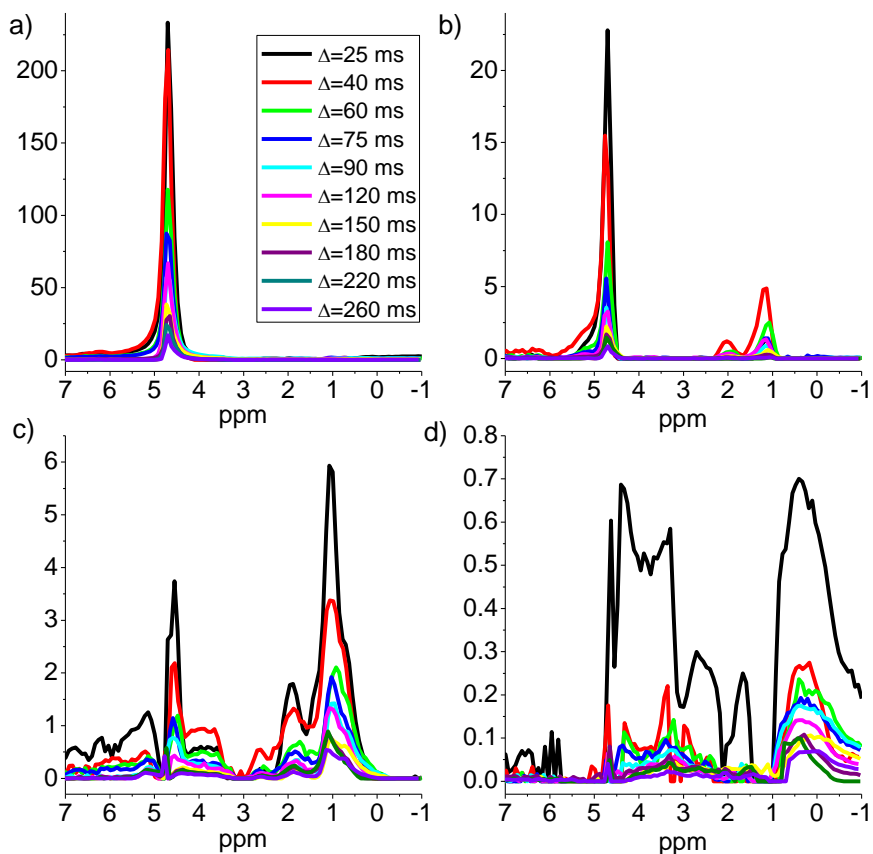

Figure 4.10: DANS as a function of diffusion observation time for component 1 (a), component 2 (b), component 3 (c) and component 4 (d) for NF algae. The colour code is the same in all four plots.

Figs, 4.10 and 4.11, show time dependency of the DANS of all the components for NF algae and SM algae, respectively. It is clear from these figures that the spectra were quite stable with increasing Δ. All components from NF algae had slower decays than the ones from NM algae indicating that the nutrient stress resulted in longer T_1's. Also, components from SM algae showed slightly slower decays in comparison to NM algae.
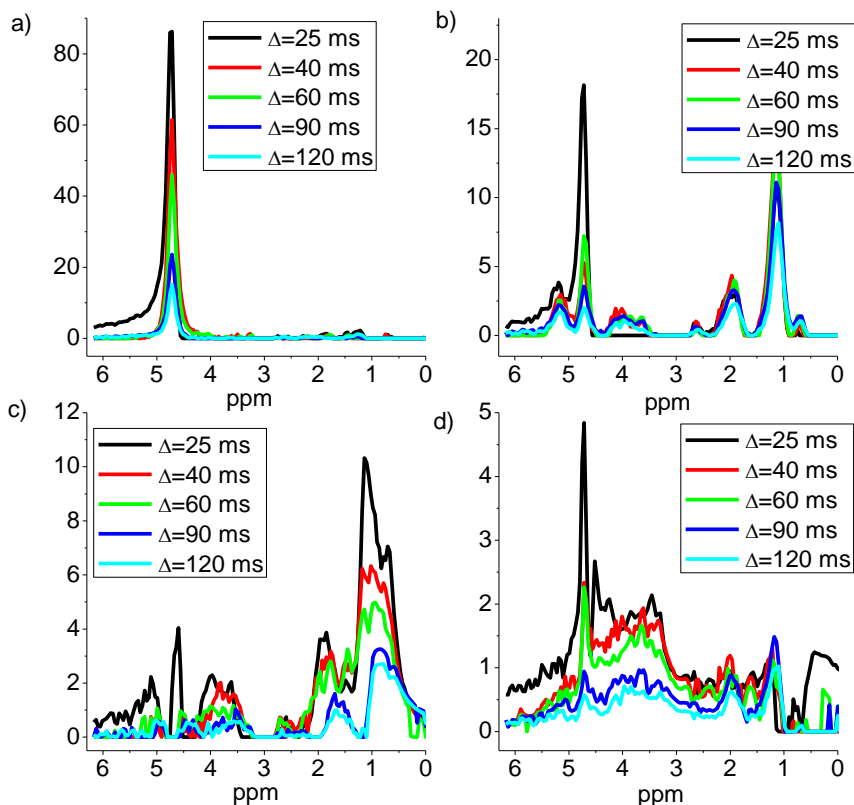

Figure 4.11: DANS as a function of diffusion observation time for component 1 (a), component 2 (b), component 3 (c) and component 4 (d) for SM algae.

4.3.3 DRCOSY measurements

Diffusion-Relaxation correlation spectroscopy (DRCOSY) experiments were performed on all the samples for a diffusion time of 40 ms to obtain the corresponding T_2's related to the *ADC*s. The DRCOSY data was analysed by both CONTIN and SplMod. The D-T_2 correlated plots for WT algae grown

in NM, NF and SM are shown in Figs. 4.12a, b and c, respectively. Table 1 gives an overview of all the results from DOSY and DRCOSY (analysed by both CONTIN and SplMod). It is clear from the table that the best agreement was between DOSY and DRCOSY analysed by CONTIN, but not by SplMod. This is because the SplMod is not really a 2D fit and it is less successful in the discrimination of T_2 components in broad distributions.

4.4 Discussion

The results summarized in Table 1 were obtained by different approaches: DOSY and DRCOSY. The discrimination of components in addition depends on the applied fitting procedure: discrete fitting with a sum of (a limited number of) exponentials (SplMod)[19], a continuous distribution (CONTIN)[26] or a 2-dimensional version of CONTIN (2d-FLI)[18] or multivariate methods[27,28]. It is well known that results of SplMod can differ substantially from those of CONTIN, depending on the differences in relative amplitude, difference in D values and how broad the distributions in the parameters are[29,30]. DOSY makes use of diffusion coefficients of different species to separate their NMR signals. In DOSY, a 1D NMR spectrum is measured for a set of gradient strengths and the set of 1D NMR spectra is further analyzed to extract the corresponding diffusion coefficients. Here, we used SplMod because of its ability to handle exponential sampling of the gradient axis and performed a 'coupled fit' of all spectral points and gradient steps, resulting in a spectral decomposition[31]. Discrimination of components largely depends on the differences in spectral characteristics and the diffusion coefficients.

DRCOSY resolves signals based on diffusion coefficients and relaxation times. DRCOSY is a combination of PGSTE and a multi echo sampling CPMG. In DRCOSY, an echo train was measured for a set of gradient strengths and the set of echo trains was further analyzed by both (2-dimensional) CONTIN and (coupled) SplMod to extract relaxation times and their correlated diffusion coefficients. As mentioned above CONTIN results of DRCOSY were in good agreement with the DOSY results.

Diffusion time dependency of the DANS of the various components (Fig. 4.7) clearly indicates the problem of proper separation of components. Components 2 and 3 are due to both water protons and lipid protons which have diffusion coefficients in the same order of magnitude but with different time dependency, which resulted in scattering of *ADC*s especially for

component 2. Also, amplitude fractions of the components were very small (<10%) in comparison to that of comp 1 and thus they were less accurate.
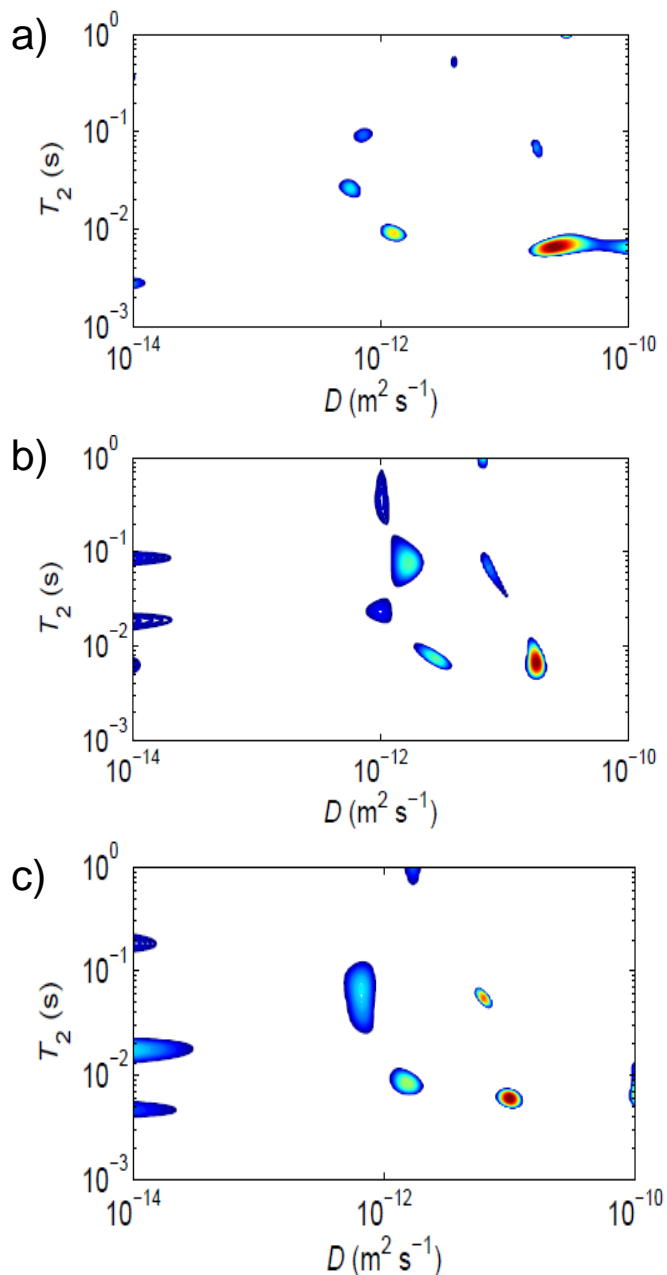

Figure 4.12: Diffusion-relaxation correlated plot at Δ=40 ms for WT *C. reinhardtii* grown in NM a), NF b) and SM c).

Table 1: 4-comp fit results of DRCOSY data analyzed by SplMod for WT algae grown in NM, NF and SM.

| | Component | DOSY | | DRCOSY | | | | |
| | | | | CONTIN | | SplMod | | |
		Relative amplitude %	ADC (μm²/s)	ADC (μm²/s)	T_2 (ms)	Relative amplitude %	ADC (μm²/s)	T_2 (ms)
NM algae	1	90	30	26	7	84	25	3
	2	5.5	9	18	70	6	9	70
	3	3	1.3	1.3, 0.7 & 0.56	10, 98 & 27	10	1.6 & 1.5	31 & 7
	4	1.5	0.013	0.01	3	--	--	--
NF algae	1	84.4	29	18	7	64	14	7
	2	8.6	4.7	7.5	64	5.5	2	280
	3	6.4	2	2.3, 1.6 &1	8, 25, 82 & 353	24	1.9	72
	4	0.6	0.018	0.01	6.5, 18 & 91	6.5	1.1	18
SM algae	1	40	17	10	6	32	1.4	6
	2	22.6	1.9	6.2	58	2	0.84	10240
	3	23.6	0.68	0.64 & 1.5	9 & 64	35.5	0.69	72
	4	13.8	0.0	0.01	5, 18 & 195	30.5	0.3	19

Notwithstanding these limitations, using DOSY and DRCOSY, we were able to discriminate and characterise chloroplast water in *C. reinhardtii* suspensions. T_2 of the chloroplast water was about 7 ms and the ADC was about 3×10^{-11} m²/s at Δ=40 ms. T_2 of the chloroplast water was not changed upon nitrogen stress and salt stress (Fig. 4.12; Table 1). However, because of the osmotic stress chloroplasts (component 1) lost about 50% water in SM algae, according to our estimates using Δ=40 ms (DOSY measurements, Fig. 4.8a) and consequently the chloroplast dimension reduced from 4.6±1.2 μm to 3.8±0.5 μm. In NF algae, changes in chloroplast water content and volume were not substantial.

The size estimated from the dependence of D(Δ) as a function of Δ (Fig. 4.4b) for component 2 from NM algae was about 1.3 μm. The component most probably represents lipid bodies. T_2 of the component was about 70 ms (Fig. 4.12a and Table 1) which is typical for lipids in oil bodies. Component 2 from NF algae had higher intensities than NM at 1.3 ppm and 2 ppm (Fig. 4.8b) indicating that the nutrient stress resulted in accumulation of lipid bodies. The size of the accumulated bodies estimated from the dependence of D(Δ) as a function of $\Delta$was about 2± 0.3μm, very well in agreement to the value reported by Siaut *et al.*[4]. T_2 of this component was about 64 ms (CONTIN fit, Fig. 4.12b). Component 2 from SM algae had also

higher intensities at 1.3 ppm, 2 ppm, 2.6 ppm and at 5.2 ppm (Fig. 4.8b) suggesting that the osmotic stress also resulted in accumulation of lipid bodies. The size of the accumulated bodies estimated from the restricted diffusion behaviour was about 1.3±0.2 μm. T_2 of the lipid bodies was about 60 ms from CONTIN fit (Fig. 4.12c).

Component 3 from NF algae and SM algae had broader peaks in the DANS spectra. *ADC*s of component 3 from NM algae, NF algae and SM algae were 1.3x10^{-12} m^2/s, 3.4x10^{-12} m^2/s and 1x10^{-12} m^2/s, respectively at Δ=25 ms. T_2's of the component from NM algae were about 10 ms, 27 ms and 98 ms and were comparable to those from NF algae.

After growth in a Nitrogen Limited (NL) continuous culture system, *C. reinhardtii* exhibits substantial changes in thylakoid protein profiles[32]. They have reduced amounts of cytochrome b$_6$f, and light-harvesting complexes, 7-fold increased amounts of NADH-PQ oxidoreductase, with major subunits of 51 kDa and 17 kDa and two novel cytochromes of 34 and 12.5 kDa are highly abundant[32]. These differences in amount of various protein complexes and pigment molecules in the thylakoid membrane could explain the substantial changes observed in the relative amplitudes of the peaks in DANS of component 4 from NM, NF and SM algae (Fig. 4.8d).

Component 4 from SM algae did not have resonances in the lower ppm region (+1 to –1) for Δ's from 40 ms – 120 ms. It might be because of fitting problem resulting from differences in relative amplitudes. For Δ=25 ms a 4-component fit is better, but for other diffusion times residuals from the lower ppm region in the 3-comp fit are better than in the 4-comp fit (cf. Residual plots presented in supplementary information). As the residuals from other ppm regions are better in the 4-comp fit for all diffusion observation times, 4 components were considered.

In order to prove that this component 4 indeed relates to pigment-protein (super) complexes in the thylakoid membrane, spinach thylakoid membrane suspensions have also been studied (See Chapter 5). The spectra of component 4 clearly show a different composition in the different systems, and change under environmental stressors, but the diffusion behaviour is very comparable and typical for such systems.
The observed changes in *ADC*s of these components might reflect the reorganization of the photosynthetic protein complexes resulting from the stress (nutrient and salt stress). An increase in diffusion was observed earlier by Iwai *et al.*[33] who measured phosphorylation dependent LHCII

diffusion in isolated thylakoid membranes of *C. reinhardtii* using fluorescence correlation spectroscopy. The diffusion was nearly 2-fold faster (ADC ˜ 2.13±1.2x10⁻¹²m²/s) under phosphorylated conditions as compared to that of de-phosphorylated ones (ADC ˜ 0.92±0.6x10⁻¹²m²/s). However, the *ADC*s calculated by them strongly differ (about 45 times faster) from our results (in the order of 10⁻¹⁴ m²/s) which in turn are in good agreement with reported values for LHCII complexes[5]. In addition, it should be noted that in recent studies, Ünlü *et al.* claimed that a free pool of LHCII exists in *C. reinhardtii*, which plays an important role in short term photo-protection mechanisms during photosynthesis[34,35].

The huge standard deviations for the ADC of this component 4 for NM and SM *C. reinhardtii* were due to insufficient diffusion attenuation of the signal. One can decrease the standard deviations in the ADC by increasing the diffusion attenuation either by increasing δ and/or g. Using stronger gradients (g) is more advantageous than longer gradient pulses as increasing δ results in more T_2-weighting and as the protein complexes already have quite short T_2's. The standard deviations were much smaller in NF *C. reinhardtii* which indirectly indicates that the diffusion was extremely slow in both NM and SM *C. reinhardtii.* Component4 was observed also in DRCOSY measurements for all NM, NF and SM algae but perhaps the insufficient attenuation resulted in such a strange appearance for the signals (Fig. 4.12). T_2 of the component was about 3 ms in NM algae and both nutrient stress and salt stress resulted in longer T_2's (cf. Table 1). Thus, rotational dynamics of the membrane protein complexes became faster in NF algae and SM algae in comparison to that of NM algae. By proper diffusion filtering, these spectra can be obtained in about 5 mins. This opens the possibility to further characterize component 4 by more advanced 2D NMR methods.

4.5 Conclusions

¹H NMR methods (DOSY and DRCOSY) were applied to study (the dynamics of) chloroplast water, lipids in oil bodies and in (thylakoid) membrane and (thylakoid) pigment-protein complexes *in vivo* in *C. reinhardtii* grown in normal medium and under stress conditions. This information has not yet been available for intact photosynthetic micro-organisms. Using restricted diffusion behaviour of chloroplast water, the size or volume of chloroplasts in *C. reinhardtii* of WT grown in normal medium, nitrogen free medium and salty medium could be estimated. Salt stress resulted in substantial changes about 17% in chloroplast size (4.6±1.2 μm in

NM and 3.8±0.5 μm in SM), related to a decrease of about 55% of the volume). T_2 of the chloroplast water was not changed upon stress.

T_2 and restricted diffusion of lipid bodies and membrane lipids could also be measured for NM, NF and SM *C. reinhardtii*. Sizes of the oil droplets as estimated from their hindered diffusion were 1.3±1 μm, 2.0±0.3 μm and 1.3±0.2 μm for NM, NF and SM *C. reinhardtii*, respectively. T_2 of lipid bodies was longer than that of membrane lipids in all the three NM, NF and SM *C. reinhardtii* and T_2 of membrane lipids was comparable in all the three NM, NF and SM *C. reinhardtii*.

Most significantly, we could study dynamics and (changes in) composition of photosynthetic pigment-protein complexes *in vivo* in WT *C. reinhardtii* grown in the three different cultures (NM, NF and SM). By proper diffusion editing these spectra can be measured in about 5 minutes at 300 MHz thus it would be even better at higher field spectrometers.

In conclusion, DOSY and DRCOSY NMR are very useful techniques to study dynamics and amount of chloroplast water, lipids in oil bodies and in (thylakoid) membrane) and (photosynthetic) pigment-protein (super) complexes *in vivo* in *C. reinhardtii* and also to probe changes in the dynamics and composition under changing environmental conditions.

Supporting information

Supporting information is included below: **S4.1.** Residual plot (3-component fit (black) and 4-component fit (red) for all diffusion times) of DANS (7 T ^{1}H DOSY experiment), of a *C. reinhardtii* suspension grown in normal medium (S-1a), nitrogen free medium (S-1b) and excess salt medium (S-1c).
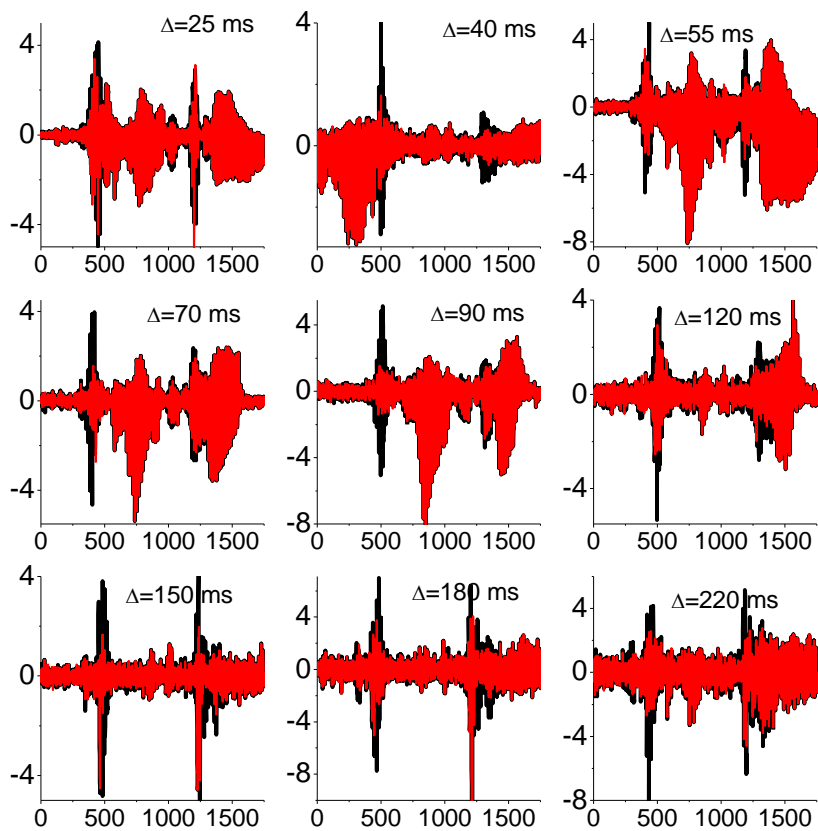
Acknowledgements

Figure S4.1a: Residual plot (3-component fit (black) and 4-component fit (red) for all diffusion times) of DANS (7 T ^{1}H DOSY experiment), of a *C. reinhardtii* suspension grown in normal medium.
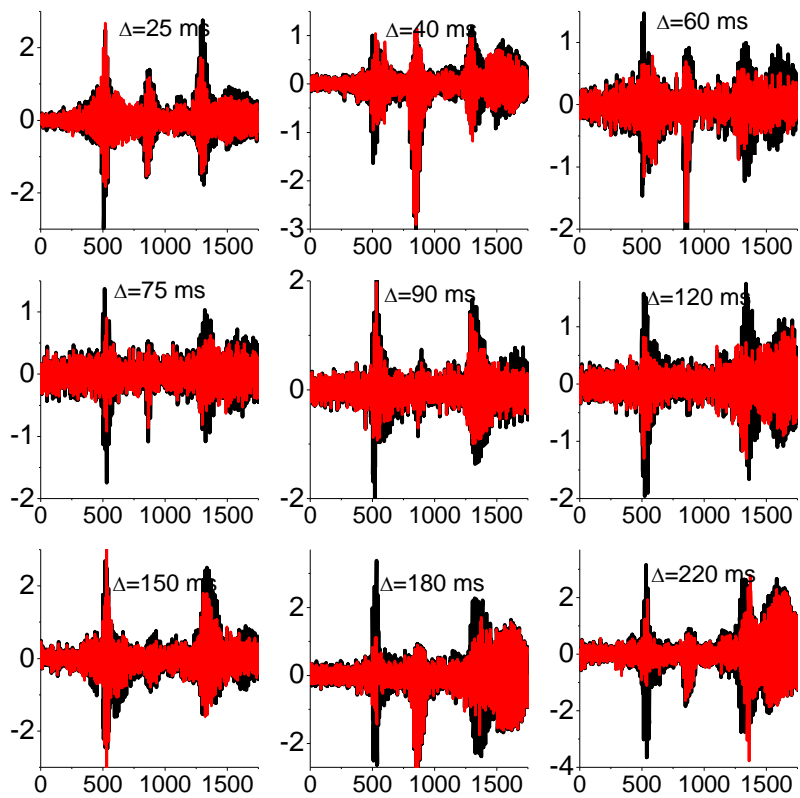
Figure S4.1b: Residual plot (3-component fit (black) and 4-component fit (red) for all diffusion times) of DANS (7 T ^{1}H DOSY experiment), of a *C. reinhardtii* suspension grown in nitrogen free medium.
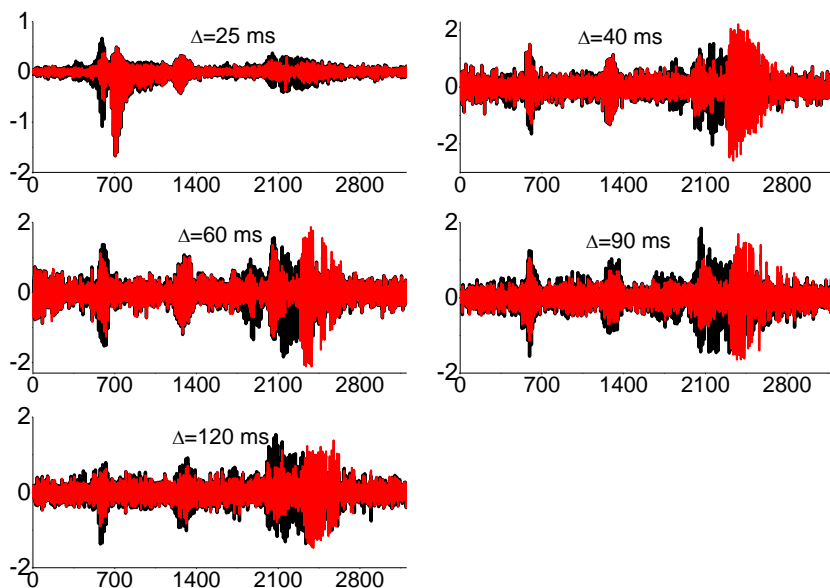
Figure S4.1c: Residual plot (3-component fit (black) and 4-component fit (red) for all diffusion times) of DANS (7 T ^{1}H DOSY experiment), of a *C. reinhardtii* suspension grown in salty medium.

References

1) Kirchhoff, H. (2013). Architectural switches in plant thylakoid membranes. Photosynthesis Research **116**(2-3): 481-487.

2) Kirchhoff, H. (2014). Structural changes of the thylakoid membrane network induced by high light stress in plant chloroplasts. Philosophical Transactions of the Royal Society B: Biological Sciences **369**(1640): 2013-0225.

3) Black, C. C., Sung, S. J. S., Toderich, K., and Voronin, P. Y. (2010).Applying photosynthesis research to increase crop yields. Bull. Georgian Natl. Acad. Sci **4**: 101-110.

4) Siaut, M., Cuiné, S., Cagnon, C., Fessler, B., Nguyen, M., Carrier, P., and Peltier, G. (2011). Oil accumulation in the model green alga Chlamydomonas reinhardtii: characterization, variability between common laboratory strains and relationship with starch reserves. BMC Biotechnology **11**(1): 7.

5) Kana, R. (2013). Mobility of photosynthetic proteins. Photosynthesis Research **116**(2-3): 465-479.

6) Blackwell, M., Gibas, C., Gygax, S., Roman, D., and Wagner, B. (1994).The plastoquinone diffusion coefficient in chloroplasts and its mechanistic implications. Biochimica et Biophysica Acta (BBA)-Bioenergetics **1183**(3): 533-543.

7) Joliot, P., Lavergne, J., and Béal, D. (1992). Plastoquinone compartmentation in chloroplasts. I. Evidence for domains with different rates of photo-reduction. Biochimica et Biophysica Acta (BBA)-Bioenergetics **1101**(1): 1-12.

8) Lavergne, J., Bouchard, J. P., and Joliot, P. (1992). Plastoquinone compartmentation in chloroplasts. II. Theoretical aspects. Biochimica et Biophysica Acta (BBA)-Bioenergetics **1101**(1): 13-22.

9) Mullineaux, C. W., Tobin, M. J., and Jones, G. R. (1997). Mobility of photosynthetic complexes in thylakoid membranes. Nature **390**(6658): 421-424.

10) Kirchhoff, H., Sharpe, R. M., Herbstova, M., Yarbrough, R., and Edwards, G. E. (2013). Differential mobility of pigment-protein complexes in granal and agranal thylakoid membranes of C3 and C4 plants. Plant Physiology **161**(1): 497-507.

11) Sarcina, M., Murata, N., Tobin, M. J. and Mullineaux, C. W. (2003). Lipid diffusion in the thylakoid membranes of the cyanobacterium *Synechococcus sp.*: effect of fatty acid desaturation. FEBS Letters **553**(3): 295-298.

12) Mullineaux, W. And Kirchhoff, H. (2010). Role of Lipids in the Thylakoid membrane dynamics. Advances in Photosynthesis and Respiration **30**: pp 283-294.

13) Gorman, D. S. and Levine, R. (1965). Cytochrome f and plastocyanin: their sequence in the photosynthetic electron transport chain of Chlamydomonas reinhardtii. Proceedings of the National Academy of Sciences of the United States of America **54**(6): 1665.

14) Stejskal, E. O. and Tanner, J. E. (1965). Spin diffusion measurements: spin echoes in the presence of a time-dependent field gradient. Journal of Chemical Physics **42**:288–292.

15) Galvosas, P., Stallmach, F., Seiffert, G., Kärger, J., Kaess, U., and Majer, G. (2001). Generation and application of ultra-high-intensity magnetic field gradient pulses for NMR spectroscopy. Journal of Magnetic Resonance **151**(2): 260-268.

16) Antalek, B. (2002) Using Pulsed Gradient Spin Echo NMR for Chemical Mixture Analysis: How to Obtain Optimum Results. Concepts in Magnetic Resonance **14**: 225-258.

17) Provencher, S.W. (1982). CONTIN: a general purpose constrained regularization program for inverting noisy linear algebraic and integral equations. Computer Physics Communications **27**(3): pp229-242.

18) Song, Y.Q., Venkataramanan, L., Hürlimann, M.D., Flaum, M., Frulla, P. and Straley, C. (2002). T 1–T 2 correlation spectra obtained using a fast two-dimensional Laplace inversion. Journal of Magnetic Resonance **154**(2): pp261-268.

19) Van Resandt, R.W., Vogel, R.H. and Provencher, S.W. (1982). Double beam fluorescence lifetime spectrometer with subnanosecond resolution: Application to aqueous tryptophan. Review of Scientific Instruments **53**(9): pp1392-1397.

20) Sen, P. N. (2004). Time-dependent diffusion coefficient as a probe of geometry. Concepts in Magnetic Resonance Part A **23**(1): 1-21.

21) Mitra, P. P., Sen, P. N., Schwartz, L. M., and Le Doussal, P. (1992). Diffusion propagator as a probe of the structure of porous media. Physical review letters **68**(24): 3555.

22) Gromova, M., Guillermo, A., Bayle, P.A. and Bardet, M. (2015). In vivo measurement of the size of oil bodies in plant seeds using a simple and robust pulsed field gradient NMR method. European Biophysics Journal **44**(3): pp121-129.

23) Nieva-Echevarría, B., Goicoechea, E., Manzanos, M. J., and Guillén, M. D. (2014). A method based on ^{1}H NMR spectral data

useful to evaluate the hydrolysis level in complex lipid mixtures. Food Research International **66**: 379-387.

24) Lindblom, G. and G. Orädd. (2009). Lipid lateral diffusion and membrane heterogeneity. Biochimica et Biophysica Acta (BBA)-Biomembranes **1788**(1): 234-244.

25) Sanders, M., Mueller, R., Menjoge, A., and Vasenkov, S. (2009). Pulsed Field Gradient Nuclear Magnetic Resonance Study of Time-Dependent Diffusion Behaviour and Exchange of Lipids in Planar-Supported Lipid Bilayers. The Journal of Physical Chemistry B **113**(43): 14355-14364.

26) Van Resandt, R.W., Vogel, R.H. and Provencher, S.W. (1982). Double beam fluorescence lifetime spectrometer with subnanosecond resolution: Application to aqueous tryptophan. Review of Scientific Instruments **53**(9): pp1392-1397.

27) Huo, R., Wehrens, R., Van Duynhoven, J. and Buydens, L.M.C. (2003). Assessment of techniques for DOSY NMR data processing. Analytica Chimica Acta **490**(1): pp231-251.

28) Nilsson, M. and Morris, G.A. (2007). Improved DECRA processing of DOSY data: correcting for non-uniform field gradients. Magnetic Resonance in Chemistry **45**(8):pp656-660.

29) Kroeker, R. M. and Henkelman, R. M. (1986). Analysis of biological NMR relaxation data with continuous distributions of relaxation times. Journal of Magnetic Resonance **69**(2): 218-235.

30) Dekkers, B.L., De Kort, D.W., Grabowska, K.J., Tian, B., Van As, H. and van der Goot, A.J. (2016). A combined rheology and time domain NMR approach for determining water distributions in protein blends. Food Hydrocolloids **60**: pp.525-532.

31) De Kort, D.W., Van Duynhoven, J.P., Hoeben, F.J., Janssen, H.M. and Van As, H. (2014). NMR nanoparticle diffusometry in hydrogels: enhancing sensitivity and selectivity. Analytical chemistry **86**(18): pp9229-9235.

32) Peltier, G. and G. W. Schmidt (1991). Chlororespiration: an adaptation to nitrogen deficiency in Chlamydomonas reinhardtii. Proceedings of the National Academy of Sciences **88**(11): 4791-4795.

33) Iwai, M., Pack, C. G., Takenaka, Y., Sako, Y., and Nakano, A. (2013). Photosystem II antenna phosphorylation-dependent protein diffusion determined by fluorescence correlation spectroscopy. Scientific Reports**3**.

34) Ünlü, C., Drop, B., Croce, R. and van Amerongen, H. 2014. State transitions in Chlamydomonas reinhardtii strongly modulate the functional size of photosystem II but not of photosystem I. Proceedings of the National Academy of Sciences **111**(9): 3460-3465.

35) Ünlü, C., Polukhina, I. and van Amerongen, H. 2016. Origin of pronounced differences in 77 K fluorescence of the green alga Chlamydomonas reinhardtii in state 1 and 2. European Biophysics Journal **45**(3):209-217.Kirchhoff, H. (2013). Architectural switches in plant thylakoid membranes. Photosynthesis Research **116**(2-3): 481-487.

5

Study of water and lipid dynamics in *Synechocystis* sp.PCC 6803 by non-invasive DRCOSY and DOSY-DANS ^{1}H NMR

Abstract

Non-invasive ^{1}H NMR methods (DOSY and DRCOSY) are used to study the dynamics of water molecules in water pools, lipids in oil bodies and in thylakoid membranes and pigment-protein complexes under complete *in vivo* conditions in a suspension of the blue-green alga *Synechocystis* sp.PCC 6803. The Diffusion Associated NMR Spectra (DANS), the corresponding diffusion coefficients and the T_2 values of the different components are compared with those observed in suspensions of *C. reinhardtii*, a unicellular green alga, and of isolated spinach thylakoids. The differences in membrane composition (ratio of the different membrane lipids) were clearly observed in the DANS of the oil bodies and the (thylakoid) membranes, but the diffusion coefficients were quite comparable. Also the DANS of the component that is assigned to the pigment-protein complexes are quite different, reflecting the differed composition. The diffusion coefficients of this component in isolated spinach thylakoids and in C. reinhardtii are very comparable, but about a factor of 10 lower with respect to that of Synechocystis at short diffusion times. The dynamics of these complexes in these systems are thus quite different. The presented methods can be used to study volume regulation of the cells and to probe changes in the water and lipid dynamics, changes in the (thylakoid) membrane organization/composition and dynamics under changing environmental conditions.

5.1 Introduction

Photosynthesis is one of the most important processes for life on earth which releases oxygen as a by-product. Photosynthesis occurs in plants, microalgae and also in some bacteria. Light dependent photosynthetic reactions take place in the thylakoid membrane and dark reactions in the stroma of the chloroplasts in plants and microalgae and in the cytosol in cyanobacteria. In order to optimize photosynthesis in changing environmental conditions the photosynthetic membrane reorganizes its protein organization. These reorganizations include state transitions that balance the excitation of the two photosystems, non-photochemical quenching, which thermally dissipates excess energy at the level of the light-harvesting antenna, and cyclic electron flow, which supplies the increased ATP demand needed for by CO2 assimilation[1].

Mobility of the pigment-protein complexes and of the thylakoid membrane lipids plays a very crucial role in the thylakoid membrane reorganization. We were able to study the mobility of the thylakoid membrane lipids in intact leaf disks and also in *C. reinhardtii* suspension (Chapters 2 and 4, respectively) using PFG ^{1}H NMR methods. In *C. reinhardtii* suspension (changes in) the dynamics of the accumulated lipid bodies upon nutrient stress and salt stress, of the membrane lipids and of the photosynthetic protein complexes were studied. Here we applied the developed PFG NMR methods to study the thylakoid membrane dynamics in the prokaryotic photosynthetic cyanobacterium*Synechocystis*sp.PCC 6803. Both *C. reinhardtii* and cyanobacteria are model systems to study photosynthesis. Synechocystis is also of interest for biofuel production and therefore we will try to detect the lipid fractions. In comparison to *C. reinhardtii* cyanobacteria like Synechocystis have a higher thylakoid membrane fraction with a different composition of the light-harvesting complexes (phycobilisomes are appressed against the thylakoid membranes) and also a different structure of the thylakoid membranes (stack of parallel sheets). We studied whether the above mentioned differences are visible in the different components that we observe with PFG ^{1}H NMR, especially the ones we assigned to (membrane) lipids and the photosynthetic pigment-protein complexes (Chapter 4). In addition to Synechocystis suspensions of isolated spinach thylakoids were measured for comparison and as a reference.

In addition to the thylakoid lipid membrane dynamics this chapter also describes Synechocystis water dynamics and the possibilities to study Synechocystis volume regulation.

5.2 Materials and Methods

5.2.1 Wild Type *Synechocystis*sp.PCC 6803

Wild Type *Synechocystis*sp.PCC 6803 cells were grown under continuous white-light illumination in BG-11 (Allen, 1968)[2] buffered with 20mM HEPES-NaOH (pH 7.5) and sodium carbonate was omitted. Synechocystis cells were shaken in a rotary shaker (100 rpm) at 30 °C and illuminated by a white lamp at 50 μmol.m^{-2}.s^{-1}. The cells were grown in 250 mL flasks with a growing volume of 100 mL and maintained in the logarithmic growth phase. The 100 mL suspension was further centrifuged to get about 800 μL of highly concentrated cells.

Spinach thylakoids were isolated from fresh spinach leaves using the method described by Caffarri *et al*[3].

5.2.2. DOSY and Diffusion Associated NMR Spectra

A special NMR (Shigemi) tube was used for all experiments in order to minimise susceptibility differences coming from the interface between liquid sample and air. All high-field ^{1}H NMR diffusometry experiments were performed at 7 T (300 MHz ^{1}H Larmor frequency) using a Bruker Avance II spectrometer equipped with a Bruker diff25 diffusion probehead, which delivers a maximum field gradient strength of 10 T m^{-1}.

DOSY NMR diffusometry were carried out using a stimulated echo experiment in combination with bipolar sine-bell shaped gradients (so-called 13-interval). The echo attenuation as a function of the experimental parameters can be described by the Stejskal-Tanner equation[4]

$$\frac{I}{I_0} = \sum_i A_i e^{-(\gamma \delta g)^2 \left(\Delta - \delta/3\right) D_i},$$

where $\frac{I}{I_0}$ is the echo attenuation, A_i the amplitude of the NMR signal of component *i*, γ the gyromagnetic ratio of the relevant nucleus (rad T^{-1} s^{-1}), δ the effective gradient pulse duration (s), *g* the gradient strength (T m^{-1}), Δ the effective diffusion time (s), and D_i the diffusion coefficient of component *i* (m^2 s^{-1}).

Stimulated echo experiments were performed in order to detect shorter T_2 components at longer diffusion observation times[5]. Bipolar gradients were used to compensate for internal field gradients, which are present at high field strengths in inhomogeneous samples. The effective gradient pulse

duration δ was set to 2 ms for Synechocystis and 3 ms for spinach thylakoids in order to have sufficient attenuation to measure the slow diffusion observed in the spinach thylakoids. The effective diffusion time Δ was varied between 20 and 60 ms for Synechocystis and between 25 and 150 ms for spinach thylakoids. The gradient intensity was varied between 1 and 8 T m^{-1} for Synechocystis and between 2 and 8 T m^{-1} for spinach thylakoids (in order to have proper attenuation).The attenuation of NMR spectra as a function of gradient intensity was analysed by fitting 1 to 4 exponential decays to the spectra using SplMod (Provencher, 1982)[6], which was set to perform a coupled exponential fit of the spectral data points. This resulted in 1 to 4 diffusion-associated NMR spectra (DANS). The procedure is similar to the DECRA curve resolution method described elsewhere[7], but SplMod is preferred because it can handle both linear and logarithmic sampling of the gradient axis[4].

Dimensions of the compartments were estimated as described in chapter 2 (Materials & Methods).

DRCOSY

Diffusion-relaxation experiments were performed on a 300 MHz spectrometer equipped with a gradient coil capable of delivering a 10 T m^{-1} field gradient. A stimulated echo-based diffusion experiment, using unipolar gradients and rectangular pulse shapes, was combined with a time-domain CPMG experiment. The effective gradient pulse duration δ was set to 2 ms and the effective diffusion time Δ was 30 ms. Gradient strength was varied between 1 and 8 T m^{-1}. An echo time of 0.2 ms was used and 2k echoes were recorded. The data was analysed using 2D Laplace transformation.

5.3 Results

5.3.1 DOSY

^{1}H diffusion was measured in a Synechocystis suspension for diffusion observation times from 20 ms to 60 ms in order to study the dynamics of water and lipids. Diffusion attenuated ^{1}H NMR spectra of Synechocystis for Δ= 30 ms are shown in Fig. 5.1. Here, medium water signal was suppressed using a diffusion−filter (first gradient-step was chosen to be 1 T/m).We were able to decompose the attenuated spectra into components with different associated diffusion coefficients (Diffusion Associated NMR Spectra, DANS) by coupled fitting of the attenuation of the individual spectral points.

Diffusion associated ^{1}H NMR spectra of Synechocystis for Δ= 30 ms are shown in Fig. 5.2. A four component fit was found to be the best for all the diffusion observation times based on residual plots (shown in supplementary data).
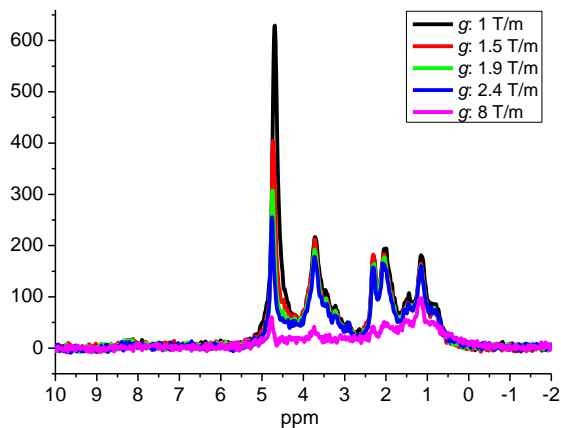

Figure 5.1: Diffusion attenuated ^{1}H NMR spectra of Synechocystis for Δ= 30 ms, δ= 2 ms, g: 1−8 T/m (medium water was already suppressed at first g-step of 1 T/m).
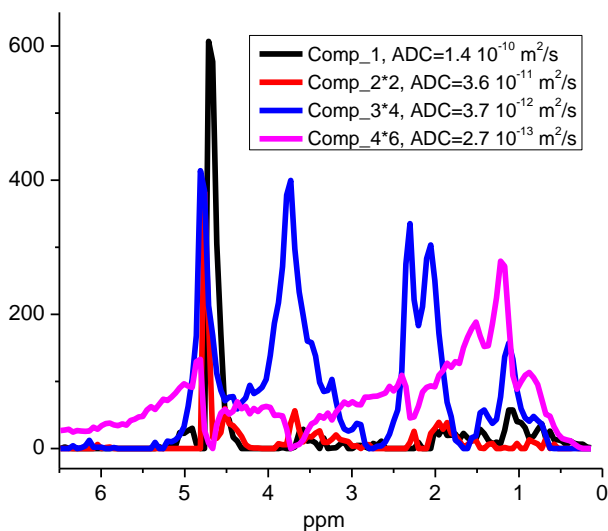

Figure 5.2: Diffusion associated ^{1}H NMR spectra of Synechocystis for Δ= 30 ms, δ= 2 ms, g: 1−8 T/m (medium water was suppressed using a D−filter). Amplitudes of the components 2, 3 and 4 were multiplied by 2, 4 and 6, respectively.

The DANS of component 1 as a function of Δ is shown in Fig. 5.3a.The amplitude fraction of this component was about 82% of the total signal at Δ=20 ms. The spectrum showed a large resonance at 4.7 ppm and minor (just above the noise level) resonances at 0.7 ppm, 1.2 ppm, 1.4 ppm, 1.7 ppm, 3.1 ppm, 3.6 ppm and 5 ppm. The behaviour of the amplitude as a function of Δ was quite different for the water resonance at 4.7 ppm and the other resonances indicating that the water protons had a shorter T_1. The apparent diffusion coefficient (ADC) of the component was 1.4×10^{-10} m^2/s at Δ=30 ms and restricted diffusion was observed (Fig. 5.3b). The size of the compartment as estimated from the Δ-dependence of D(Δ) was about 8.5 μm. This value fits quite well with the size of a Synechocystis cell, indicating that the component stems mainly from water inside Synechocystis.

The DANS of component 2 as a function of $\Delta$is shown in Fig. 5.3c. The amplitude fraction of the component was about 5% of the total signal at Δ=20 ms. The spectrum showed a very large resonance at 4.7 ppm and small resonances at 4.45 ppm, 3.6 ppm, 2.2 ppm, 1.9 ppm and 1.8 ppm. The ADC of the component was 3.6×10^{-11} m^2/s at Δ=30 ms. Probably, it was from both water protons (4.7 ppm) and lipid protons diffusing at about the same rates. It might represent lumenal water and lipid bodies. The water protons have a shorter T_1 than the other protons as manifest from the amplitude behaviour of the signals as a function of Δ (Fig. 5.3c).

The DANS of component 3 as a function of Δ is shown in Fig. 5.3e. The amplitude fraction of the component was about 8% of the total signal at Δ=20 ms. The spectrum showed resonances at chemical shifts of lipid protons such as CH_3(0.7–0.9 ppm), CH_2(1.1 ppm), CH_2CH_2COO (1.62 ppm), CH_2–CH=CH (2.02–2.09 ppm), CH–OH (3.4–4 ppm) and α, β glycosidic bonds (4–5 ppm)[8]. Also for this component the amplitude behaviour as a function of Δ was different for the resonance at 4.7 ppm and for the other resonances. The corresponding ADC was about 3.7×10^{-12} m^2/s at Δ=30 ms. Component 3 showed restricted diffusion (Fig. 5.3f). The DANS and ADC of component 4 as a function of Δ are presented in Figs. 5.3g and 5.3h, respectively. The amplitude fraction of this component was about 5% of the total signal at Δ=20 ms and the spectrum shows quite broad resonances. The amplitudes of the resonances around 4-6 ppm decay faster than those around 1 ppm with increasing Δ, indicating differences in T_1 values of the spins. The ADC of the component was 2.7×10^{-13} m^2/s at Δ=30 ms.
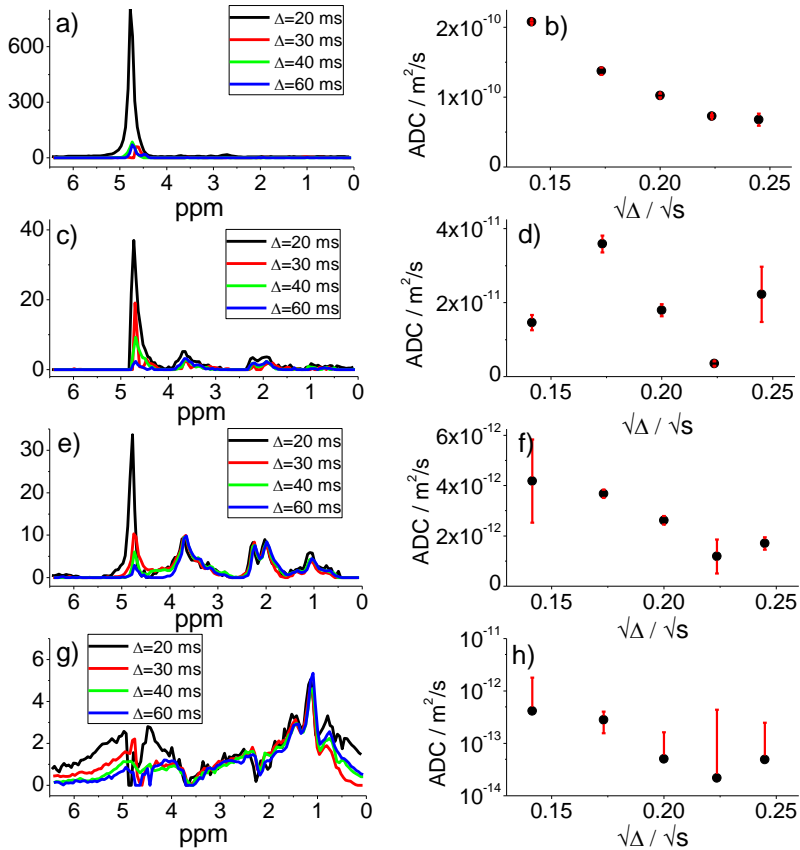
Figure 5.3: DANS as a function of diffusion labelling time Δ for components 1 (a), 2 (c), 3 (e) and 4 (g) and *ADC*s as a function of diffusion labelling time Δ for components 1 (b), 2 (d), 3 (f) and 4 (h) for Synechocystis suspension.

Diffusion was also measured for a suspension of spinach thylakoids, mainly to compare the lipid/protein composition and dynamics with the components observed in Synechocystis. Because the observed diffusion was slower in the spinach thylakoids suspension, diffusion was measured with δ=3 ms and *g*: 2-8 T/m. A three component fit was found to be the best for all Δ from 20 ms to 150 ms. The time dependency of the DANS of all the three components and the associated diffusion behaviour are shown in Fig. 5.4.

The behaviour of the amplitude as a function of Δ was quite different for the water resonance at 4.7 ppm and the other resonances for both components 1 and 2. For component 3, the amplitudes of the resonances around 4-6 ppm decay faster than those around 1 ppm with increasing Δ as observed for component 4 from the Synechocystis suspension.
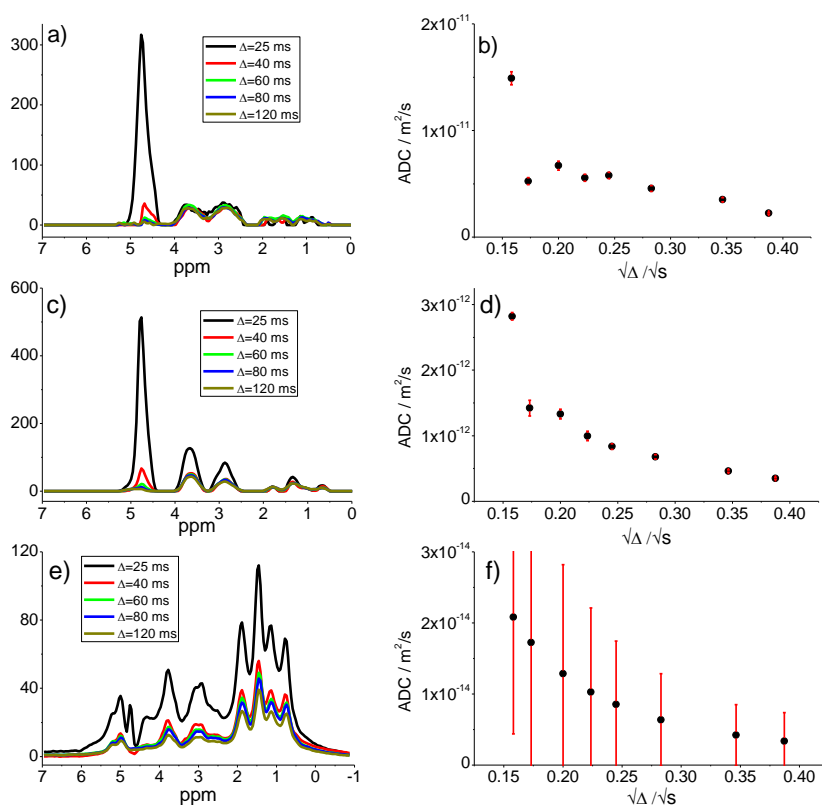

Figure 5.4: DANS as a function of diffusion labelling time Δ for components 1 (a), 2 (c) and 3 (e) and *ADC*s as a function of diffusion labelling time Δ for components 1 (b), 2 (d) and 3 (f) for spinach thylakoids suspension.

5.3.2 DRCOSY

Diffusion-Relaxation correlation spectroscopy (DRCOSY) experiments were performed on a Synechocystis suspension for a diffusion time of 30 ms to determine the corresponding T_2's of the ADC's. The DRCOSY data was fit

by both CONTIN and SPLMOD. The D-T_2 correlated plot resulting from the CONTIN fit is shown in Fig. 5.5. Four diffusion distributions were observed.
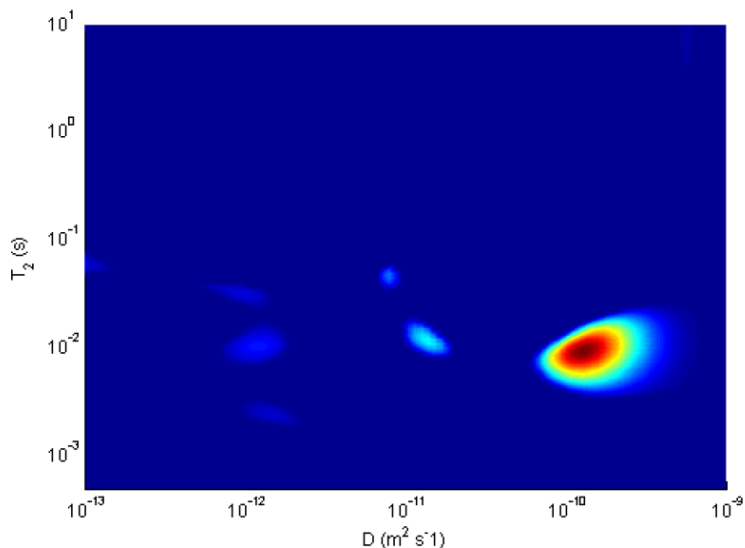

Figure 5.5: Diffusion-T_2 relaxation correlated plot for Synechocystis suspension at Δ=30 ms.

Table 1 shows the 4-comp fit results of DRCOSY data analyzed by SPLMOD. The ADC of component 1 from the CONTIN fit was 1.8×10^{-10} m²/s and was about 3-fold slower in the SPLMOD fit. This component showed diffusion similar to that of component 1 as observed with DOSY experiments. The T_2 of this component from both CONTIN and SPLMOD was about 10 ms which is quite close to the T_2 of chloroplast water in *Ficus benjamina* leaf disks. Therefore, the component was assigned to Synechocystis water.

Component 2 showed an ADC similar to that of component 2 as observed with DOSY experiments. The component had two T_2's in the order of about10 ms and 50-60 ms from CONTIN and T_2 of the component was only about 3 ms from SPLMOD.

The ADC of component 3 as obtained from the DRCOSY measurements was 1.5×10^{-12} m²/s, which corresponds to component 3 of the DOSY measurements. The component had T_2 values around 3, 10 and 35 ms as

Table 1: Four component fit results of DRCOSY data (cf. Fig. 5.6) analyzed by SPLMOD

	Comp 1	Comp 2	Comp 3	Comp 4
Fraction	0.87	0.035	0.08	0.015
T_2 (s)	0.009	0.003	0.028	0.076
ADC (m^2/s)	5×10^{-11}	5×10^{-12}	3.2×10^{-12}	1.2×10^{-12}

obtained from the CONTIN fit and around 28 ms when applying SPLMOD. The ADC of the component 4 from the DRCOSY measurements was 1.2×10^{-12} m^2/s when applying SPLMOD and was $1\text{-}2\times10^{-13}$ m^2/s as obtained from the CONTIN fit which is close to the value of component 4 as obtained from the DOSY measurements. The T_2's of the signal were 3 ms (SPLMOD) and 60 ms (CONTIN).

5.4 Discussion

In order to suppress the medium water to be able to detect the Synechocystis water, the first gradient step was chosen to be 1 T/m instead of 2 T/m as used in *C. reinhardtii* suspensions, because of higher mobility of water and lipids in the Synechocystis suspension in comparison to suspension of *C. reinhardtii* cells and spinach thylakoids (Figs. 5.6b-5.8b). Calculated D_0's of cell water were about 4.4×10^{-10} m^2/s and 3.5×10^{-10} m^2/s in Synechocystis and *C. reinhardtii* suspensions, respectively. The calculated D_0 of chloroplast water in *C. reinhardtii* suspension was about 6×10^{-11} m^2/s. Thus, in order to observe chloroplast water and other slower components the first gradient step was chosen to be 2 T/m in *C. reinhardtii* suspension.

Because of the different structure of Synechocystis, only one (cellular) water pool (other than the lumenal water pool) was observed whereas two water pools (cytoplasmic water and chloroplast water) were observed in *C. reinhardtii* (Chapters 2 and 4). In Fig. 5.6 we compared the related spectra and ADC's as a function of Δ for these water pools. Water of both *C. reinhardtii* and Synechocystis was more mobile and less restricted than the

chloroplast water of *C. reinhardtii* (Fig. 5.6b). T_2's of the cell water (Fig. 2.2 from Chapter 2) and chloroplast water (Fig. 4.14 from Chapter 4) from *C. reinhardtii* were around 15 ms and 3 ms, respectively. T_2 of the Synechocystis water was about 10 ms.
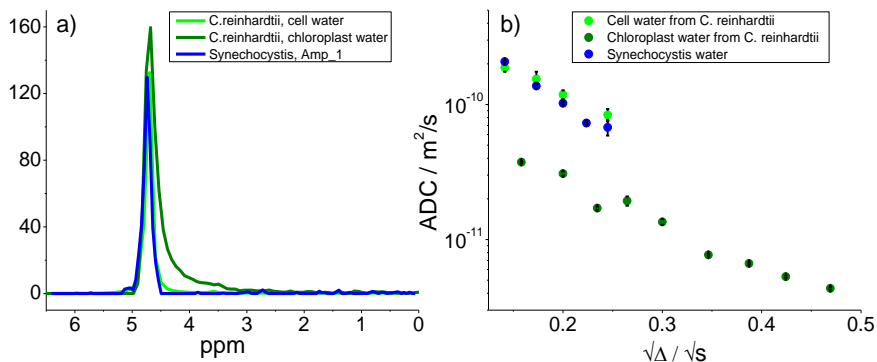

Figure 5.6: DANS at Δ=40 ms (a) and ADC as a function of diffusion labelling time Δ (b) for cell water (green) and chloroplast water (olive) of *C. reinhardtii* and Synechocystis water (blue).

Component 1 from spinach thylakoids suspension may represent water restricted to grana, the lumen water pool and sorbitol (originating from the isolation procedure) as the DANS of the component had a large water peak at short Δ values and relatively smaller signals from sorbitol and lipids. In case of *C. reinhardtii*, component 2 showed higher intensity signals at lower ppm upon nutrient stress and salt stress (Fig. 4.8b in Chapter 4) because of the accumulated lipid bodies. Component 2 from Synechocystis may also have contributions from lipid bodies and the component had two T_2's in the order of about 10 ms and 50-60 ms (Fig. 5.5).
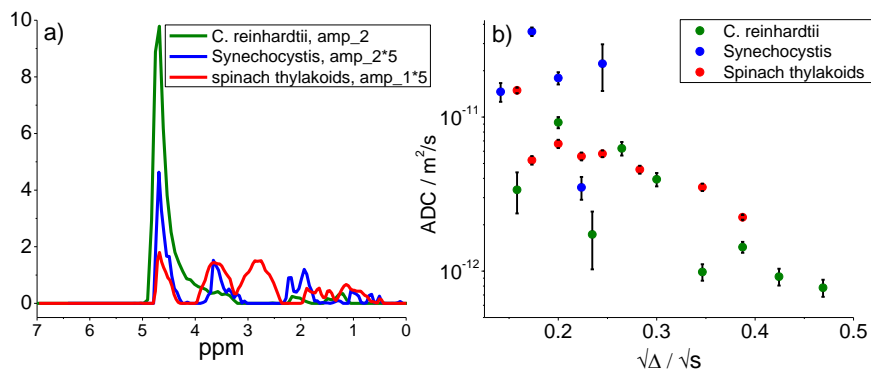
Figure 5.7: DANS at Δ=40 ms (a) and ADC as a function of diffusion labelling time Δ (b) for component 2 from *C. reinhardtii* (olive) and Synechocystis (blue, amplitude was multiplied by 5) and for the component 1 from spinach thylakoids suspension (red, amplitude was multiplied by 5).

In Fig. 5.8 the DANS (a) and diffusion behaviour (b) of membrane lipids from *C. reinhardtii*, the component 3 from the Synechocystis and component 2 from spinach thylakoids are compared. All the three systems had resonances below 2.2 ppm and above 3.3 ppm though their relative amplitudes were quite different. Synechocystis has an intense doublet at around 2-2.3 ppm, *C. reinhardtii* at 1.1 ppm (comparable to Synechocystis at 1.1 ppm) and the spinach thylakoids show high intensity at 1.37 ppm and around 3.3 ppm. Both Synechocystis and spinach thylakoids have intense signals at 4.7 ppm and at 3.7 ppm, *C. reinhardtii* only at 4.7 ppm. Only spinach thylakoids has a resonance at 2.7 ppm and only Synechocystis has a resonance at 2.3 ppm. The lipid compositions of cyanobacteria, algae and higher plants are very similar although the ratios can differ[9]. All the above mentioned differences in the spectra may be due to a difference in the various lipid ratios. If the DGDG fraction is higher, then the signal at 3.4-4 ppm can be higher such as in Synechocystis and if the SQDG fraction is more than the –CH2 resonance at 1.0-1.2 ppm can be higher. Nuzzo *et al.*[10] and Masuda *et al.*[11] reported quantitative analysis of the lipids in microalgal samples, which clearly indicated that the lipid ratios are quite different in the three samples. The T_2's of the membrane lipids from Synechocystis were about 3, 10 and 35 ms (Fig. 5.5 and Table 5.1).
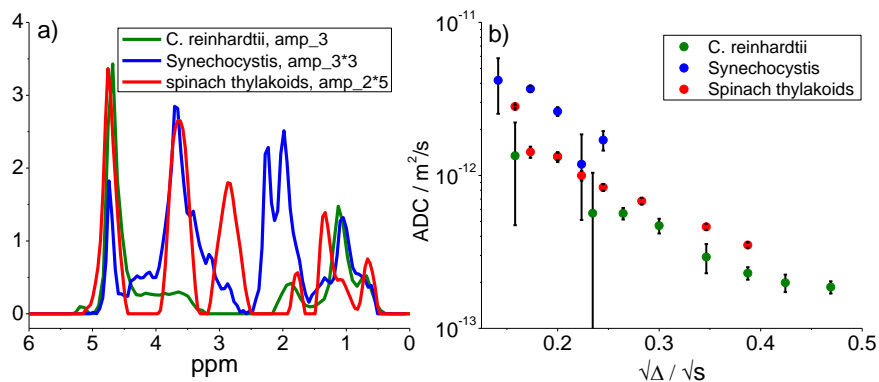
Figure 5.8: DANS at Δ=40 ms (a) and ADC as a function of diffusion labelling time Δ (b) for component 3 from *C .reinhardtii* (olive) and Synechocystis(blue, amplitude was multiplied by 3) and for the component 2 from spinach thylakoids suspension (red, amplitude was multiplied by 5).

Sarcina *et al*. (2003) found a diffusion coefficient of a lipid soluble marker in cells of the cyanobacterium *Synechococcus*PCC 7942, using Fluorescence Recovery After Photobleaching (FRAP), of about $0.3×10^{-12}$ m^2/s[12]. Membrane lipid diffusion in *C. reinhardtii* was in that order, $0.1-1×10^{-12}$ m^2/s, but the observed diffusion of component 3 in Synechocystis was faster ($0.9-3.6×10^{-12}$ m^2/s) indicating that the diffusion in (thylakoid) membranes can be quite different in different systems.

The spectra of component 4 for Synechocystis and *C. reinhardtii* and component 3 for spinach thylakoids show substantial differences but the *ADC*s are comparable at long diffusion observation times (Fig. 5.9). The ADC of component 4 at Δ=50 ms from Synechocystis was about $2×10^{-14}$ m^2/s and was in the order of the ADC of component 3 from spinach thylakoids and component 4 from *C. reinhardtii* (Fig. 5.9b). The diffusion coefficient of phycobilisomes on the thylakoid membrane surface in *Synecoccocus* PCC 7942 is about $3×10^{-14}$ m^2/s[13] which is in the order of ADC of component 4 at Δ=50 ms and thus component 4 from Synechocystis may have contributions from phycobilisomes. T_2's of the component were 3 ms and 60 ms. The diffusion coefficient of LHCII (light-harvesting complex II of plants and green algae) was reported to be $0.8×10^{-14}$ m^2/s in isolated spinach thylakoid membranes by Consoli *et al.*[14]. This value fits quite well to the ADC of the slowest component from both spinach thylakoids and *C.*

reinhardtii. So the slowest component from both spinach thylakoids and *C. reinhardtii* might have some contribution from LHCII. By proper diffusion filtering, the spectra of component 4 can be obtained in about 5 mins choosing only the last gradient step. This opens the possibility to further characterize the component by more advanced 2D NMR methods.
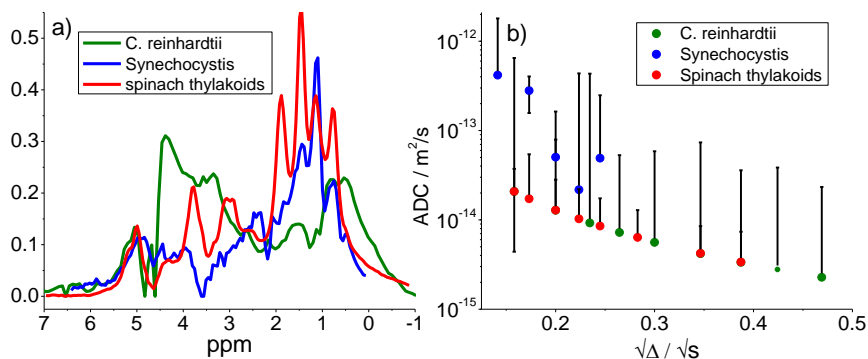

Figure 5.9: DANS at Δ=40 ms (a) and ADC as a function of diffusion labelling time Δ (b) for component 4 from *C. reinhardtii* (olive) and Synechocystis(blue) and for the component 3 from spinach thylakoids suspension (red).

5.5 Conclusions

Synechocystis water can be detected using ^{1}H NMR DOSY and DRCOSY experiments with an appropriate D-filter. The ADC of the water was about 1×10^{-10} m^2/s at Δ=30 ms and T_2 was about 10 ms. Thus, it is possible to measure T_2 and ADC of the Synechocystis water even at low field strengths and using a maximum gradient strength of 1 T/m. Hindered diffusion of the water was observed and the estimated size from the hindered diffusion was about 8.5 μm, which corresponds to the size of a Synechocystis cell. Using the cell water signal it is possible to study Synechocystis volume regulation and to probe changes in the water dynamics under changing environmental conditions.

In addition (thylakoid) membrane lipids and their dynamics have been studied in both Synechocystis and spinach thylakoids suspensions. Diffusion NMR is a completely *in vivo* approach to study the membrane dynamics in Synechocystis. Using this approach we were able to detect the difference in thylakoid membrane composition in Synechocystis, *C. reinhardtii* and spinach thylakoids. It is also possible to probe the changes in

the membrane organization/composition and dynamics under changing environmental conditions by this technique. The T_2's of component 2 (perhaps lumenal water and lipid bodies) from Synechocystis were about 10 ms and 50-60 ms. The T_2's of the membrane lipids were about 3, 10 and 35 ms. The slowest component from Synechocystis might have contributions from phycobilisomes but further research has to be done for complete characterization.

Supporting information

Supporting information is included below: **S5.1:** Residual plot (3-component fit (black) and 4-component fit (red) for all diffusion times) of DANS (7 T ^{1}H DOSY experiment), of a *Synechocystis* suspension. **S5.2:** Residual plot (2-component fit (black), 3-component fit (red) and 4-component fit (blue) for all diffusion times) of DANS (7 T ^{1}H DOSY experiment), of a spinach thylakoids suspension.
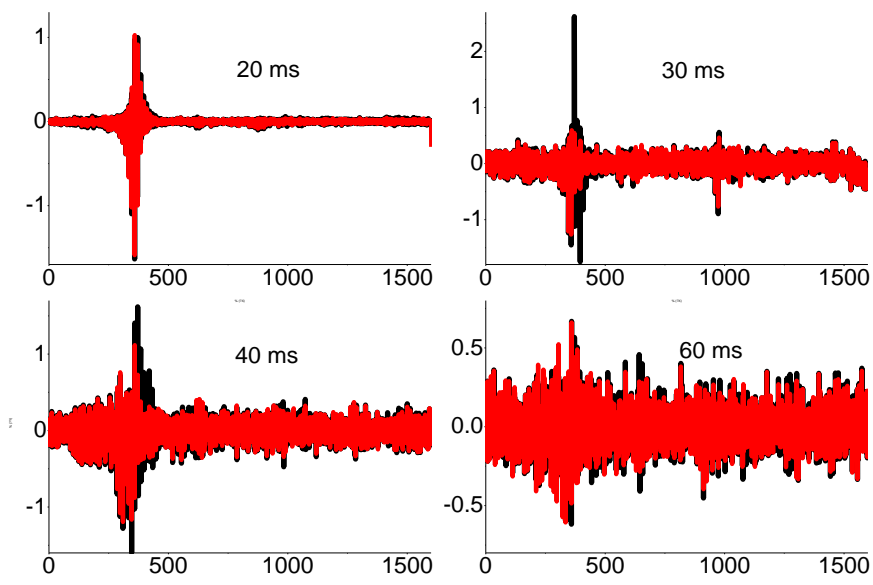
Acknowledgements

Figure S5.1: Residual plot (3-component fit (black) and 4-component fit (red) for all diffusion times) of DANS (7 T ^{1}H DOSY experiment), of a *Synechocystis* suspension.
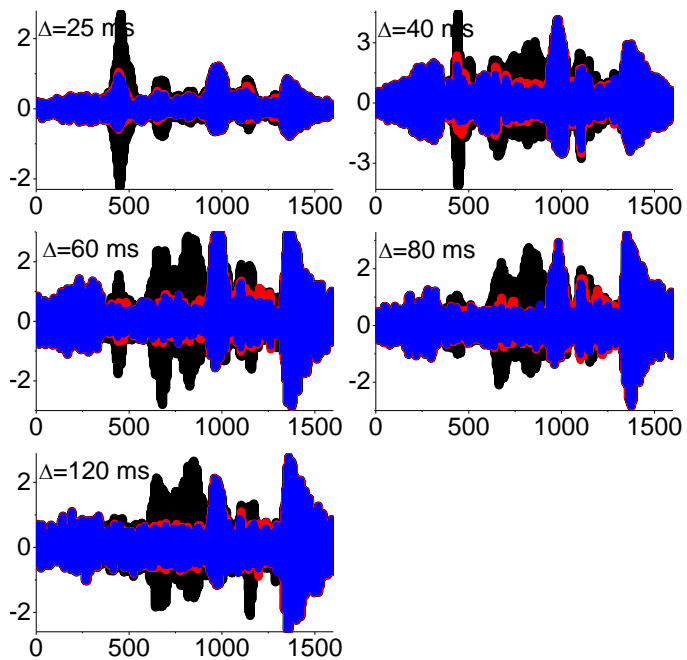
Figure S5.2: Residual plot (2-component fit (black), 3-component fit (red) and 4-component fit (blue) for all diffusion times) of DANS (7 T ^{1}H DOSY experiment), of a spinach thylakoids suspension.

References

1) Minagawa, J. and Tokutsu, R. (2015). Dynamic regulation of photosynthesis in Chlamydomonas reinhardtii. The Plant Journal **82**(3): 413-428.

2) Allen, M. M. (1968). Simple conditions for growth of unicellular blue-green algae on plates 1, 2. Journal of Phycology **4**(1): 1-4.

3) Caffarri, S., Kouril, R., Kereiche, S., Boekema, E. J., and Croce, R. (2009). Functional architecture of higher plant photosystem II supercomplexes. EMBO Journal **28**: 3052–3063.

4) Stejskal, E. O. and Tanner, J. E. (1965). Spin diffusion measurements: spin echoes in the presence of a time-dependent field gradient. Journal of Chemical Physics **42**: 288–292.

5) Antalek, B. (2002). Using Pulsed Gradient Spin Echo NMR for Chemical Mixture Analysis: How to Obtain Optimum Results. Concepts in Magnetic Resonance **14**: 225-258.

6) Provencher, S. W. (1982). A constrained regularization method for inverting data represented by linear algebraic or integral equations. Computer Physics Communications **27**(3): 213-227.

7) Windig, W. and Antalek, B. (1997). Direct exponential curve resolution algorithm (DECRA): a novel application of the generalized rank annihilation method for a single spectral mixture data set with exponentially decaying contribution profiles. Chemometrics and Intelligent Laboratory Systems **37**(2): 241-254.

8) Nieva-Echevarría, B., Goicoechea, E., Manzanos, M. J., andGuillén, M. D. (2014). A method based on 1H NMR spectral data useful to evaluate the hydrolysis level in complex lipid mixtures. Food Research International **66**: 379-387.

9) Wada H, Murata N. 2009. Lipids in photosynthesis: essential and regulatory functions. The Netherlands: Springer.

10) Nuzzo, G., Gallo, C., d'Ippolito, G., Cutignano, A., Sardo, A., and Fontana, A. (2013). Composition and quantitation of microalgal lipids by ERETIC 1H NMR method. Marine Drugs **11**(10): 3742-3753.

11) Masuda, S., Harada, J., Yokono, M., Yuzawa, Y., Shimojima, M., Murofushi, K., Tanaka, H., Masuda, H., Murakawa, M., Haraguchi, T. and Kondo, M. 2011. A monogalactosyldiacylglycerol synthase found in the green sulfur bacterium Chlorobaculumtepidum reveals important roles for galactolipids in photosynthesis. The Plant Cell **23**(7):2644-2658.

12) Sarcina, M., Murata, N., Tobin, M. J., and Mullineaux, C. W. (2003). Lipid diffusion in the thylakoid membranes of the cyanobacterium Synechococcus sp.: effect of fatty acid desaturation. FEBS Letters **553**(3): 295-298.

13) Sarcina, M., Tobin, M. J., and Mullineaux, C. W. (2001). Diffusion of Phycobilisomes on the Thylakoid Membranes of the Cyanobacterium Synechococcus 7942 effects of phycobilisome size, temperature and membrane lipid composition. Journal of Biological Chemistry **276**(50): 46830-46834.

14) Consoli, E., Croce, R., Dunlap, D. D., and Finzi, L. (2005). Diffusion of light-harvesting complex II in the thylakoid membranes. EMBO Reports **6**(8): 782-786.

6

General discussion

The aim of this thesis was to explore the use of PFG NMR approaches to study dynamics of chloroplast water, thylakoid membrane lipids and proteins in photosynthetically active systems by making use of naturally available probe molecules and effects of different environmental conditions on the dynamics of these molecules. In order to provide easy understanding, this chapter is divided into two sections; the first section is about dynamics of chloroplast water in leaves and in photosynthetic microorganisms and the second section is about dynamics of (thylakoid) membrane lipids and proteins in photosynthetic microorganisms.

6.1 Section I (dynamics of chloroplast water)

Although chloroplast water amounts to around 10–30% of the total leaf water, a very limited number of NMR studies of chloroplasts *in vivo* in relation to leaf water content has been published. McCain *et al.*[1] reported that chloroplast water can be discriminated from non-chloroplast water by using an orientation-dependent NMR spectrum of a leaf. Because of susceptibility differences coming from loosely bound manganese ions near the thylakoid membrane chloroplast water can be shifted with respect to non-chloroplast water[1]. However, DOSY measurements on leaf disks of *F. benjamina* and *A. platanoides* (Chapter 2) clearly revealed that even vacuolar water can be shifted from the (bulk) water resonance (4.7 ppm) and also that chloroplast water can have resonances at 4.7 ppm. Thus, discrimination of chloroplast water based on spectral characteristics only is not correct. More recently, Musse *et al.*[2] characterized various cell compartments in *Brassica napus* leaves by monitoring leaf senescence using low-field ^1H NMR relaxometry, light and electron microscopy[2]. They concluded that chloroplast water can be observed as a water pool with a T_2 of about 20 ms, and can easily be distinguished from the other T_2 pools. However, the observed T_2 of chloroplast water can be affected by exchange and thus the discrimination of chloroplast water from other water pools in leaves is not always reliable. As described in chapter 2 our approaches (DOSY and DRCOSY) are applicable in general to all types of leaves (irrespective of the orientation dependence) and at all available field strengths using very short diffusion times that minimize effects of exchange.

Using this approach we were able to discriminate chloroplast water successfully not only in leaf disks but also in the intact photosynthetic microorganism *C. reinhardtii*. Translational dynamics of the chloroplast water in the above mentioned three systems was about comparable, the diffusion coefficient being in the order of 3×10^{-11} m^2 s^{-1} at Δ=25 ms at 20^0 C. This is the first report on translational dynamics of chloroplast water so far, to the best of our knowledge. This work is useful to track changes in leaf tissues and subcellular compartments, e.g. during leaf development, senescence and drought, and in turn to help to understand the relation between chloroplast water and photosynthesis and the changes in it by combining with other studies such as fluorescence and gas exchange for instance.

Although previous studies[3,4,5,6,7] on Chloroplast Volume Regulation(CVR), the process by which chloroplasts import or export osmolytes to maintain a constant volume in a changing environment, were done only on *in vitro* systems, the studies showed that CVR is essential for efficient photosynthesis. McCain *et al.*[6,7] studied CVR for the first time in intact leaf disks using ^{1}H NMR spectroscopy based on the abovementioned assumption (shifted peak uniquely corresponds to chloroplast water) which is not correct (cf. Chapter 2). As we were able to detect chloroplast water accurately under complete *in vivo* conditions (using ^{1}H DOSY and DRCOSY methods), we tried to study CVR in leaf disks of *F. benjamina* and *A. platanoides* as a function of dehydration. The approaches DOSY and DRCOSY have been applied to follow the behaviour of the different water pools (water in different leaf tissues and in chloroplasts) during dehydration. The effect of sub-epidermal cells (present in *F. benjamina*, not present in *A. platanoides*) on the dehydration behaviour of chloroplast is demonstrated. Chloroplasts appeared to be less sensitive than other compartments (such as vacuoles for instance) to moderate dehydration stress in leaf disks of both *F. benjamina* and *A. platanoides*. With extended stress, chloroplasts became equally sensitive as vacuoles in *A. platanoides* but they were still less sensitive in *F. benjamina* because of the buffer role of sub-epidermal cells. This demonstrates that Chloroplast Volume Regulation (CVR) can be studied.

Also, to find out correlation between chloroplast water volume and photosynthetic rates, PS II efficiency (F_v/F_m) was measured using PAM fluorometry but actually high PS II efficiency does not necessarily mean high photosynthetic rates. Thus in order to study the relation between chloroplast volume and photosynthetic activity under complete *in vivo* conditions our

NMR measurements should be combined with other methods more directly related to photosynthetic activity, such as gas exchange measurements. We found a non-linear correlation between chloroplast water volume and PS II efficiency. To a critical value of chloroplast water content, PS II efficiency was 0.35 and below 20 % of AWRF$_{chloroplast}$ (Amount of (chloroplast) Water Relative to Fresh) PS II efficiency declined gradually. Perhaps, a photo-protection mechanism of PS II is related to chloroplast water content.

We also studied nutrient stress and osmotic stress effects of algae. T_2 of the chloroplast water did not change upon nitrogen stress and salt stress (Fig. 4.12; Table 4.1). In Nitrogen Free (NF) algae, changes in chloroplast water content and volume were trivial. At 100 mM excess salt stress chloroplasts lost about 50% water (DOSY measurements at Δ=40 ms, Fig. 4.8a, Chapter 4) and consequently the chloroplast dimension reduced from 4.6±1.2 μm to 3.8±0.5 μm. It is possible to probe changes in chloroplast water volume and dimensions (although not precisely as estimated by time dependent diffusion of chloroplast water) in *C. reinhardtii* suspension using ¹H DOSY NMR under changing environmental conditions (nitrogen starvation and excess salt). By combining this research with other techniques such as gas exchange, it would be possible to study relation between chloroplast water volume and photosynthesis under various environmental conditions.

6.2 Section II

In addition to chloroplast water dynamics, lipids in lipid bodies, (thylakoid) membrane lipids and most probably protein pigment complexes could be observed and their dynamics were studied. In intact leaf systems, T_2 of the membrane lipids is on the order of 5 ms, their apparent diffusion coefficient is 2.7×10^{-12} m²/s at Δ=12 ms and 5×10^{-13} m²/s at Δ=290 ms. Hindered diffusion of the lipids was also observed. It is possible to probe changes in membrane dynamics under changing environmental conditions using the hindered diffusion of membrane lipids.

It is clear from DOSY measurements on *C. reinhardtii* suspensions that both nutrient stress and salt stress result in an accumulation of lipids in lipid bodies. The apparent diffusion coefficient (ADC) of the lipid bodies was 2×10^{-12} m²/s at Δ=220 ms which is close to the ADC (0.79×10^{-12} m²/s at Δ=400 ms) of TAGs in lipid bodies in seeds[8]. The size of the accumulated bodies was about 2±0.3 μm in NF algae, in very good agreement with the value reported by Siaut *et al.*[9] and it was about 1.3±0.2 μm in SM algae. Thus, ¹H DOSY and DRCOSY measurements are very useful to study

accumulated lipid bodies in algae. Study of accumulated lipid bodies has applications in bio-fuel production. As we already have an idea about characteristics (ADC and T_2) of lipid bodies even inexpensive low field DRCOSY measurements can be used to study the lipid bodies and that in turn helps to study *in vivo* effects of growth/environmental conditions easily at low cost.

ADC's of membrane lipids from NM algae, NF algae and SM algae were 1.3×10^{-12} m^2/s, 3.4×10^{-12} m^2/s and 1×10^{-12} m^2/s, respectively at Δ=25 ms at 20⁰ C. The T_2 of the component of NM algae were about 7 ms and 30 ms, whereas for NF algae it was about 23 ms. Thus nutrient stress resulted in longer T_2 values, reflecting higher mobility of the membrane lipids of *C. reinhardtii*. The T_2 of the membrane lipids from Synechocystis was in the order of 20 ms (Fig. 5.6 and Table 5.1, Chapter 5).The lipid compositions of cyanobacteria, algae and higher plants are very similar, although the ratio between the different lipids differ[10]. All the observed differences in the spectra (of membrane lipids, Fig. 5.9 from chapter 5) may be due to a difference in the various lipid ratios for plants and cyanobacteria. Nuzzo *et al.* reported a quantitative analysis of lipids in microalgal samples which clearly indicates that the lipid ratios are quite different in the three samples[11].

In addition to the lipid bodies and membrane lipids, a very intriguing component was observed in the photosynthetic microorganisms (*C. reinhardtii* and Synechocystis) and also in isolated spinach thylakoid suspensions. The Diffusion Associated NMR Spectrum (DANS) of the component from *C. reinhardtii* suspension had substantial changes due to nutrient stress and salt stress which indicates that the component might have contributions from thylakoid membrane protein (super) complexes, because after growth in a Nitrogen Limited (NL) continuous culture system *C. reinhardtii* exhibits substantial changes in thylakoid protein profiles[12]. These differences in amount of various protein complexes and pigment molecules in the thylakoid membrane could explain the substantial changes observed in the relative amplitudes of the peaks in DANS of this component from NM, NF and SM algae (Fig. 4.8d, chapter 4).

Also, the spectra of this component for Synechocystis, *C. reinhardtii* and spinach thylakoids showed substantial differences but the ADC's were comparable at long diffusion observation times (Fig. 5.10, Chapter 5). The ADC of the component at Δ=50 ms from Synechocystis is about 2×10^{-14}

m^2/s and is in the order of the ADC of the component from spinach thylakoids and from *C. reinhardtii* (Fig. 5.10b, Chapter 5). The diffusion coefficient of phycobilisomes on the thylakoid membrane surface in *Synecoccocus* PCC 7942 is about 3×10^{-14} m^2/s[13] which is in the order of the ADC of the component at Δ=50 ms and thus the component from Synechocystis might have contributions from phycobilisomes. The T_2's of the component were 3 ms and 60 ms. The diffusion coefficient of the major light-harvesting complex LHCII was reported by *Consoli et al.*[14] to be 0.8×10^{-14} m^2/s in isolated spinach thylakoid membranes. This value fits quite well with the ADC of the slowest component from both spinach thylakoids and *C. reinhartdtii*. So the slowest component from both spinach thylakoids and *C. reinhartdtii* might have some contribution from LHCII. By proper diffusion filtering, the spectrum of the component can be obtained in about 5 mins choosing only the last gradient step. This (diffusion edited spectrum combined with more advanced 2D NMR methods) opens a new way to study the photosynthetic proteins because the approach does not need any of the following requirements such as expensive isotope labelling, low temperatures to have solid state samples (thus possible to study the proteins in native conditions) and long-range crystalline structures.

References

1) McCain, D. C., Selig, T. C., and Markley, J. L. (1984). Some plant leaves have orientation-dependent EPR and NMR spectra. Proceedings of the National Academy of Sciences **81**: 748-752.

2) Musse, M., De Franceschi, L., Cambert, M., Sorin, C., Le Caherec, F., Burel, A., and Leport, L. (2013). Structural changes in senescing oilseed rape leaves at tissue and subcellular levels monitored by Nuclear Magnetic Resonance Relaxometry through water status. Plant Physiology **163**: 392-406.

3) Robinson, S. P. (1985). Osmotic adjustment by intact isolated chloroplasts in response to osmotic stress and its effect on photosynthesis and chloroplast volume. Plant Physiology **79**(4): 996-1002.

4) Gupta, A. S. and G. A. Berkowitz (1988). Chloroplast osmotic adjustment and water stress effects on photosynthesis. Plant Physiology **88**(1): 200-206.

5) Santakumari, M. and G. A. Berkowitz (1991). Chloroplast volume: cell water potential relationships and acclimation of photosynthesis to leaf water deficits. Photosynthesis Research **28**(1): 9-20.

6) McCain, D. C. (1995). Combined effects of light and water stress on chloroplast volume regulation. Biophysical Journal **69**(3): 1105.

7) McCain, D. C. and J. Markley (1992). In vivo study of chloroplast volume regulation. Biophysical Journal **61**: 1207-1212.

8) Gromova, M., Guillermo, A., Bayle, P.A. and Bardet, M. (2015). In vivo measurement of the size of oil bodies in plant seeds using a simple and robust pulsed field gradient NMR method. European Biophysics Journal **44**(3): pp121-129.

9) Siaut, M., Cuiné, S., Cagnon, C., Fessler, B., Nguyen, M., Carrier, P., and Peltier, G. (2011). Oil accumulation in the model green alga Chlamydomonas reinhardtii: characterization, variability between common laboratory strains and relationship with starch reserves. BMC Biotechnology **11**(1): 7.

10) Wada H, Murata N. 2009. Lipids in photosynthesis: essential and regulatory functions. The Netherlands: Springer.

11) Nuzzo, G., Gallo, C., d'Ippolito, G., Cutignano, A., Sardo, A., and Fontana, A. (2013). Composition and quantitation of microalgal lipids by ERETIC 1H NMR method. Marine drugs **11**(10): 3742-3753.

12) Peltier, G. and G. W. Schmidt (1991). Chlororespiration: an adaptation to nitrogen deficiency in Chlamydomonas reinhardtii. Proceedings of the National Academy of Sciences **88**(11): 4791-4795.

13) Hatch D, Boardman NK. 2014. Photosynthesis: The Biochemistry of Plants. California: Academic Press, INC.

14) Sarcina, M., Tobin, M. J., and Mullineaux, C. W. (2001). Diffusion of Phycobilisomes on the Thylakoid Membranes of the Cyanobacterium Synechococcus 7942 effects of phycobilisome size, temperature and membrane lipid composition. Journal of Biological Chemistry **276** (50): 46830-46834.

7

Summary

1) Using ^{1}H DOSY and DRCOSY methods with appropriate D-filter, it was possible to discriminate chloroplast water from other water pools in leaf disks of *Ficus benjamina* and *Acer platanoides* and also in suspension of green algae *Chlamydomonas reinhardtii*. *Synechocystis* water was also detected in *Synechocystis* suspension using the methods.

2) Also, we were able to study dehydration effects on leaf cellular compartments in leaf disks of *F. benjamina* and *A. platanoides*. We conclude from the study that subepidermal cells (present only in *F. benjamina*) serve as water storage pools and help plants to survive under dehydrating conditions by preventing chloroplast water loss.

3) Algal water and chloroplast water were observed in suspension of green algae *Chlamydomonas reinhardtii.* Using restricted diffusion behaviour of chloroplast water, the size or volume of chloroplast in *C. reinhardtii* of WT grown in normal medium (NM), nitrogen free medium (NF) and salty medium (SM) could be estimated. Salt stress resulted in substantial changes about 17 % in chloroplast size (4.6±1.2µm in NM and 3.8± 0.5µm in SM), related to a decrease of about 47 % of the volume. T_2 of the chloroplast water increased by about a factor 2 for both NF algae and SM algae in comparison to that of the NM algae.

4) In leaf disks and in suspensions of *Synechocystis*, *C. reinhardtii* and spinach thylakoids, membrane lipids were observed. To the best of our knowledge, no other lipid diffusion measurements in intact leaf systems have been reported. Hindered diffusion of the lipids was also observed. It would be possible to probe changes in membrane dynamics under changing environmental conditions using the hindered diffusion of membrane lipids.

5) T_2 and restricted diffusion of lipid bodies and membrane lipids was measured for NM, NF and SM *C. reinhardtii*. Nutrient stress and salt stress had substantial effect on lipid production (lipid bodies) and dynamics of membrane lipids. Estimated sizes of the lipid bodies from their hindered diffusion were 1.3µm, 2 ± 0.3µm and 1.3 ± 0.2µm for NM, NF and SM *C. reinhardtii,* respectively. T_2 of lipid bodies was longer than that of membrane lipids in all the three NM,

NF and SM *C. reinhardtii* and T_2 of membrane lipids was longer in NF and SM *C. reinhardtii* than that of NM *C. reinhardtii*.

6) Most significantly, we could study dynamics and (changes in) composition of photosynthetic pigment-protein complexes *in vivo* in WT *C. reinhardtii* grown under the three different cultures (NM, NF and SM) and also in suspensions of *Synechocystis* and spinach thylakoids. By proper diffusion editing these spectra can be measured in about 4 minutes at 300 MHz thus it would be even better at higher field spectrometers. This opens the possibility to apply 2D NMR methods for further characterisation of the spectral components.

Acknowledgements

Training and Education

		Education Statement of the Graduate School	
		Experimental Plant Sciences	
Issued to:		**Shanthadevi Pagadala**	
Date:		**6 June 2017**	
Group:		**Laboratory of Biophysics**	
University:		**Wageningen University & Research**	
1) Start-up phase			date
►	**First presentation of your project**		
	Title: 1H and 31P in vivo NMR methods to study thylakoid membrane phase, time dependent lipid diffusion and exchange		Jan 10, 2012
►	**Writing or rewriting a project proposal**		
	Writing a review or book chapter		
►	**MSc courses**		
	BIP 30806: Advances in Magnetic Resonance, Wageningen, NL		Mar-Apr 2012
►	**Laboratory use of isotopes**		
		Subtotal Start-up Phase	7.5 credits*
2) Scientific Exposure			date
►	**EPS PhD student days**		
	EPS PhD student day 2013, Leiden, NL		Nov 29, 2013
►	**EPS theme symposia**		
	EPS Theme 3 Symposium-'Metabolism and Adaptation', Amsterdam, NL		Mar 22, 2013
	EPS Theme 3 Symposium-'Metabolism and Adaptation', Wageningen, NL		Mar 11, 2014
	EPS Theme 3 Symposium-'Metabolism and Adaptation', Wageningen, NL		Mar 14, 2017
►	**NWO Lunteren days and other National Platforms**		
	Dutch Meeting on molecular and cellular biophysics, Veldhoven, NL		Oct 01-02, 2012
	Dutch Meeting on molecular and cellular biophysics, Veldhoven, NL		Sep 30-Oct 01, 2013
	Annual meeting 'Experimental Plant Sciences' 2014, Lunteren, NL		Apr 14-15, 2014
	Annual meeting 'Experimental Plant Sciences' 2015, Lunteren, NL		Apr 13-14, 2015
►	**Seminars (series), workshops and symposia**		
	Symposium 'Measuring the Photosynthesis phenome', Wageningen, NL		Jul 07-09, 2014
►	**Seminar plus**		
►	**International symposia and congresses**		
	MR in food conference, Wageningen, NL		Jun 27-29, 2012
	EUROMAR, Hersonissos, Crete, Greece		Jun 30-Jul 05, 2013
►	**Presentations**		
	Talk: FOM meeting 2011, Amsterdam, NL		Oct 19, 2011

Talk: FOM meeting 2012, Utrecht, NL	Mar 14, 2012
Poster: Dutch meeting 2012, Veldhoven, NL	Oct 01, 2012
Talk: FOM meeting 2012, Amsterdam, NL	Oct 29, 2012
Talk: FOM meeting 2013	Mar 07, 2013
Poster: EUROMAR, Hersonissos, Crete, Greece	Jul 02, 2013
Talk: FOM meeting 2014, Groningen, NL	May 13, 2014
Poster: Ampere NMR School 2014, Zakopane, Poland	Jun 24, 2014
Talk: FOM meeting 2015, Utrecht, NL	Jun 12, 2015
► **IAB interview**	
Meeting with a member of the International Advisory Board of EPS	Jan 05, 2015
► **Excursions**	
Subtotal Scientific Exposure	16.6 credits*
3) In-Depth Studies	date
► **EPS courses or other PhD courses**	
Postgraduate course 'In vivo NMR', Wageningen, NL	Dec 10-20, 2012
Ampere NMR school, Zakopane, Poland	Jun 22-28, 2014
► **Journal club**	
► **Individual research training**	
Subtotal In-Depth Studies	4.8 credits*
4) Personal development	date
► **Skill training courses**	
FOM course 'Taking charge of PhD project', Utrecht, NL	Apr 18 & 25, 2012
FOM course 'Art of presenting science', Utrecht, NL	Sep 14, 28 -Oct 12, 2012
FOM course 'Art of scientific writing', Utrecht, NL	Mar 01, 15 -Apr 05, 2013
► **Organisation of PhD students day, course or conference**	
► **Membership of Board, Committee or PhD council**	
Subtotal Personal Development	3.1 credits*
TOTAL NUMBER OF CREDIT POINTS*	32.0
Herewith the Graduate School declares that the PhD candidate has complied with the educational requirements set by the Educational Committee of EPS which comprises of a minimum total of 30 ECTS credits	
* A credit represents a normative study load of 28 hours of study.	